

**Climate in the Eastern Mediterranean through the Holocene  
inferred from Turkish stalagmites**

Inauguraldissertation  
der Philosophisch-naturwissenschaftlichen Fakultät  
der Universität Bern

vorgelegt von  
**Ozan Mert Göktürk**  
aus der Türkei

Leiter der Arbeit:  
SNF-Prof. Dr. Dominik Fleitmann  
Institut für Geologie und Oeschger Centre for Climate Change Research  
Universität Bern



**Climate in the Eastern Mediterranean through the Holocene  
inferred from Turkish stalagmites**

Inauguraldissertation  
der Philosophisch-naturwissenschaftlichen Fakultät  
der Universität Bern

vorgelegt von  
**Ozan Mert Göktürk**  
aus der Türkei

Leiter der Arbeit:  
SNF-Prof. Dr. Dominik Fleitmann  
Institut für Geologie und Oeschger Centre for Climate Change Research  
Universität Bern

Von der Philosophisch-naturwissenschaftlichen Fakultät angenommen.

Bern, 10. Mai 2011

Der Dekan:  
Prof. Dr. Silvio Decurtins



**Climate in the Eastern Mediterranean through the Holocene  
inferred from Turkish stalagmites**

Dissertation

submitted to the Faculty of Science of the University of Bern  
for the degree of Doctor of Science (Dr. phil. nat.)

by

**Ozan Mert Göktürk**

from Turkey

Supervisor:

SNF-Prof. Dr. Dominik Fleitmann

Institute of Geological Sciences and Oeschger Centre for Climate Change Research  
University of Bern



*“Real science is all about trying to prove your theory wrong. You do everything you can to prove it wrong, then have other people do what they can to prove it wrong. When all of you fail at doing that, when the theory has been refined such that it fits all the evidence and you can't figure out how else to test it, then it is most likely the truth. **That** is what scientific rigor is about. It isn't about coming up with a theory, ignoring data you don't like, showing it to a few people who agree with you, and saying 'Ok, we proved this true and nobody else can look at it.'“*

*Richard P. Feynman (1918 – 1988), Physicist*





---

# TABLE OF CONTENTS

<b>ABSTRACT</b> .....	<b>V</b>
<b>THANKS ! – TEŞEKKÜRLER !</b> .....	<b>VII</b>
<b>1 INTRODUCTION AND OUTLINE OF THE THESIS</b> .....	<b>1</b>
<b>1.0</b> Foreword .....	1
<b>1.1</b> Aim of This Work .....	1
<b>1.2</b> Why Turkey? .....	1
<b>1.3</b> Stalagmites as Natural Archives .....	5
<b>1.4</b> Methods .....	5
<b>1.4.1</b> <sup>230</sup> Th Dating .....	6
<b>1.4.2</b> Stable Isotope Analysis .....	6
<b>1.5</b> Outline of the Thesis .....	7
<b>1.6</b> References .....	8
<b>2 CLIMATE ON THE SOUTHERN BLACK SEA COAST DURING THE HOLOCENE: IMPLICATIONS FROM THE SOFULAR CAVE RECORD</b> .....	<b>13</b>
<b>2.1</b> Abstract .....	13
<b>2.2</b> Introduction .....	14
<b>2.3</b> Sofular Cave: Climatic and Environmental Setting .....	15
<b>2.4</b> Material and Methods .....	17
<b>2.5</b> Results and Proxy Quality .....	17
<b>2.5.1</b> Chronology .....	17
<b>2.5.2</b> Stable Isotope Profiles .....	17
<b>2.5.2.1</b> δ <sup>13</sup> C .....	18
<b>2.5.2.2</b> δ <sup>18</sup> O .....	22
<b>2.5.3</b> Growth Rate and Diameter .....	25
<b>2.5.4</b> Initial <sup>234</sup> U/ <sup>238</sup> U .....	25
<b>2.6</b> Discussion .....	26
<b>2.6.1</b> Holocene Climate Variability on the Southern Black Sea Coast .....	26
<b>2.6.1.1</b> The Early Holocene: 11.6 – 9.6 ka BP .....	26
<b>2.6.1.2</b> The 'Hypsithermal': 9.6 – 5.4 ka BP .....	26
<b>2.6.1.3</b> Mid- to Late Holocene: 5.4 ka BP – Present .....	27
<b>2.6.2</b> Comparison with Eastern Mediterranean and Monsoon Records .....	29
<b>2.6.3</b> Wet Period during Sapropel I: .....	30
<b>2.6.3.1</b> Timing .....	30
<b>2.6.3.2</b> Possible Mechanisms .....	31
<b>2.7</b> Summary and Conclusions .....	34

---

	Acknowledgements .....	35
<b>2.8</b>	References .....	35
<b>3</b>	<b>LATE HOLOCENE WINTER TEMPERATURES IN THE EASTERN MEDITERRANEAN AND THEIR RELATION TO CULTURAL CHANGES: THE KOCAIN CAVE RECORD .....</b>	<b>41</b>
<b>3.1</b>	Abstract .....	41
<b>3.2</b>	Introduction .....	42
<b>3.3</b>	Kocain Cave: Climatic and Environmental Setting .....	44
<b>3.4</b>	Material and Methods .....	46
<b>3.5</b>	Results and Discussion .....	48
<b>3.5.1</b>	Chronology and Growth Rates .....	48
<b>3.5.2</b>	Stable Isotope Profiles and Their Interpretation .....	48
<b>3.5.2.1</b>	$\delta^{13}\text{C}$ .....	48
<b>3.5.2.2</b>	$\delta^{18}\text{O}$ .....	52
<b>3.5.3</b>	Implications for Late Holocene Climate and Cultural Changes in the Eastern Mediterranean .....	53
<b>3.5.3.1</b>	Synchronicity of Cold Periods with Global Glacier Advances .....	55
<b>3.5.3.2</b>	Minoan Warm Period, 4.2 ka BP Event and the Bronze Age Collapse .....	55
<b>3.5.3.3</b>	Roman Warm Period and Medieval Climate Anomaly .....	57
<b>3.5.3.4</b>	Little Ice Age and the Decline of the Ottoman Empire .....	58
<b>3.5.3.5</b>	The Degree of Warmth in the Modern Era .....	59
<b>3.6</b>	Summary and Conclusions .....	59
<b>3.7</b>	References .....	60
<b>4</b>	<b>DECIPHERING THE CLIMATE SIGNAL: A NEW LATE HOLOCENE STALAGMITE RECORD FROM THE SOUTHEAST BALKAN .....</b>	<b>67</b>
<b>4.1</b>	Abstract .....	67
<b>4.2</b>	Introduction .....	68
<b>4.3</b>	Uzuntarla Cave: Climatic and Environmental Setting .....	68
<b>4.4</b>	Material and Methods .....	70
<b>4.5</b>	Results and Discussion .....	70
<b>4.5.1</b>	Chronology .....	70
<b>4.5.2</b>	Stable Isotope Profiles and Their Interpretation .....	72
<b>4.5.2.1</b>	$\delta^{18}\text{O}$ .....	72
<b>4.5.2.2</b>	$\delta^{13}\text{C}$ .....	74
<b>4.5.3</b>	Implications for Past Climate .....	75
<b>4.5.3.1</b>	Minoan Warm Period and the Bronze Age Collapse .....	75
<b>4.5.3.2</b>	Iron Age cold and Roman warm periods .....	77

---

---

	<b>4.5.3.3</b> The Oort Minimum and the Little Ice Age .....	77
<b>4.6</b>	Summary and Conclusions .....	78
<b>4.7</b>	References .....	78
<b>5</b>	<b>RECORDS FROM OVACIK AND YENESU CAVES .....</b>	<b>83</b>
<b>5.1</b>	Abstract .....	83
<b>5.2</b>	Introduction .....	83
<b>5.3</b>	Ovacik and Yenesu Caves .....	83
<b>5.4</b>	Material and Methods .....	84
<b>5.5</b>	Results and Discussion .....	84
<b>5.5.1</b>	Chronology and Growth Rates .....	84
<b>5.5.1.1</b>	O-1 .....	85
<b>5.5.1.2</b>	O-4 .....	85
<b>5.5.1.3</b>	Ye-4 .....	86
<b>5.5.2</b>	Stable isotope profiles and their comparison with those of Sofular and Uzuntarla caves .....	86
<b>5.5.2.1</b>	O-1 .....	86
<b>5.5.2.2</b>	O-4 .....	88
<b>5.5.2.3</b>	Ye-4 .....	88
<b>5.6</b>	Conclusions .....	90
<b>5.7</b>	References .....	90
<b>6</b>	<b>SUMMARY AND FINAL CONCLUSIONS .....</b>	<b>93</b>
<b>6.1</b>	Summary .....	93
<b>6.2</b>	Final Conclusions and Outlook .....	95
<b>6.3</b>	References .....	96
<b>A</b>	<b>DATA .....</b>	<b>99</b>
<b>B</b>	<b>PUBLICATIONS .....</b>	<b>99</b>
<b>C</b>	<b>CONFERENCE CONTRIBUTIONS .....</b>	<b>109</b>
<b>D</b>	<b>DECLARATION .....</b>	<b>111</b>
<b>E</b>	<b>CURRICULUM VITAE .....</b>	<b>113</b>

---



---

## ABSTRACT

The Eastern Mediterranean is not only a modern global warming hot-spot, but also has a long history of human civilization that has apparently been affected by past climatic variations. Detailed studies on Holocene climate are therefore of critical importance for this region, as the area is climatically rather complex and our current level of knowledge does not allow a thorough understanding of the regional impact of large scale climate forcings. This work contributes to the issues of past climate in the Eastern Mediterranean, by presenting six new proxy records that span the Holocene either partially or completely. The records are based on the  $^{230}\text{Th}$  (U-series) chronologies and the high resolution (sub-decadal) stable isotope ( $\delta^{13}\text{C}$  and  $\delta^{18}\text{O}$ ) profiles of stalagmites collected from caves in three different climatic zones of Turkey. In each chapter, one stalagmite record is carefully examined to reach the most plausible interpretation of its stable isotope profile and growth characteristics, in terms of climatic variations and environmental changes during the Holocene. This is achieved with a) the comparison of the recent part of each proxy time series with the available meteorological records from a nearby station; b) the comparison of the entire length of each proxy time series with the available paleoclimate records covering the Holocene. The climatic, geological and geomorphological features of the specific cave sites are also considered in the interpretations.

Three of the six records mentioned above provide conclusive information concerning the Holocene climatic variations in Turkey and the Eastern Mediterranean. The Sofular Cave record is from the southern Black Sea coast (northern Turkey), where the modern rainfall regime and variability are significantly different from those of the typical Mediterranean sites. This record indicates a remarkable increase in rainfall amount and intensity during the early to mid-Holocene (~ 9.6 to 5.4 ka BP), and marks one of the northernmost points in the greater Eastern Mediterranean area where a roughly simultaneous wet period was previously reported. Enhanced evaporation in fall and winter due to high sea surface temperatures, and/or a regional summer monsoon mechanism involving both the Black and Mediterranean seas must have led to a much wetter climate in the entire area. The  $\delta^{13}\text{C}$  record from the Kocain Cave in southern Turkey is unique in that it is probably a direct winter temperature proxy for the second part of the Holocene, indicated by its good match with the meteorological records and clear expression of the well known cold periods. This record can be key to understanding both the mechanisms that led to the inferred winter temperature variations, as well as the impact of these variations on the human societies in this region. For instance, the Little Ice Age is found to have been persistently cold and generally dry in western Anatolia, which supports the proposed role of cold winters and drought in the uprisings in the 16<sup>th</sup> century Ottoman Empire; while contradicting the notion of a continuous negative mode of the North Atlantic Oscillation during this period. The third record, from the Uzuntarla Cave in northwestern Turkey, provides mixed proxies for more than one climatic parameter. Yet, with the aid of other available records, it can be used to infer valuable clues concerning past climate. Interpretation of the other three records remain ambiguous since it is not clear which factors determined their isotopic variations. Nevertheless, they are useful for assessing the limitations of stalagmites as natural archives of climate, especially when sub-millennial time scales are concerned. All in all, the new records presented here are a remarkable step towards a well distributed and denser network of high quality climate proxy records, as well as demonstrating the potentials of stalagmites for paleoclimate research.



---

## THANKS ! - TEŞEKKÜRLER !

Dominik, I would sincerely like to thank you for letting me participate in this exciting project. During the last four years, I found the opportunity to improve my knowledge and to gain experience in many things – even our frequent clashes were educational :-) Thanks for keeping your rigor while approaching my work, yes I complained sometimes, but at the end I learned a lot.

Seraina, without your support at work, and your friendship while not working, this would have been very difficult. Merci viu viu mau.

Robyn, thank you for being such an enthusiastic and patient teacher in the lab.

Daenu, my Sofular paper will be published soon and I am not sure if someone will ever read it as carefully as you did! Thanks for all your help and the pure enthusiasm. It was a pleasure being your office mate.

Naki hocam, bana dört yıl boyunca abilik ettiniz, yabancı olduğum bu yerde arkamda her zaman birinin olduğunu hissettim sayenizde. Sağ olun.

Valentina, Janos, Sally and Mareike... This was once said by Mevlana: *“Not the ones who speak the same language, but the ones who feel the same way can understand each other”*. Thank you for being around, you made everything easy.

Dea, you cheered me up in the office, helped me through problems, and listened all my gossip so well! :-) A hearty and bloody thank you from your barbarian!

Okan hocam, bu projeye bizden, genç birini de katma fikri sizindi. Bütün bunları yapabilmeme vesile olduğunuz ve tüm desteğiniz için size teşekkür ederim. Umarım kendimi iyi yetiştirebilmişimdir.

Ben bu işlere sırf havanın ve iklimin *delisi* olduğum için girdim. *“Yapma demiyorum hobi olarak gene yap”* demeyen, *“kapı gibi mühendis diploman var, gir bir yere para kazan”* diye kafa ütülemeyen, tutkuyla yaptıklarımda bana sonuna kadar destek olan herkese, özellikle *Not Defteri*'min müdavimlerine, Sertan Abi'ne, anneme, babama ve Altan'a çok teşekkür ederim. Taylan, Ali ve Deniz; aynı yolun yolcusu sevgili meslektaşlarım, kendimi yalnız hissetmememi sağladığınız için size minnettarım.

Son olarak... Bir erkek bir işi ne büyük iştahla başarırsa başarsın, eğer *o kadının* hayranlığını kazanamıyorsa mutlu olamaz. Bütün bu hengamenin ortasında karşıma çıkıp hayatıma yön veren, ona anlam ve umut katan Ruken'im, teşekkürlerin en büyüğü sana...





# CHAPTER 1

## INTRODUCTION AND OUTLINE OF THE THESIS

### 1.0 Foreword

Having been studying paleoclimatology for some years, I am realizing how much my perception of weather and climate has since changed. Now whenever 'normal' friends ask me in awe, for example, after three consecutive very warm winters, if it will ever again snow in Istanbul, I dare to say: "Come on, this is perhaps *just* a 10-year long warm spell due to a shift in the NAO (*-what the hell is that Ozan?*), it hasn't been warm long enough yet to worry". This reply is probably owing to the fact that, in one of my stalagmite records, a single measurement tells me about the winter temperatures of that decade (see Chapter 3), and there are as many as 2476 data points in the last 5700 years, fluctuating up and down in between extremes! The knowledge of how warm and how cold it can actually get makes one a boring realist.

However, this boring realism can sometimes get quite telling as well. Today, once in every three autumns on the Black Sea coast of Turkey, a devastating flood occurs. One of my stalagmites shows signs of even bigger and much more frequent floods that occurred some 7000 years ago (see Chapter 2), when summers and in turn Black Sea waters in fall were probably much warmer, giving rise to monster convective clouds. I try to provoke people's imagination by telling my story and warn them that current global warming can have similar consequences. Sustained cold is as bad as heat: In the 16<sup>th</sup> century Ottoman Anatolia, people left their home towns for ever, probably due to repeating, unrelenting winters (see Chapter 3). Even a single winter of cold like that one in the past, has the potential to create an energy crisis today, and to change the lives of millions of people (Watson, 2008; TWGI, 2010).

### 1.1 Aim of This Work

The aim of this PhD thesis is to construct highly resolved and well dated records of past climate using stalagmites collected from caves in Turkey. Interpretation of these records in terms of local, regional and larger scale climate dynamics is also an integral part. The Holocene (last ~11700 years in geological history) is the target time frame, as it is the current interglacial (warm period) during which human civilization flourished (Fig. 1.1). Another aim is to assess the strengths and limitations of stalagmites as paleoclimate recorders for the Holocene, as the much lower amplitude climatic and environmental changes within this time frame (compared to glacial-interglacial shifts) are not always well expressed in natural archives.

### 1.2 Why Turkey?

Turkey is a key area to study Holocene climate, because of two main reasons: The first and obvious one is its historical significance. For example, the largest and best preserved Neolithic site found so far, Çatalhöyük (~9.5 – 7.7 ka BP), is in Central Anatolia (Hodder, 1997). In fact, borderlands of the Eastern Mediterranean sea were the cradle of

civilizations throughout human history, for example during the Bronze Age (Drews, 1993), when Hittite Empire and the Minoans reigned in Anatolia and Crete, respectively. Understanding past climate in Turkey is therefore crucial to explain climatically-induced cultural and societal changes.

The second -yet equally important- motivation to work in Turkey is again its position, but this time from a climatic point of view. The country, owing to its location, is affected by three major climatic systems; providing opportunity to gather information on the strength, geographical extent and interaction of these in the past. Being in mid-latitudes (36°N - 42°N), Turkey is under the influence of North Atlantic climate in winter, through westerlies blowing across the Mediterranean. The strength of these westerlies (thus the degree of North Atlantic control) is modulated by the North Atlantic Oscillation (NAO), whose negative mode leads to stronger westerly circulation and warmer&wetter conditions over the Eastern Mediterranean (Hurrell, 1995; Hurrell and VanLoon, 1997). On the other hand, invasion of cold, continental air masses from the north depends more on the East Atlantic / Western Russia (or, as defined later, the North Sea – Caspian (NCP)) pattern (Barnston and Livezey, 1987; Kutiel and Benaroch, 2002); with the positive mode leading to cooler&drier times. While these are the two teleconnections controlling the main aspects of winter climate over Turkey (Krichak et al., 2002; Türkeş and Erlat, 2009), the summer regime is defined largely by changes in the Indian monsoon and its extensions into the Middle East (Raichich et al., 2003; Ziv et al., 2004). An enhanced Indian monsoon means a stronger descending branch of the Hadley cell over Turkey, and drier conditions.

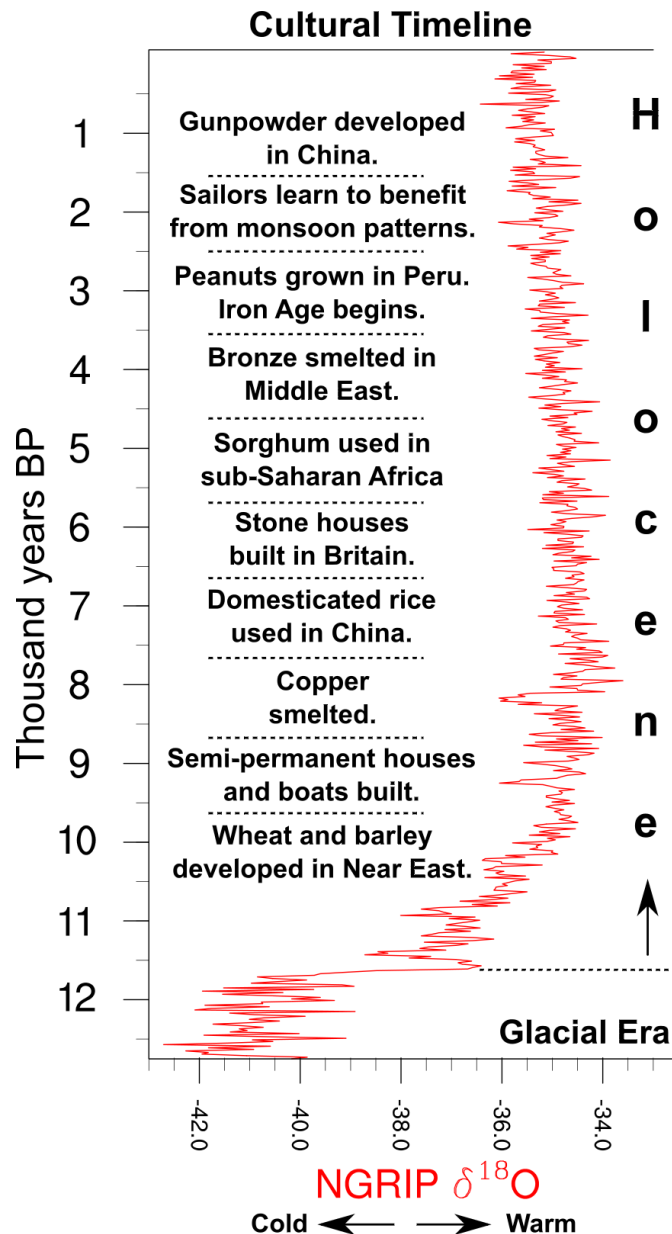


**Fig. 1.1:** Timeline of important human developments during the Holocene, along with the δ<sup>18</sup>O (per mil) record from the North Greenland Ice Core Project (NGRIP, Svensson et al., 2008). 'BP' stands for 'before present', where present is defined as 1950. Figure partly adapted from NCDC (2008).



Black Sea (**BLS**): uniform rainy with a maximum in autumn, temperate  
 Marmara (Mediterranean to Black Sea) Transition (**MRT**): uniform rainy with a warm and light rainy summer  
 Mediterranean (**MED**): markedly seasonal with a cool and heavy rainy winter and a hot dry summer; humid and semi-humid subtropical  
 Continental Mediterranean (**CMED**): seasonal with a rainy winter and spring and a severe hot dry summer; semi-arid subtropical  
 Mediterranean to Central Anatolia Transition (**MEDT**): moderate rainy winter and spring  
 Continental Central Anatolia (**CCAN**): cool rainy spring and cold rainy winter; warm and light rainy summer; semi-arid steppe  
 Continental Eastern Anatolia (**CEAN**): cool rainy spring and early summer with a very cold and snowy winter; semi-humid steppe and highland

**Fig. 1.2:** Turkey (approximate borders marked with full white lines), as divided into its climatic zones (dashed white lines) mainly according to the seasonality of rainfall (Türkeş, 1996). Locations of caves from which the stalagmites mentioned in this thesis originate are shown with red dots. Detailed information about the caves and their climatic settings can be found in individual chapters.

These broad generalizations may seem adequate to describe the factors governing climatic variations in Turkey, but the issue is more complex. Anatolia is surrounded by water masses on three sides, and has a complex topography (Fig. 1.2). The two mountain chains extending from east to west, namely the North Anatolian in the north and the Taurus in the south, climatically isolate the interior plateau from coastal areas by blocking warm and humid maritime air (see also Chapter 3). This leads to stark differences both in temperature and rainfall, especially during winter. The Black Sea itself is another complicating factor. Originally dry and cool continental air masses coming from the north pass over the Black Sea, are humidified and then forced upwards by the North Anatolian mountains. This is a process that enhances precipitation in northern and eastern parts of Turkey. A year round wet, oceanic climate is observed on the northern coastline of the country (see also Chapter 2). In fact, all these local factors can be traced in the studies that

tried to link larger scale phenomena with Turkey's climatic variations. Although their work is often cited to show that winter precipitation variability in Turkey is largely controlled by the NAO, Cullen and deMenocal (2000) was able to explain only 27% of the variability with this pattern.

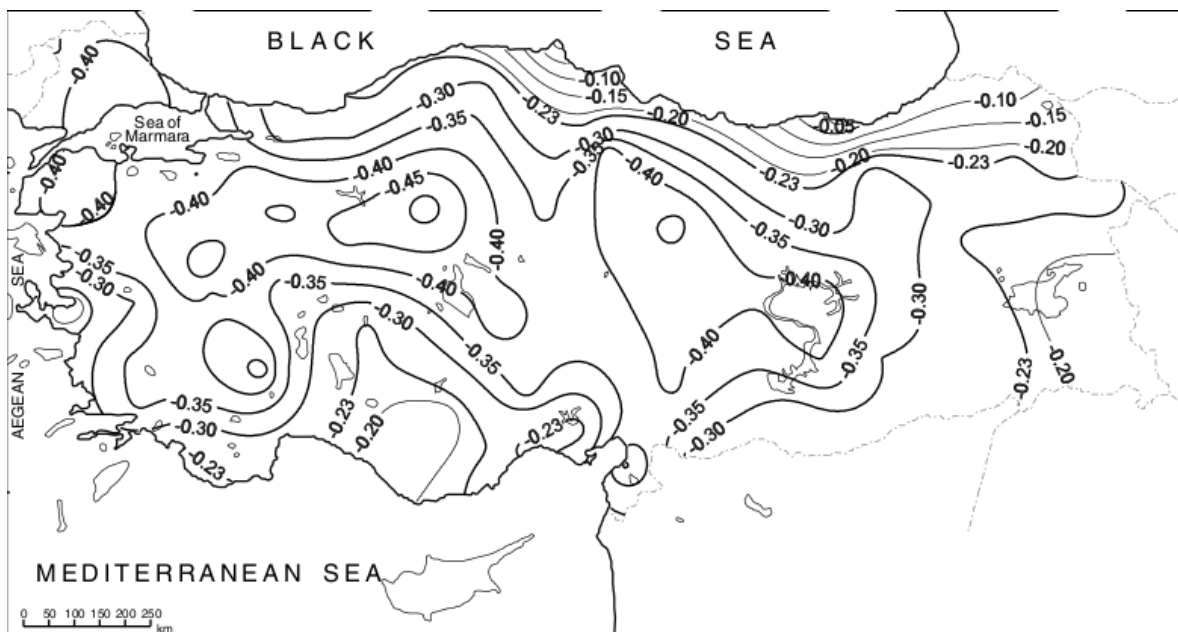


**Fig. 1.3:** Correlation coefficients between the winter NAO index and the winter precipitation time series of 78 stations in Turkey. Figure taken from Türkeş and Erlat (2003). Bold lines indicate statistically significant (level 95%) correlations.

Later, Türkeş and Erlat (2003) found that the Black Sea climate zone in Turkey is detached from the southern and western parts of the country in terms of the response to the NAO (Fig. 1.3). The effect of water masses over the climate of the Eastern Mediterranean region is even more evident in the linkages with the NCP. Regions exposed to northern maritime trajectories (Crete, Israel and the Black Sea zone in Turkey) receive more precipitation during the positive (cool) phase of this teleconnection pattern (Kutiel et al., 2002), demonstrating that “warm&wet” generalization does not always hold.

Despite the fact that the mentioned irregularities may well lead to inconclusive results concerning some aspects of past climate dynamics; with a correct interpretation of the data in hand, they can well be very useful for providing answers to some interesting questions: What could have been the outcome of significantly *warmer* or *colder* conditions than today, in terms of the effects of teleconnection patterns? Could borders of modern climatic zones have shifted, even within the *quasi-stable* Holocene time frame? Could a local climate of the present have been quite widespread, due to some factor surpassing a certain threshold? For example, did the stronger summer insolation during the early to mid-Holocene (Liu et al., 2004) really lead to much drier summers in the Eastern Mediterranean (Tzedakis, 2007), or did it create local monsoon rains (Arz et al., 2003), which are almost non-existent today? This thesis is an attempt to contribute to the discussions of past climate, by providing data from a region of climatic complexities.

Records of Holocene climate in and around Turkey are now not too few. They have been

mostly obtained from marine (e.g. Lamy et al., 2006; Marino et al., 2009) and lake deposits (Roberts et al., 2008 and references therein; Kuzucuğlu et al., 2011), also trees (Akkemik et al., 2008 and references therein). However, marine and lacustrine records often have large dating uncertainties and low temporal resolution, whereas tree proxies have a very limited skill to register variations in winter climate (Hughes, 2002; Mangini et al., 2007). With their precise dating and ability to record various aspects of the climate system depending on the specific cave site, stalagmites are good alternatives. They were extensively used to reconstruct past climate in other parts of the globe (McDermott, 2004; Fairchild et al., 2006; Lachniet, 2009).

### 1.3 Stalagmites as Natural Archives

Speleothems, which are composed of calcite or aragonite, form when dissolved calcium carbonate ( $\text{CaCO}_3$ ) is redeposited in caves. In the dissolution region of karstic areas (Fig. 1.2), infiltrating rainwater or snowmelt reacts with  $\text{CO}_2$  and forms carbonic acid ( $\text{H}_2\text{CO}_3$ ), which has the ability to dissolve the carbonate bedrock. Resulting calcium ( $\text{Ca}^{2+}$ ) and bicarbonate ( $\text{HCO}_3^-$ ) ions

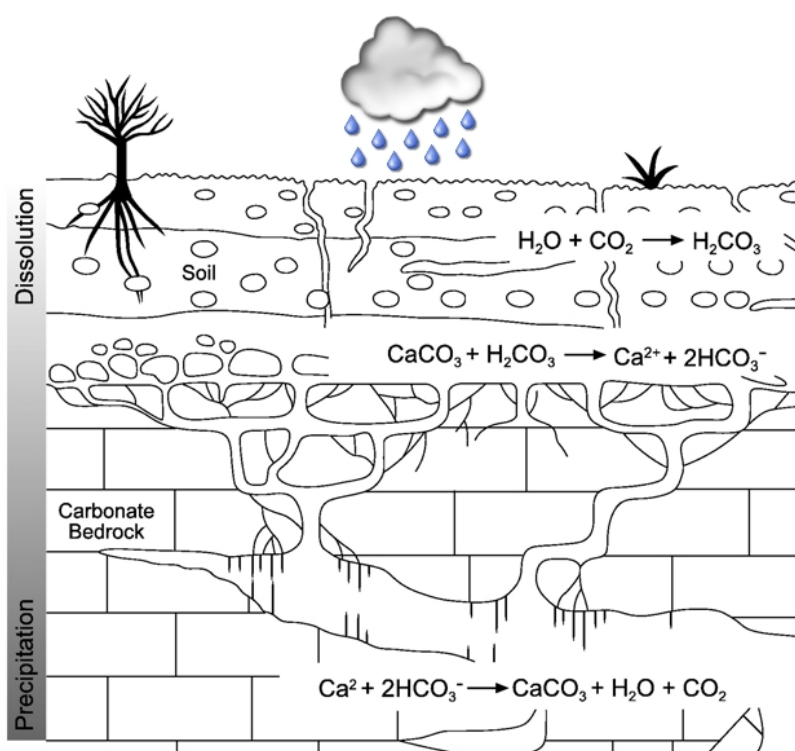


**Fig. 1.4:** A simple schematic showing chemical steps of speleothem formation. Adapted from Fairchild et al. (2006).

are then carried by seepage waters into the cave, where  $\text{CO}_2$  is degassed to form the  $\text{CaCO}_3$  once again, this time as stalagmites, stalactites and flowstones.

As the formation of cave deposits is initiated by rain or snowfall, and is continued with the processes in the soil, various characteristics of stalagmites are sensitive to climatic variations. For example, a long pause in stalagmite growth can imply extremely arid conditions, or permafrost. In order to know how fast the stalagmite grew or when the growth ceased,

the sample must be dated. Likewise, a distinct change in the oxygen isotopic composition of the speleothem calcite, which can be inferred from stable isotope analysis, may be the indication of a change in the isotopic composition of the rainfall source (i.e. sea or ocean). Methods will be briefly presented in the next section.

### 1.4 Methods

Obtaining past climatic (and environmental) information from stalagmites proceeds on two main courses. The first one is dating, results of which can be used as independent proxies,

as mentioned earlier. The second includes all analyses other than dating, aiming to obtain any kind of environmental signal hidden in the cave deposit. Particular methods used in this work are outlined below.

### 1.4.1 <sup>230</sup>Th Dating

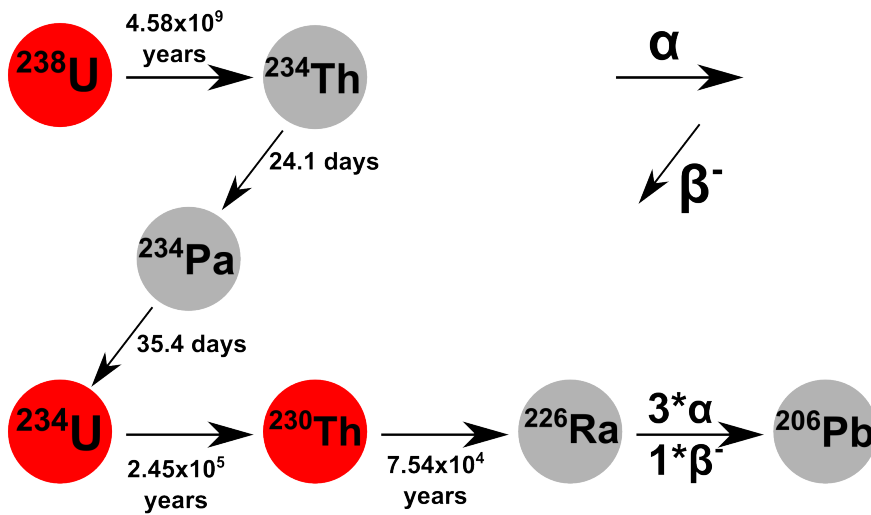


**Fig. 1.5:** <sup>238</sup>U decay chain. Measured isotopes during the <sup>230</sup>Th dating procedure have red backgrounds. Horizontal arrows denote alpha decay, whereas diagonal arrows show beta decay. Half-lives of the decaying isotopes are indicated near each arrow, except for <sup>226</sup>Ra. Schematic was adapted from Fankhauser (2008).

Age determination of stalagmites used in this thesis was performed through <sup>230</sup>Th dating, which is also known as uranium-series or U-Th dating. This standard methodology for dating carbonate deposits is based on a fundamental difference between the physical properties of the two elements in the <sup>238</sup>U decay chain: Uranium is soluble in water, but Thorium is not. Therefore, a trace amount of natural Uranium is transported into the cave by seepage

waters and is incorporated in the stalagmite by the time it is deposited; while Thorium, under ideal conditions, is absent. This gives the opportunity to calculate how much time has elapsed since the calcite deposited, using the measured amounts of <sup>230</sup>Th, <sup>234</sup>U and <sup>238</sup>U, as the half-lives of these radioactive isotopes are known (Fig. 1.3). Detailed information on the method and its main problems can be found in specific dating literature or in textbooks (e.g. Cheng et al., 2000; Richards and Dorale, 2003), as well as in the upcoming chapters.

As by-products of this procedure, and depending on how many dates are obtained from the analyzed stalagmite, one can construct **growth rate** and **initial <sup>234</sup>U/<sup>238</sup>U ratio** time series, both of which can be standalone proxy records for past climate (Fairchild et al., 2006; Fairchild et al., 2009); as it will be demonstrated in Chapter 2.

### 1.4.2 Stable Isotope Analysis

As the stalagmite is composed of CaCO<sub>3</sub>, it is possible to measure its carbon and oxygen stable isotopic composition ( $\delta^{13}\text{C}$  and  $\delta^{18}\text{O}$ ) on the material removed from its main growth axis (Fig. 1.4). Before these elements are finally deposited as CaCO<sub>3</sub> in the cave, isotopic fractionation between their standard (<sup>12</sup>C and <sup>16</sup>O) and heavy stable (<sup>13</sup>C, <sup>17</sup>O, <sup>18</sup>O) isotopes occur in many processes which are sensitive to climatic and environmental factors, thus  $\delta^{13}\text{C}$  and  $\delta^{18}\text{O}$  can be proxies for various climatic parameters.  $\delta$  notation is used to express the per mil (parts per thousand) difference of the heavy to light isotope ratio of the sample relative to the standard (in our case, 'Vienna Pee Dee Belemnite'). That is,  $\delta^{13}\text{C}$  is the

difference of the  $^{13}\text{C}/^{12}\text{C}$  ratio in the sample from the  $^{13}\text{C}/^{12}\text{C}$  ratio in the standard, divided by the  $^{13}\text{C}/^{12}\text{C}$  ratio in the standard and multiplied by 1000. The same applies for  $\delta^{18}\text{O}$ , this time with  $^{18}\text{O}/^{16}\text{O}$  ratios.

$\delta^{13}\text{C}$  variations in stalagmites is governed by processes in the soil-bedrock-cave system, which are partly related to rainfall and temperature above the cave (Fairchild et al., 2006). On the other hand,  $\delta^{18}\text{O}$  is controlled by atmospheric temperature, isotopic composition of moisture source, evaporation, and the amount and seasonality of precipitation; all of which determine the oxygen isotopic composition of infiltrating water (McDermott, 2004; Lachniet, 2009). Therefore, it is no surprise that in the abstract of a detailed and careful study on a Scottish stalagmite, Baker et al. (2011) conclude that “neither  $\delta^{13}\text{C}$  nor  $\delta^{18}\text{O}$  can be interpreted as a simple paleoclimate proxy” at their site. This recent statement is a warning against the danger of careless and simplistic interpretations of these proxies, as they can be influenced by the many factors outlined above, some of which can operate in opposing directions at the same time (see chapters 2 and 4). For example, at a site where summer rainfall is more abundant during cooler years, cooling signal (a decline in  $\delta^{18}\text{O}$ ) can be easily blurred or even neutralized by summer precipitation, which has significantly higher  $\delta^{18}\text{O}$  than that of winter. At this point, a comparison of the recent section of the stalagmite record with nearby meteorological records is essential (Jex et al., 2011): an approach that is central to the aim of this PhD thesis as well.

Stable isotope analysis is done also on rainwater samples, in order to determine  $\delta\text{D}$  (deuterium) and  $\delta^{18}\text{O}$  values of atmospheric precipitation. This can help understand which of the climatic parameters mentioned in the above paragraph play roles in determining the isotopic composition of rainwater, which in turn becomes dripwater in the cave. In Chapter 2, this technique is demonstrated.

## 1.5 Outline of the Thesis

In **Chapter 2**, a stalagmite record covering the entire Holocene, from the Sofular Cave in northern Turkey where a year-round wet climate prevails (Fig. 1.2), is presented. This record does not only bring insights into the issues of early to mid-Holocene climatic trends in the Eastern Mediterranean region, but also proves that a multi-proxy approach can be crucial for the correct interpretation of stalagmite proxies.

In **Chapter 3**, a winter temperature record based on the  $\delta^{13}\text{C}$  profile of a stalagmite from the Kocain Cave in southern Turkey (Fig. 1.2) is presented. This record has the potential to be a key record for the Eastern Mediterranean for the last ~5700 years, as it has numerous interesting implications concerning the role of climate changes in shaping cultural history.

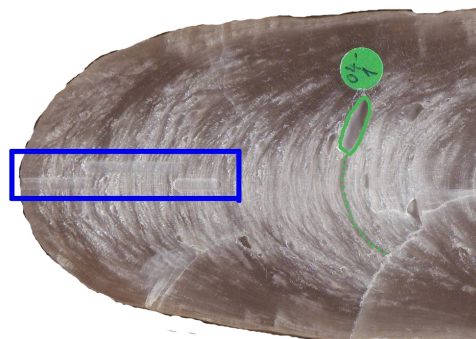


**Fig. 1.6:** Trenches opened on the polished inner surface of a stalagmite half. Material was removed for  $^{230}\text{Th}$  dating (green) and stable isotope (blue) analyses.

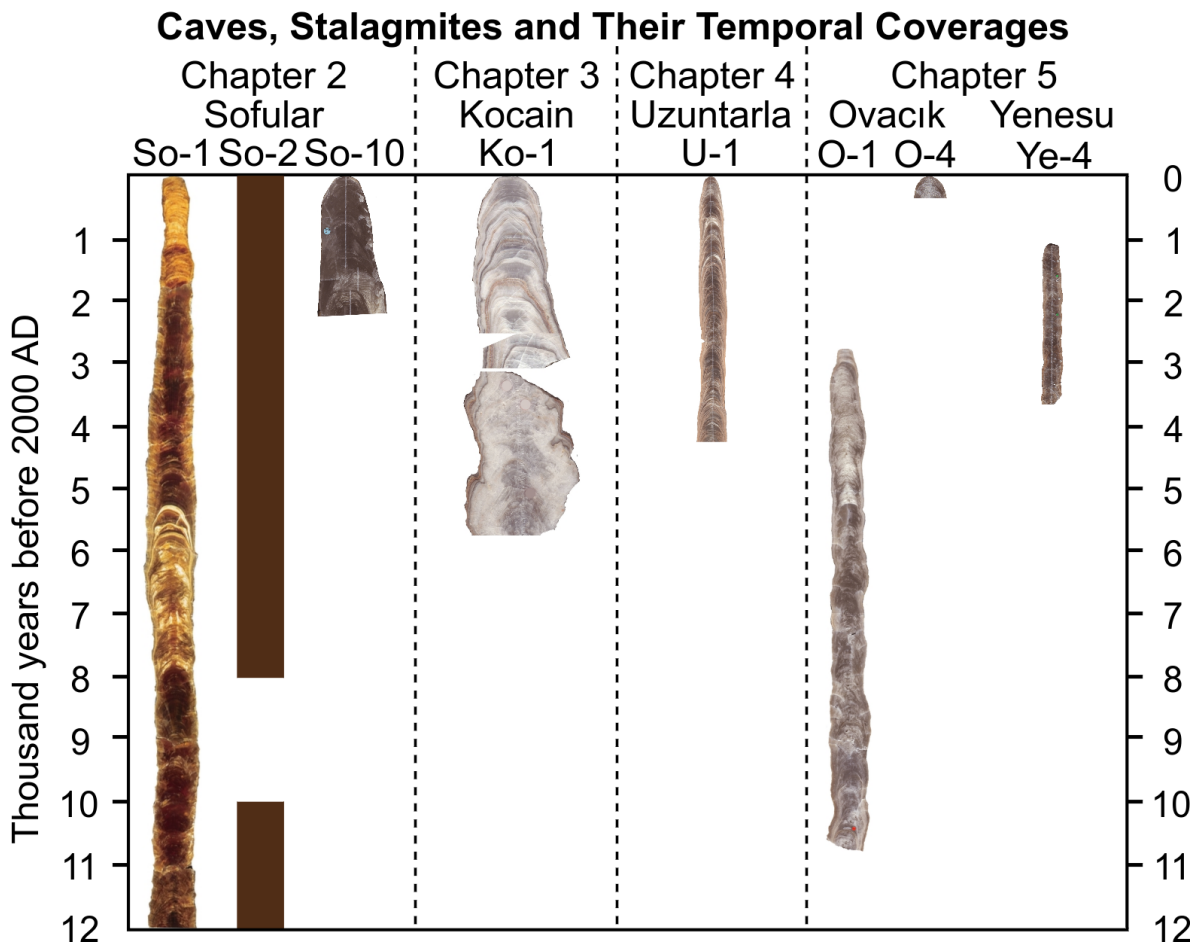


**Fig. 1.7:** Temporal coverage of the stalagmites analyzed in this work. Tips of each sample shows the start and end times of its stable isotope chronology. Note that intermediate parts of the stalagmites may not match with the corresponding points in the time scale, as growth rates often change.

In **Chapter 4**, presenting a stalagmite record from the Uzuntarla Cave in northwestern Turkey (Fig. 1.2), it will be demonstrated that both  $\delta^{13}\text{C}$  and  $\delta^{18}\text{O}$  can be influenced by more than one climatic factor, yet this can be exploited to infer useful paleoclimatic information with the aid of nearby records, i.e. the Kocain Cave record in Chapter 3.

In **Chapter 5**, preliminary results of currently inconclusive efforts on three stalagmites from Ovacık and Yenesu caves (Fig. 1.2) will be presented. It will be shown that non-recent stalagmites whose proxy time series cannot be compared with meteorological records are not very useful.

**Chapter 6** includes the summary and final conclusions.

## 1.6 References

- Akkemik, U., D'Arrigo, R., Cherubini, P., Köse, N., Jacoby, G.C., 2008. Tree-ring reconstructions of precipitation and streamflow for north-western Turkey. *Int J Climatol* 28, 173-183.
- Arz, H., Lamy, F., Patzold, J., Muller, P., Prins, M., 2003. Mediterranean moisture source for an early-Holocene humid period in the northern Red Sea. *Science* 300, 118-121.
- Baker, A., Wilson, R., Fairchild, I.J., Franke, J., Spötl, C., Matthey, D., Trouet, V., Fuller, L., 2011.



- High resolution  $\delta^{18}\text{O}$  and  $\delta^{13}\text{C}$  records from an annually laminated Scottish stalagmite and relationship with last millennium climate. *Global and Planetary Change*, doi:10.1016/j.gloplacha.2010.12.007.
- Barnston, A.G., Livezey, R.E., 1987. Classification, seasonality and persistence of low-frequency atmospheric circulation patterns. *Mon Weather Rev* 115, 1083-1126.
- Cheng, H., Edwards, R.L., Hoff, J., Gallup, C.D., Richards, D.A., Asmerom, Y., 2000. The half-lives of uranium-234 and thorium-230. *Chem Geol* 169, 17-33.
- Cullen, H.M., deMenocal, P.B., 2000. North Atlantic influence on Tigris-Euphrates streamflow. *Int J Climatol* 20, 853-863.
- Drews, R., 1993. *The End of the Bronze Age: Changes in Warfare and the Catastrophe ca. 1200 B.C.*, Princeton University Press, Princeton, NJ.
- Fairchild, I., Treble, P., 2009. Trace elements in speleothems as recorders of environmental change. *Quaternary Sci Rev* 28, 449-468.
- Fankhauser, A., 2008. Climate variability recorded in a 50,000-year old stalagmite from northern Turkey. Master thesis, Institute of Geological Sciences, University of Bern.
- Hodder, I., 1997. 'Always momentary, fluid and flexible': towards a reflexive excavation methodology. *Antiquity* 71, 691-700.
- Hughes, M.K., 2002. Dendrochronology in climatology: The state of the art. *Dendrochronologia* 20, 95-116.
- Hurrell, J.W., 1995. Decadal trends in the North-Atlantic Oscillation - regional temperatures and precipitation. *Science* 269, 676-679.
- Hurrell, J.W., VanLoon, H., 1997. Decadal variations in climate associated with the north Atlantic oscillation. *Climatic Change* 36, 301-326.
- Jex, C.N., Baker, A., Eden, J.M., Eastwood, W.J., Fairchild, I.J., Leng, M.J., Thomas, L., Sloane, H.J., 2011. A 500 yr speleothem-derived reconstruction of late autumn-winter precipitation, North East Turkey. *Quaternary Research*, In Press, doi:10.1016/j.yqres.2011.01.005.
- Krichak, S., Kishcha, P., Alpert, P., 2002. Decadal trends of main Eurasian oscillations and the Eastern Mediterranean precipitation. *Theor Appl Climatol* 72, 209-220.
- Kutiel, H., Benaroch, Y., 2002. North Sea-Caspian Pattern (NCP) - an upper level atmospheric teleconnection affecting the Eastern Mediterranean: Identification and definition. *Theor Appl Climatol* 71, 17-28.
- Kutiel, H., Maheras, P., Türkeş, M., Paz, S., 2002. North Sea Caspian Pattern (NCP) - an upper level atmospheric teleconnection affecting the eastern Mediterranean - implications on the regional climate. *Theor Appl Climatol* 72, 173-192.
- Kuzucuoğlu, C., Dörfler, W., Kunesch, S., Goupille, F., 2011. Mid- to late-Holocene climate change in central Turkey: The Tecer Lake record. *The Holocene* 21, 173-188.
- Lachniet, M., 2009. Climatic and environmental controls on speleothem oxygen-isotope values. *Quaternary Sci Rev* 28, 412-432.
- Lamy, F., Arz, H.W., Bond, G.C., Bahr, A., Patzold, J., 2006. Multicentennial-scale hydrological changes in the Black Sea and northern Red Sea during the Holocene and the Arctic/North Atlantic oscillation. *Paleoceanography* 21, PA1008.
- Mangini, A., Verdes, P., Spötl, C., Scholz, D., Vollweiler, N., Kromer, B., 2007. Persistent influence of the North Atlantic hydrography on central European winter temperature during the last 9000 years. *Geophys Res Lett* 34, L02704.
- Marino, G., Rohling, E., Sangiorgi, F., Hayes, A., Casford, J., Lotter, A., Kucera, M., Brinkhuis, H., 2009. Early and middle Holocene in the Aegean Sea: interplay between high and low latitude climate variability. *Quaternary Sci Rev* 28, 3246-3262.
- McDermott, F., 2004. Palaeo-climate reconstruction from stable isotope variations in speleothems: a review. *Quaternary Sci Rev* 23, 901-918.
- NCDC (National Climatic Data Center), 2008. Summary of 10,000 Year Scale. <http://www.ncdc.noaa.gov/paleo/ct/10k.html>, retrieved on 30.04.2011.
- Liu, Z., Harrison, S., Kutzbach, J., Otto-Bliesner, B., 2004. Global monsoons in the mid-Holocene and oceanic feedback. *Clim Dynam* 22, 157-182.

- Raichich, F., Pinardi, N., Navarra, A., 2003. Teleconnections between Indian monsoon and Sahel rainfall and the Mediterranean. *Int J Climatol* 23, 173-186.
- Richards, D.A., Dorale, J.A., 2003. Uranium-series chronology and environmental applications of speleothems. *Reviews in Mineralogy and Geochemistry* 52, 407-460.
- Roberts, N., Jones, M., Benkaddour, A., Eastwood, W., Filippi, M., Frogley, M., Lamb, H., Leng, M., Reed, J., Stein, M., Stevens, L., Valero-Garces, B., Zanchetta, G., 2008. Stable isotope records of Late Quaternary climate and hydrology from Mediterranean lakes: the ISOMED synthesis. *Quaternary Sci Rev* 27, 2426-2441.
- Svensson, A., Andersen, K.K., Bigler, M., Clausen, H.B., Dahl-Jensen, D., Davies, S.M., Johnsen, S.J., Muscheler, R., Parrenin, F., Rasmussen, S.O., Roethlisberger, R., Seierstad, I., Steffensen, J.P., Vinther, B.M., 2008. A 60 000 year Greenland stratigraphic ice core chronology. *Clim Past* 4, 47-57.
- Thomas White Global Investing, 2010. Argentina: record winter casts shadow on country's growth. <http://www.thomaswhite.com/explore-the-world/postcard/2010/argentina-cold-front-energy-crisis.aspx>, retrieved on 11.03.2011.
- Türkeş, M., 1996. Spatial and temporal analysis of annual rainfall variations in Turkey. *Int J Climatol* 16, 1057-1076.
- Türkeş, M., Erlat, E., 2003. Precipitation changes and variability in turkey linked to the North Atlantic oscillation during the period 1930-2000. *Int J Climatol* 23, 1771-1796.
- Türkeş, M., Erlat, E., 2009. Winter mean temperature variability in Turkey associated with the North Atlantic Oscillation. *Meteorol Atmos Phys* 105, 211-225.
- Tzedakis, P.C., 2007. Seven ambiguities in the Mediterranean palaeoenvironmental narrative. *Quaternary Sci Rev* 26, 2042-2066.
- Watson, I., 2008. Crisis looms as bitter cold, blackouts hit Tajikistan. <http://www.npr.org/templates/story/story.php?storyId=18784716>, retrieved on 11.03.2011.
- Ziv, B., Saaroni, H., Alpert, P., 2004. The factors governing the summer regime of the eastern Mediterranean. *Int J Climatol* 24, 1859-1871.





---

**CHAPTER 2****CLIMATE ON THE SOUTHERN BLACK SEA COAST  
DURING THE HOLOCENE:  
IMPLICATIONS FROM THE SOFULAR CAVE RECORD\***

O.M.Göktürk<sup>1,2</sup>, D.Fleitmann<sup>1,2</sup>, S.Badertscher<sup>1,2</sup>, H.Cheng<sup>3,4</sup>, R.L.Edwards<sup>4</sup>,  
M.Leuenberger<sup>5</sup>, A.Fankhauser<sup>1</sup>, O.Tüysüz<sup>6</sup>, J.Kramers<sup>1</sup>

1: Institute of Geological Sciences, University of Bern, Bern, Switzerland.

2: Oeschger Centre for Climate Change Research, University of Bern, Bern, Switzerland.

3: Institute of Global Environmental Change, Xi'an Jiaotong University,  
Xi'an, Shaanxi, China.

4: Department of Geology and Geophysics, University of Minnesota-Twin Cities,  
Minneapolis, Minnesota, USA.

5: Division of Climate and Environmental Physics, Institute of Physics,  
University of Bern, Bern, Switzerland.

6: Eurasia Institute of Earth Sciences, Istanbul Technical University, Istanbul, Turkey.

**2.1 Abstract**

We present the updated Holocene section of the Sofular Cave record from the southern Black Sea coast (northern Turkey); an area with considerably different present-day climate compared to that of the neighboring Eastern Mediterranean region. Stalagmite  $\delta^{13}\text{C}$ , growth rates and initial ( $^{234}\text{U}/^{238}\text{U}$ ) ratios provide information about hydrological changes above the cave; and prove to be more useful than  $\delta^{18}\text{O}$  for deciphering Holocene climatic variations. Between  $\sim 9.6$  and  $5.4$  ka BP (despite a pause from  $\sim 8.4$  to  $7.8$  ka BP), the Sofular record indicates a remarkable increase in rainfall amount and intensity, in line with other paleoclimate studies in the Eastern Mediterranean. During that period, enhanced summer-time insolation either produced much stronger storms in the following fall and winter through high sea surface temperatures, or it invoked a regional summer monsoon circulation and rainfall. We suggest that one or both of these climatic mechanisms led to a coupling of the Black Sea and the Mediterranean rainfall regimes at that time, which can explain the observed proxy signals. However, there are discrepancies among the Eastern Mediterranean records in terms of the timing of this wet period; implying that changes were probably not always occurring through the same mechanism. Nevertheless, the Sofular Cave record does provide hints and bring about new questions about the connection between regional and large scale climates, highlighting the need for a more extensive network of high quality paleoclimate records to better understand Holocene climate.

\* Accepted for publication in *Quaternary Science Reviews*

## 2.2 Introduction

Climatic variations on the longer, glacial/interglacial and millennial time scales are known to be very large in both amplitude and areal extent. In contrast, Holocene climatic fluctuations have been much smaller in amplitude and were often spatially incoherent (Wanner et al., 2008). Therefore, construction of regional climate records of either temperature or precipitation is now regarded as a key objective of current and future paleoclimate research (PAGES, 2009). Such records are crucial for our understanding of the nature of these regional, low-amplitude climate changes that took place during the Holocene. An area with insufficient spatial coverage of well-dated and highly resolved paleoclimate records is Turkey. To date, several records, most of which were derived from lake sediments (e.g., Roberts et al., 2008 and references therein), deliver information on Holocene climate variability in central and southern parts of the country (Fig. 2.1a), whereas no information exists for the entire Black Sea coast of Turkey. This area, however, has noticeably different climate characteristics compared to the rest of Turkey (Fig. 2.1b and 2.2; Türkeş, 1996), best expressed with its lack of summer aridity and much weaker relationship of winter precipitation variability with the North Atlantic Oscillation (Türkeş and Erlat, 2003). Thus, the question is as to whether the climate and the environment at the southern Black Sea coast have been coupled with larger-scale climate patterns in Turkey and the neighboring regions in the Eastern Mediterranean during the Holocene. To answer this fundamental question, we present a precisely dated and highly resolved stalagmite record from Sofular Cave at the Black Sea coast that covers the entire Holocene.

One of the outstanding issues concerning Holocene climate in the Eastern Mediterranean region is the changes in the amount and -possibly- the seasonality of rainfall before the mid-Holocene, especially during the sapropel deposition period between ~ 9-6 ka BP (Rohling et al., 2009a). While a marked moisture increase in the Eastern Mediterranean during the early to mid-Holocene is mostly agreed upon (Harrison et al., 1996; Bar-Matthews et al., 1997; Kallel et al., 1997; Rossignol-Strick, 1999; Arz et al., 2003; Roberts et al., 2008), the cause and mechanisms of this are still subject of controversial discussions. It has been suggested that summer rainfall, not a characteristic of the modern Mediterranean climate, must have been present during early to mid-Holocene in addition to the increased winter precipitation (Rohling, 1994; Rossignol-Strick, 1999). This hypothesis raised criticisms, most notably by Tzedakis (2007), who claimed, based on pollen evidence and the relationship between Indian Monsoon and Eastern Mediterranean summer regimes, that Mediterranean summers were even drier during this time.

Another problem is related to the duration, characterization and the degree of the impact of Holocene Rapid Climate Changes (RCCs) in the Eastern Mediterranean (Mayewski et al., 2004). Of those RCCs, the ones that occurred at 8.2 and 4.2 ka BP are the best documented (Rohling et al., 2009b and references therein), yet uncertainties exist as to how temperature and precipitation patterns were affected, and for how long. For instance, the 8.2 ka event appears to be superimposed on a longer term cooling extending from 8.6 to 8.0 ka BP (Rohling and Palike, 2005). There is also evidence for the influence of other RCCs at around 6.0 – 5.2 and 3.1 – 2.9 ka BP (Weninger et al., 2009); but again neither the spatial coherency of the events nor any particular climatic mechanism that led to the observed proxy signals has been agreed upon.

In this paper, we update and present the Holocene section of the Sofular Cave stalagmite record from the Black Sea coast of northern Turkey (Fleitmann et al. 2009), to improve the understanding of the problems outlined above. Almost bordering the Mediterranean yet having noticeably different climate characteristics (Fig. 2.1), the southern Black Sea area provides a unique opportunity to study the impact and geographical extent of Holocene climate changes in the Eastern Mediterranean. Fleitmann et al. (2009) have shown that first-order climatic shifts such as Greenland interstadials, Bølling-Allerød and Younger Dryas are clearly and accurately reflected in the Sofular record. Therefore, the question remains as to whether the climate and the environment around Sofular Cave have been coupled with larger scale patterns, as well as with the neighboring regions also during the Holocene, and if so, what were the mechanisms behind this coupling. Detailed analysis of the Sofular record and its relationship with other paleoclimate records will help answer these questions.

### 2.3 Sofular Cave: Climatic and Environmental Setting

Sofular Cave (41°25'N, 31°57'E; 440 meters asl), is located very close to the Black Sea, on the northern foothills of the Akçakoca Mountain range, a part of the North Anatolian mountain chain in Turkey. (Fig. 2.1). The cave is situated within the Lower Cretaceous unit, close to a marl-limestone contact, and the vegetation above consists of trees and shrubs. The modern climate in this area exhibits a significantly different rainfall regime compared to the neighboring regions in the Eastern Mediterranean, despite similar large scale influences from the North Atlantic, Eurasia and Monsoon realms. According to the

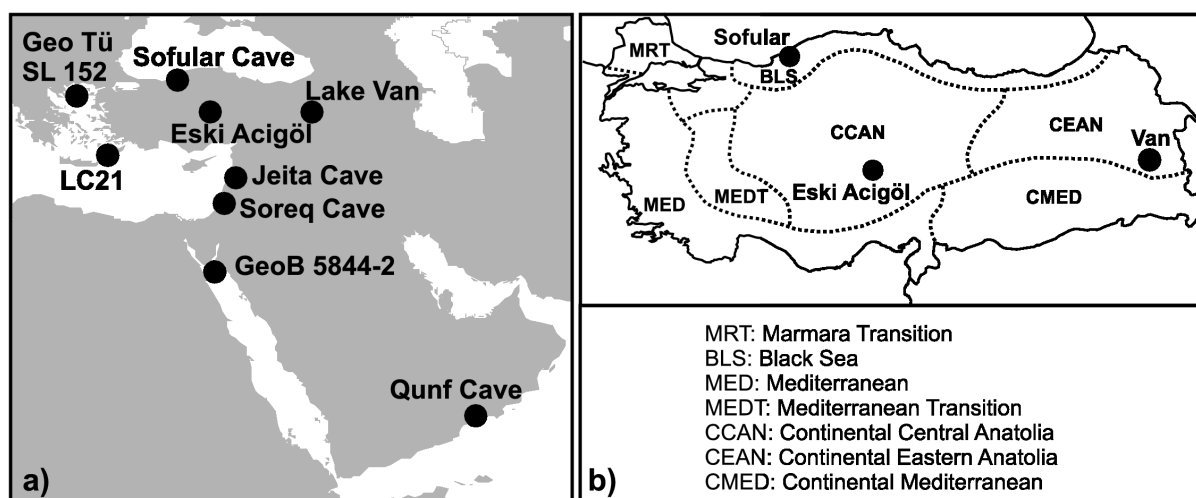


**Fig. 2.1: Location map.** a) Geographical locations of paleoclimate records plotted in Fig. 2.9 and 2.10.  
b) Climate zones in Turkey defined mainly by seasonality of rainfall (Türkeş, 1996).

updated Köppen-Geiger climate classification, a warm temperate, fully humid maritime climate is observed in the closest meteorological station of Zonguldak (Kottek et al., 2006), with a mean annual temperature of 13.3°C and precipitation of around 1200 mm (Fig. 2.2, red dots). Even though the majority of this precipitation falls in autumn and winter, rainfall in summer can be quite high, with single events reaching up to 150 mm. This leads to year-round moist conditions (Fig. 2.2a). The dominance of northerly winds blowing from the Black Sea help maintain high humidity levels (Trewartha, 1966; Fleitmann et al.,

2009). Therefore, moist summers sustain dense vegetation, prevent wildfires and constitute the main difference from the typical summer-dry Mediterranean climate, as well as from the continental climate of the Anatolian steppe. (Fig. 2.2a) Consequently, annual precipitation at the meteorological station of Zonguldak has never been below 800 mm in the last 80 years, indicating that this area is not prone to droughts. This distinct character of rainfall in the Black Sea region of Turkey (Türkeş, 1996) and its very weak relationship with the modern North Atlantic Oscillation (Türkeş and Erlat, 2003) were previously pointed out. Correlations of seasonal precipitation amounts in Zonguldak with those of other stations in Turkey are often low, if not statistically insignificant (Fig. 2.2, lower panel).

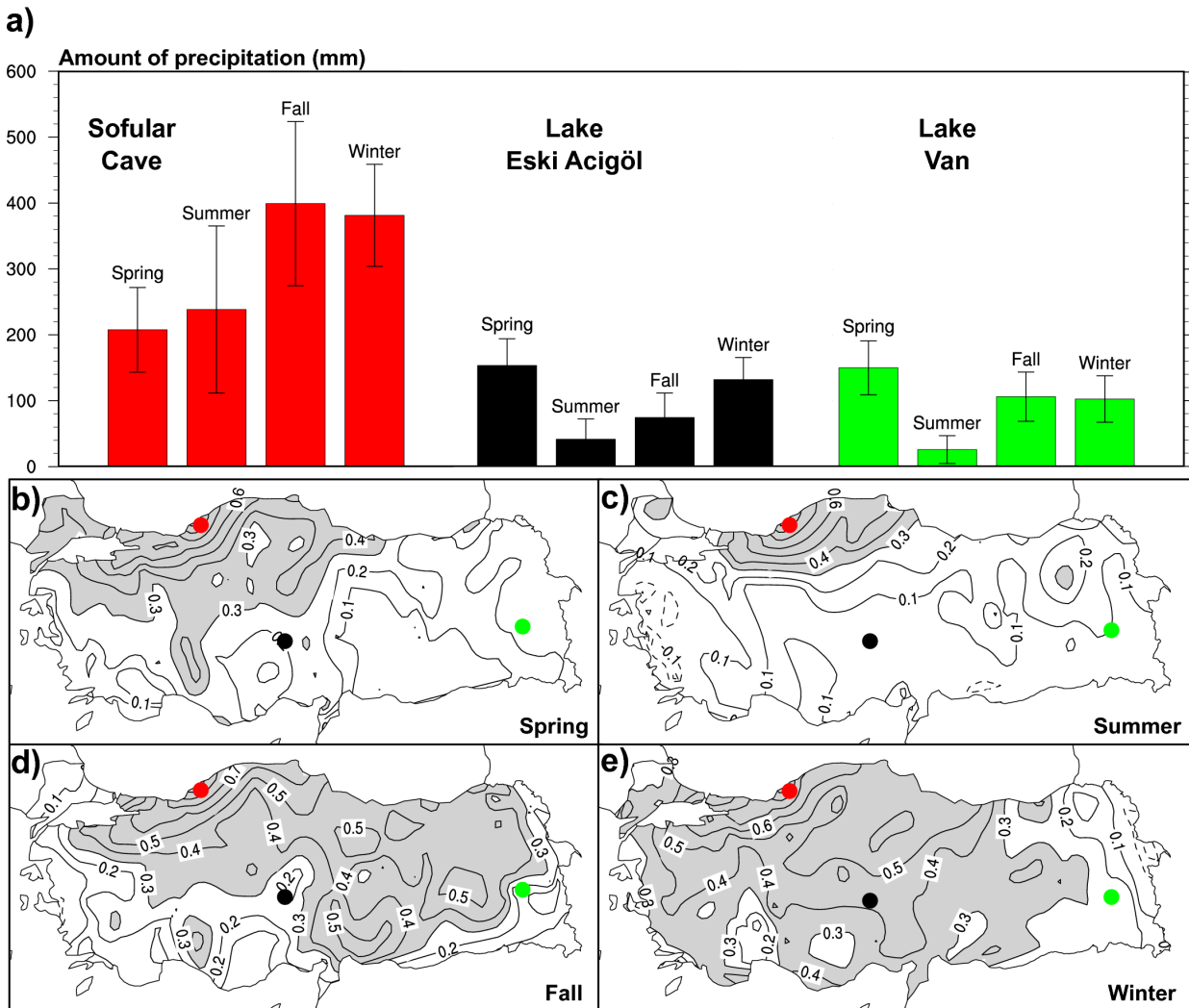


**Fig. 2.2.: Climate characteristics at and around Sofular Cave.** a) Seasonal precipitation amounts at sites Sofular Cave, Lake Eski Acıgöl and Lake Van. Also shown over each seasonal precipitation value is its standard deviation. b, c, d, e) Correlation coefficients of Sofular's seasonal precipitation time series with those of the other meteorological stations in Turkey for spring (MAM), summer (JJA), fall (SON) and winter (DJF). Gray shaded areas mark the statistically significant (95% according to Student's t-test) correlations. Full contours represent positive correlations, whereas the dotted contours denote negative correlations. Locations of Sofular Cave, Lake Eski Acıgöl and Lake Van are marked by dots with the relevant colors. Station data were obtained from the State Meteorological Service of Turkey and previously quality controlled by Göktürk et al. (2008). The closest meteorological stations to Sofular Cave, Lake Eski Acıgöl and Lake Van are Zonguldak, Nevşehir and Van (respectively).



Even in winter, when higher correlations are observed compared to other seasons (Fig. 2.2e), precipitation pattern can be different in the Black Sea climate zone (Fig. 2.1b). An extreme case is the Mount Pinatubo winter of 1991-92. Over that interval, while western Anatolia had its coldest and driest winter between 1940 and 2005 due to a lack of Mediterranean cyclones, precipitation was close to average in Sofular area, and above average in the eastern parts of the coastal Black Sea region in Turkey. Explaining this peculiarity, Fleitmann et al. (2009) show that the present-day winter precipitation over this region is enhanced by a negative temperature anomaly and demonstrate also that the moisture source has predominantly been the Black Sea, at least for the last 50 ka. In other words, interaction between Black Sea surface waters and relatively cooler air masses from north generates a substantial amount of precipitation in the Sofular area, in addition to precipitation associated with the cyclonic activity over the entire Eastern Mediterranean region (Bozkurt and Sen, 2009). This process is analogous to the formation of 'lake-effect' precipitation downwind of the Great Lakes in North America, further enhanced in the southern Black Sea coast due to strong orographic effects (Türkeş et al, 2003).

## 2.4 Material and Methods

Stalagmite So-1, sampled in the Sofular Cave in August 2005, provides time series of carbon and oxygen stable isotopes ( $\delta^{13}\text{C}$  and  $\delta^{18}\text{O}$ ) that cover the last 50 ka (Fleitmann et al., 2009). In this paper, our focus is on the Holocene section of the So-1 record, which we have recently improved with nine additional  $^{230}\text{Th}$  dates (Appendix A). Two other stalagmites from Sofular Cave, So-2 and So-10, were also analyzed in order to support our master So-1 record.  $^{230}\text{Th}$  dating was performed on multi-collector inductively coupled plasma mass spectrometers at the Minnesota Isotope Laboratory, University of Minnesota, USA (MC-ICP-MS, Thermo-Finnigan-Neptune); and at the Institute of Geological Sciences, University of Bern, Switzerland (Nu Instruments MC-ICP-MS). Stable isotope measurements were performed at the Institute of Geological Sciences, University of Bern, Switzerland; on a Finnigan Delta V Advantage mass spectrometer equipped with an automated carbonate preparation system (Gas Bench-II). Further details on  $^{230}\text{Th}$  dating method and the stable isotope analyses are provided by Fleitmann et al. (2009).

## 2.5 Results and Proxy Quality

### 2.5.1 Chronology

Depth-age models for all stalagmites are given in Fig. 2.3. The age model of the Holocene So-1 record is based on forty one  $^{230}\text{Th}$  dates with chronological uncertainties ranging between 0.29% and 7.46% around an average of 1.29%. Holocene chronologies of So-2 and So-10 records are based on four  $^{230}\text{Th}$  dates for each stalagmite (Appendix A). Almost all  $^{230}\text{Th}$  dates are in stratigraphic order (Fig. 2.3).

### 2.5.2 Stable Isotope Profiles

The So-1 stable isotope profile has a very high 5.4 years of average temporal resolution, covering the entire Holocene. The So-2 record encompasses most of the Holocene, but has a lower temporal resolution (~ 50 years) than the So-1 and has a growing hiatus from 8 to 10

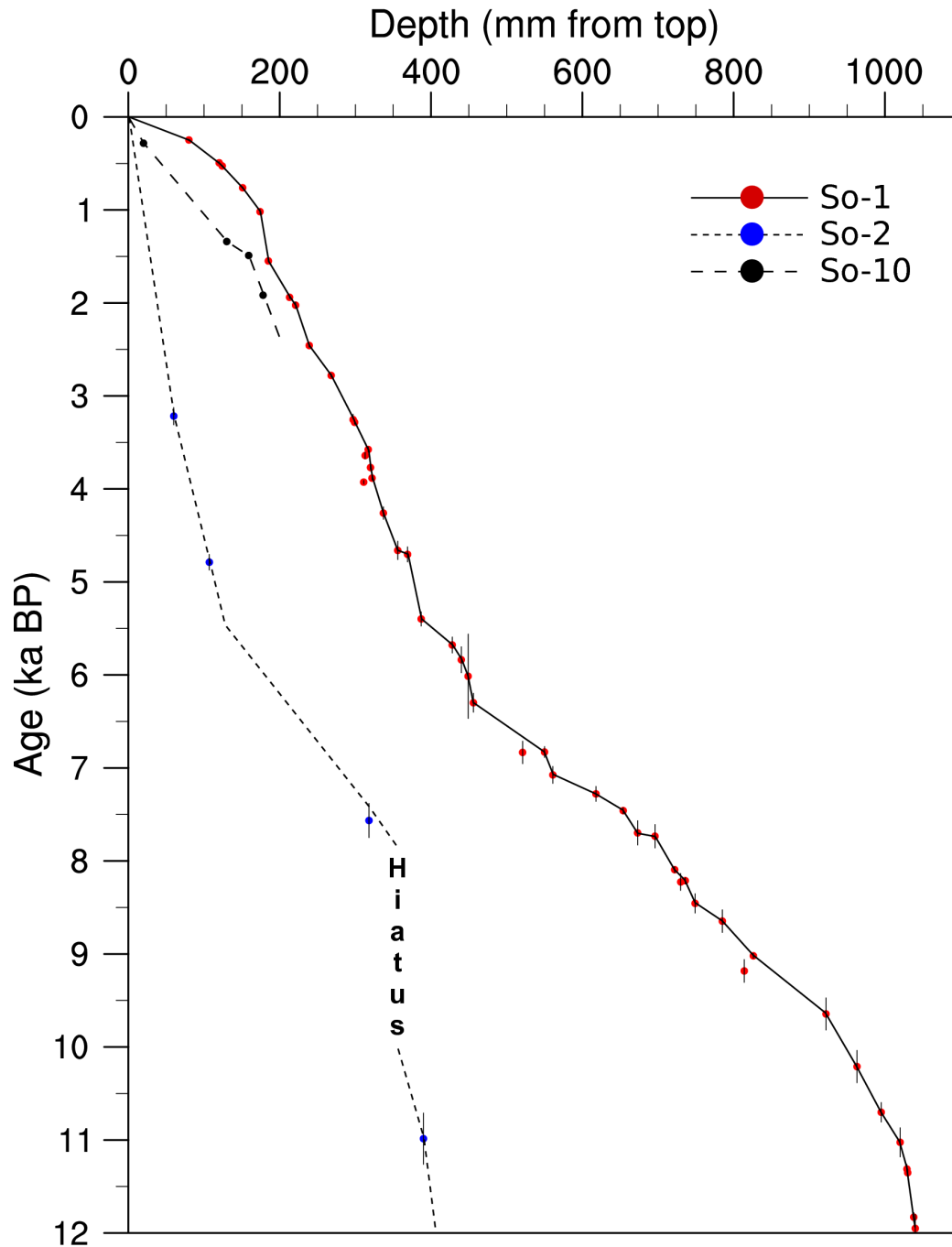


**Fig. 2.3: Stalagmite age models.** Holocene age models of the stalagmites So-1, So-2 and So-10; on an age-depth scale. Colored dots are the  $^{230}\text{Th}$  dates with their uncertainties shown as bars over each of them. Linear interpolation was performed to construct the age models between consecutive  $^{230}\text{Th}$  dates. 'BP' refers to before present (1950).

ka BP; while the So-10 record spans the last ~ 2200 years with 5 year resolution.

### 2.5.2.1 $\delta^{13}\text{C}$

Except for the higher values up to  $-8.7\text{‰}$  (VPDB) in the last 500 years of the record, the Holocene  $\delta^{13}\text{C}$  values in stalagmite So-1 varies between  $\sim -11.5$  and  $-9.5\text{‰}$  (Fig. 2.7a),

indicating the domination of C3 vegetation above the cave. There is no persistent long term trend. In Fig. 2.4, a comparison of our main record, So-1, with the supplementary records So-2 and So-10 is presented. Taking the expected mismatch arising from the less robust age models of So-2 and So-10 (Fig. 2.3) into account, these two supplementary records agree reasonably well with So-1 throughout the Holocene. Moreover, the pre-Holocene section of So-1 was used previously and was shown to accurately reflect climatic and environmental changes (Fleitmann et al., 2009). Therefore, we use the stalagmite So-1 record in the reconstruction of Holocene conditions as well, and simply refer to it as the Sofular record.

Variations in  $\delta^{13}\text{C}$  in stalagmites are often related to changes in vegetation and soil microbial activity above the cave, which in turn, are controlled by temperature and precipitation as long as open system conditions prevail (McDermott, 2004). Higher temperatures and rainfall lead to lower  $\delta^{13}\text{C}$  calcite values (McDermott, 2004; Fairchild et al., 2006), as demonstrated in several earlier works done in temperate regions (Hellstrom et al., 1998; Genty et al., 2003; Genty et al., 2006).  $\text{CO}_2$  degassing of cave drip water can be an additional factor influencing  $\delta^{13}\text{C}$  in calcite, whereas the rate of  $\text{CO}_2$  degassing can be related to the drip rate (Baker et al., 1997) and cave air  $\text{PCO}_2$  (Spötl et al. 2005). Lower drip rates, indicative of drier climate conditions, lead to enhanced degassing of  $\text{CO}_2$  and to higher calcite  $\delta^{13}\text{C}$  values. Anthropogenic land cover change can also be traced in stalagmite  $\delta^{13}\text{C}$ , since disturbed or destroyed vegetation will also lead to higher  $\delta^{13}\text{C}$  (Baldini et al., 2005). Overall, interpretation of  $\delta^{13}\text{C}$  values is not straightforward given the contrasting effects of the soil-bedrock-cave system that can arise under certain conditions. For instance, although an increase in rainfall is usually expected to result in lower  $\delta^{13}\text{C}$  for stalagmites from temperate regions (Fairchild et al., 2006), torrential rain events can lead to higher  $\delta^{13}\text{C}$  (Bar-Matthews et al., 1999) due to shorter residence times

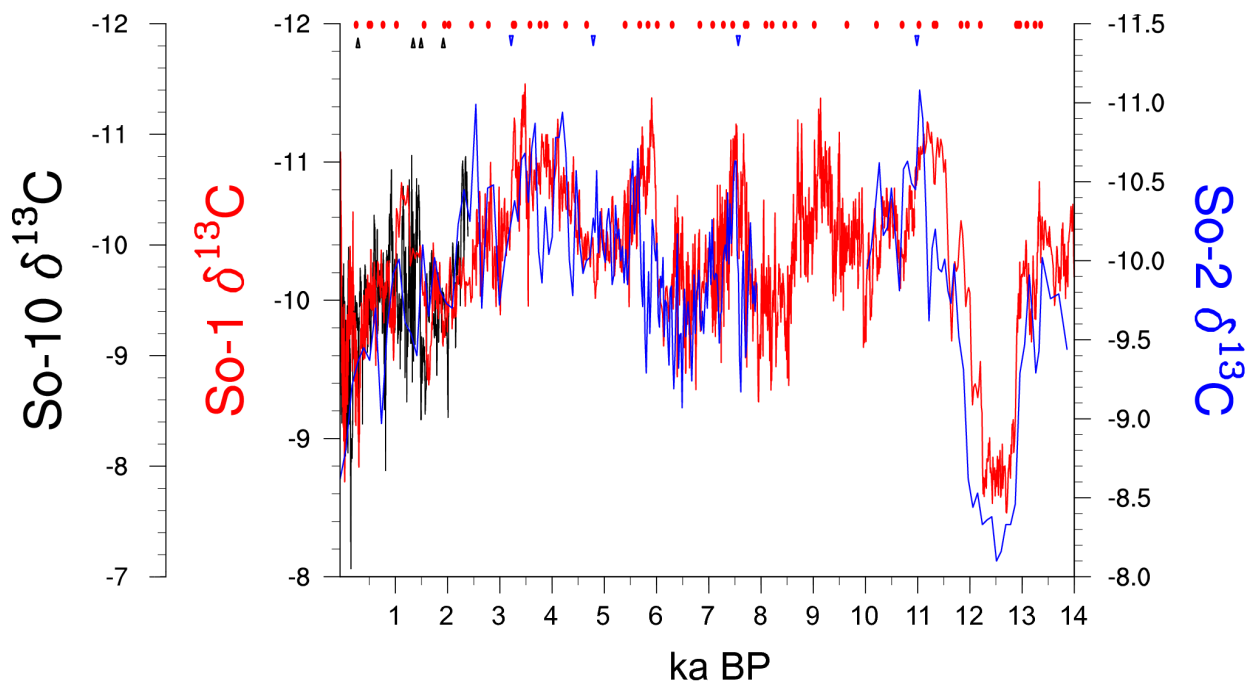


**Fig. 2.4: Isotope profile comparison of Sofular stalagmites.** Holocene  $\delta^{13}\text{C}$  profiles of the Sofular cave stalagmites So-1, So-2 and So-10. All axes are descending.  $^{230}\text{Th}$  age control points are marked with colored dots and triangles. 'BP' refers to before present (1950).

of water in the soil and to a lack of equilibration between soil water and soil CO<sub>2</sub> (Baker et al., 1997).

We interpret the Holocene Sofular  $\delta^{13}\text{C}$  record to reflect fluctuations in effective moisture, as modern day warm temperate climate prevailed around this region throughout the

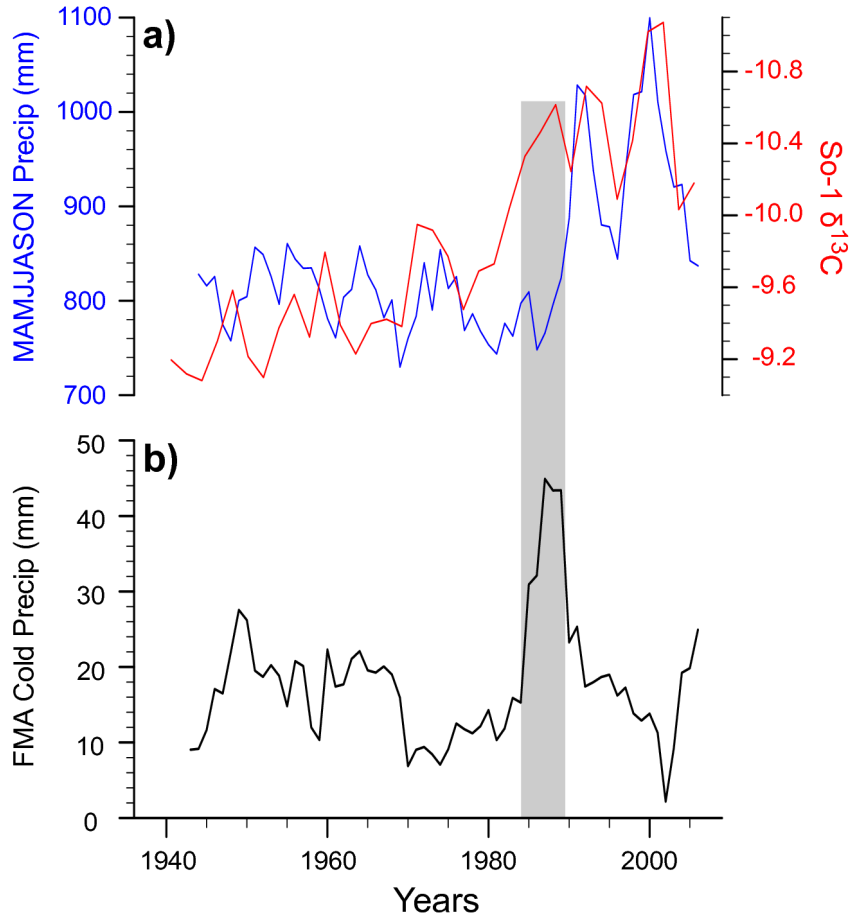


**Fig. 2.5:  $\delta^{13}\text{C}$  and present-day climate.** Relationship between meteorological observations and Sofular (stalagmite So-1)  $\delta^{13}\text{C}$  record. Climate data belong to the nearby meteorological station Zonguldak. **a)** March to November precipitation total (5-year running average) versus unsmoothed  $\delta^{13}\text{C}$  values (note descending axis). **b)** Sum of the precipitation values of those days in February, March and April, when the daily mean temperature is below 0°C; representing snowfall that stay on the ground. 5-year running average values are shown. Gray shade marks the cold and snowy late 1980s.

period (Rossignol-Strick, 1999; Kotthoff et al., 2008), consistently creating favorable conditions for vegetation activity, and significantly reducing the effects of temperature variations. In their pollen-based temperature reconstruction, Davis et al. (2003) estimated the fluctuation range of area-averaged winter temperatures as  $\sim 2^\circ\text{C}$  for southeast Europe, while the same parameter was found to be greater than  $10^\circ\text{C}$  for the coldest month during the last glacial period in Italy (Allen et al., 1999). Furthermore, the similarity of  $\delta^{13}\text{C}$  fluctuations in Sofular Cave stalagmites (Fig. 2.4) suggests that cave- and sample-specific effects are rather small and  $\delta^{13}\text{C}$  can be used as a climate proxy.

To further support the interpretation of the Sofular  $\delta^{13}\text{C}$  record as effective moisture, we made several comparisons of the most recent part of the Sofular  $\delta^{13}\text{C}$  record (stalagmite

So-1) with various parameters derived from the meteorological records of the nearby station, Zonguldak. Fig. 2.5a shows that the best match with the  $\delta^{13}\text{C}$  record is achieved by using the combined spring, summer and fall precipitation amount (accounting -on average- for 70% of total annual rainfall). The apparent mismatch in the late 1980s may be explained by the exceptionally cold and snowy late winter-early spring conditions at that time (Fig. 2.5b). This might have caused the snow cover to remain until the growing season and to operate as an additional source of effective moisture for the vegetation, as snow infiltrates more efficiently than rain does (Earman et al., 2006; Jemcov and Petric, 2009), thus lowering the  $\delta^{13}\text{C}$  values. A visible correspondence of  $\delta^{13}\text{C}$  with annual temperature or annual water excess could not be identified (Fig. 2.S1).

Our observation that more negative values of  $\delta^{13}\text{C}$  correlate better with the spring-summer-fall precipitation amount than they do with annual water excess, has an important implication. That is, *effective* precipitation above the Sofular Cave is the precipitation which falls when the vegetation and soil microbial activity is high, reflecting the influx of biogenic  $\text{CO}_2$  in the growing season (Baker et al., 1997). Moreover, moisture loss during warm season due to evapotranspiration is rather small. Considering the high atmospheric humidity throughout the year, this can be expected. It should also be noted

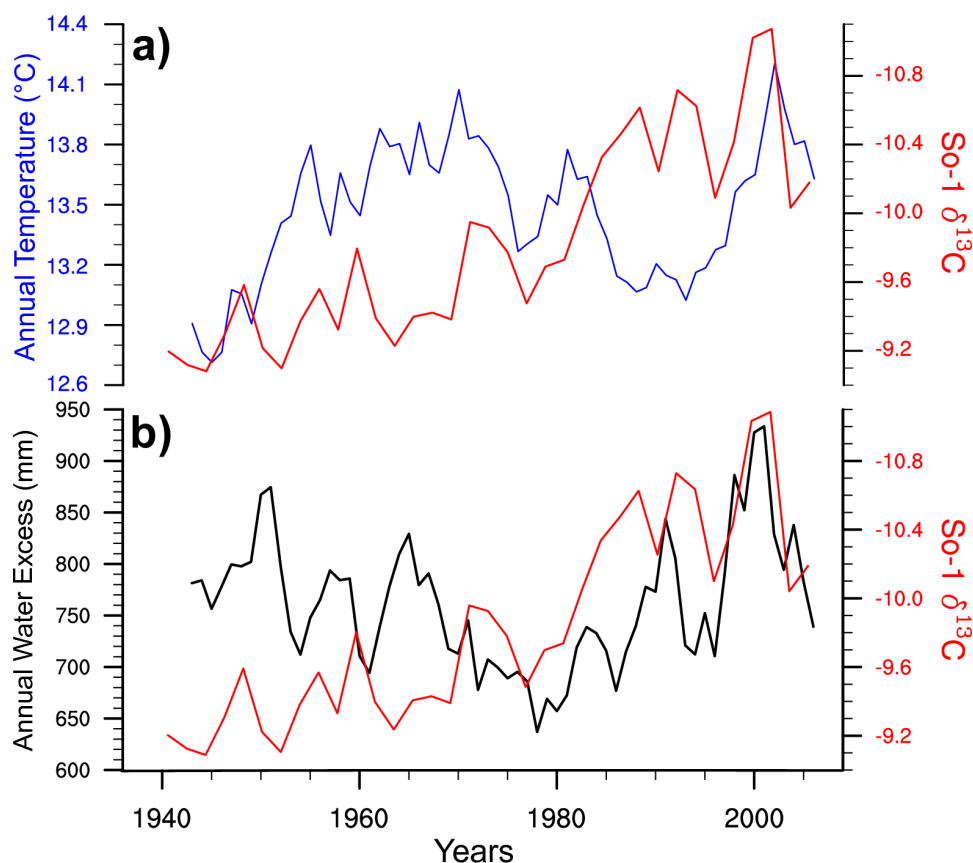


**Fig. 2.S1:  $\delta^{13}\text{C}$  and present-day climate (as a supplement to Fig. 2.5).** Relationship between meteorological observations and Sofular (stalagmite So-1)  $\delta^{13}\text{C}$  record. Climate data belong to the nearby meteorological station Zonguldak. **a)** Annual temperature (5-year running average) versus unsmoothed  $\delta^{13}\text{C}$  values (note descending axis). **b)** Annual water excess (5-year running average, calculated after Thornthwaite (1948)) versus unsmoothed  $\delta^{13}\text{C}$  values (note descending axis).

that the temporal resolution for the most recent part of the Sofular record is 2.5 years and there is no precise (i.e. annual) age control, therefore a perfect overlap of meteorological indicators and the isotope profile cannot be expected.

### 2.5.2.2 $\delta^{18}\text{O}$

The Sofular  $\delta^{18}\text{O}$  profile shows values of around -12.0‰ at the beginning of the Holocene and up to -7.4‰ in the most recent part of the record, with a very clear upward trend that stabilizes at ~ 6.0 ka BP (Fig. 2.7d). The Sofular  $\delta^{18}\text{O}$  record cannot be interpreted in a straightforward manner in terms of climate, since  $\delta^{18}\text{O}$  can be influenced by a number of variables including temperature, seasonality and amount of precipitation, storm tracks and the isotopic composition of rainfall source (McDermott, 2004; Fleitmann et al., 2009; Lachniet, 2009). As seasonality of precipitation is highly variable (Fig. 2.2, upper panel) and intense rainfall events are common in the Sofular area (Bozkurt and Sen, 2009), it is not clear to what extent our  $\delta^{18}\text{O}$  record was affected by each of these factors during the Holocene. Isotope measurements of rainwater samples collected over one year (2008-2009) close to Sofular Cave also reveal that it is not trivial to link  $\delta^{18}\text{O}$  variations to specific meteorological variables. Fig. 2.6 shows the relationship between the oxygen isotopic composition of rainwater and temperature, as well as the precipitation amount. Although the rainwater  $\delta^{18}\text{O}$  values seem primarily to follow seasonal temperature variations ( $r = 0.66$ ; “temperature effect”), intense rainfall events in summer and fall have a clear

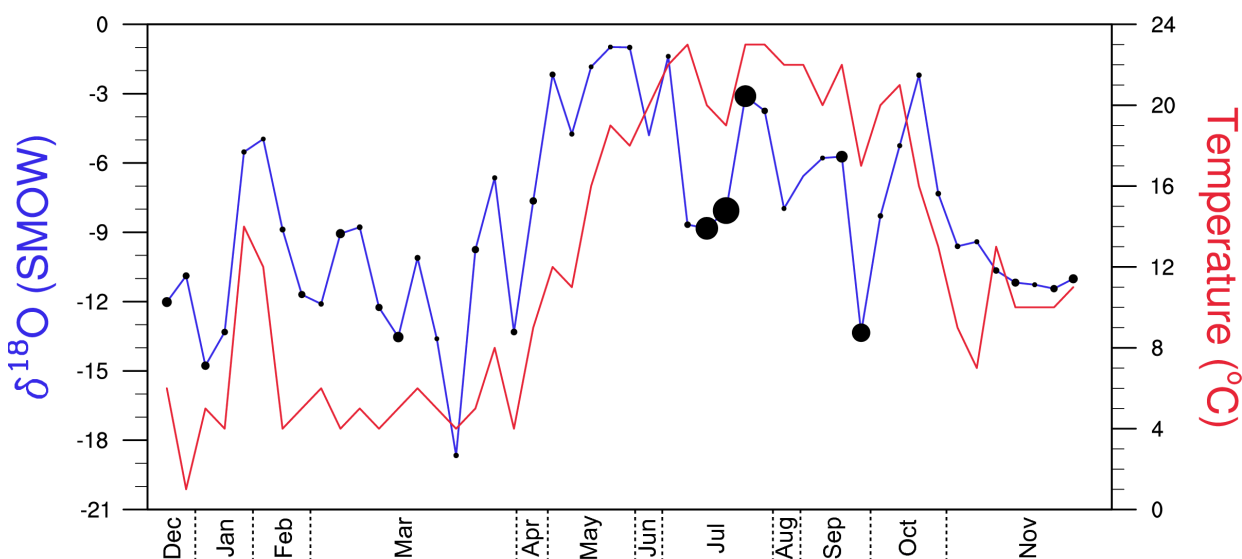


**Fig. 2.6: Rainwater  $\delta^{18}\text{O}$  and climate.** Comparison between the  $\delta^{18}\text{O}$  values of the rainwater samples (blue curve) collected from December 2008 to November 2009, and the air temperature at the time of sampling (red curve). Each black dot represents one daily sample and its size is proportionate to the amount of rainfall on that day. The biggest dot (on July 15<sup>th</sup>) is equivalent to a daily rainfall total of 109 mm. Meteorological data belong to the station Bartın and were obtained from the State Meteorological Service of Turkey.

signature of the amount effect, that blur the correlation of  $\delta^{18}\text{O}$  with seasonality due to their disproportionate contribution to groundwater recharge. Nevertheless, on long time scales, the Sofular  $\delta^{18}\text{O}$  record reflects the isotopic composition of its main moisture source, the Black Sea (Fleitmann et al., 2009; Badertscher et al., 2011). This is revealed by the close match between Sofular  $\delta^{18}\text{O}$  and a marine  $\delta^{18}\text{O}$  record (core GeoB7608-1, Bahr et al., 2006) from the western Black Sea, between ~ 25 and 8 ka BP (Fig. 2.8a), especially at ~ 16

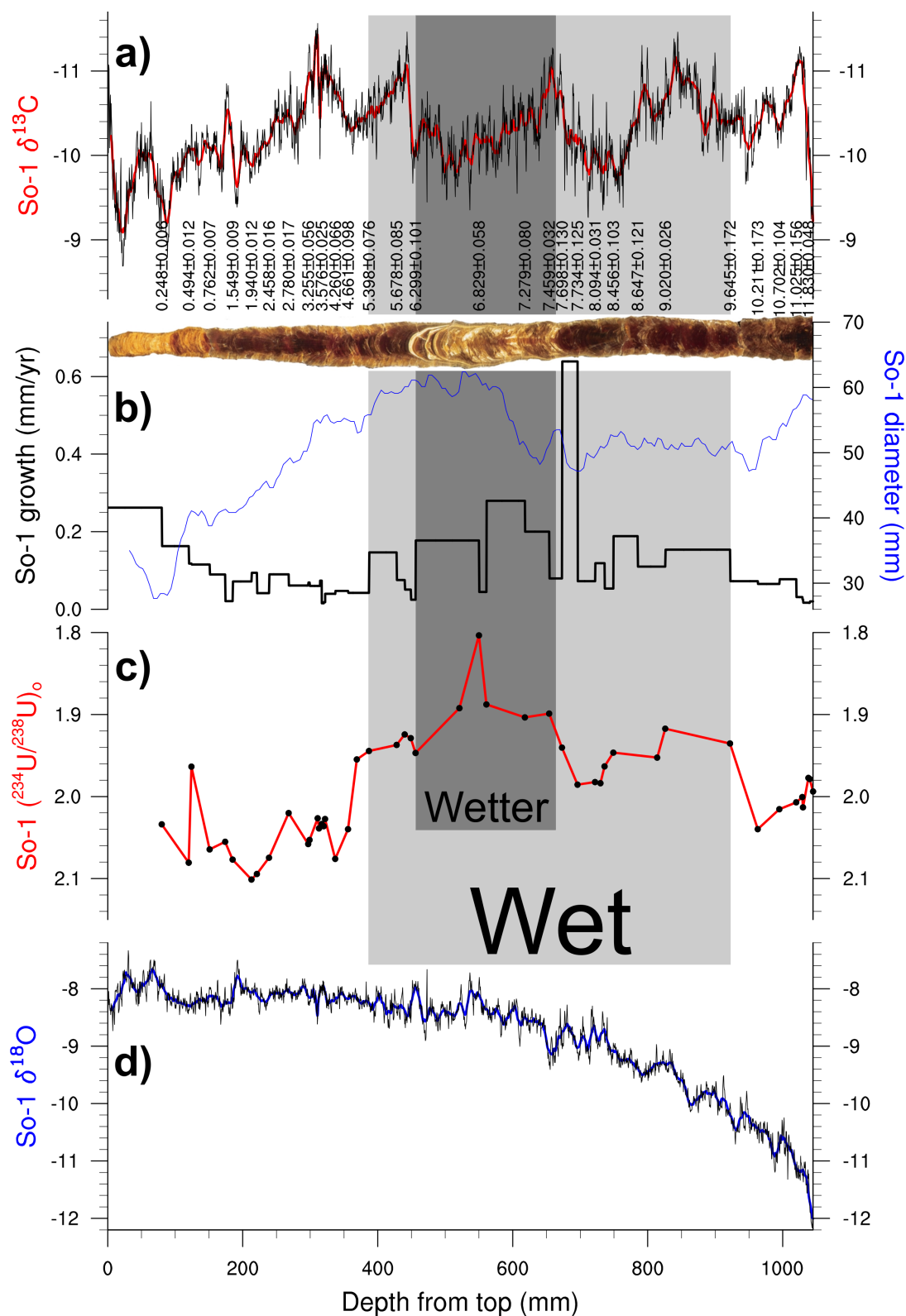


**Fig. 2.7: All Sofular proxies.** Parameters of the Sofular Cave stalagmite So-1's Holocene record on a depth scale. An image of the stalagmite is also shown, along with 28 of the  $^{230}\text{Th}$  dates (ka BP) and their associated uncertainties. To avoid overlapping, not all  $^{230}\text{Th}$  dates are shown. **a)**  $\delta^{13}\text{C}$  (VPDB) record. Black curve: raw data. Red curve: 19-point running average. Note descending axis. **b)** Growth rate (mm/yr) and diameter (mm). **c)** Initial  $^{234}\text{U}/^{238}\text{U}$  ratio, calculated by the method described by Kaufman et al. (1998). Note descending axis. **d)**  $\delta^{18}\text{O}$  (VPDB) record. Black curve: raw data. Blue curve: 19-point running average.

ka BP when the Black Sea was flooded by glacial meltwater from the north (Fleitmann et al., 2009; Badertscher et al., 2011).

For the entire 50 ka-long record of stalagmite So-1, there is a high and negative correlation ( $r = -0.76$ ) between  $\delta^{18}\text{O}$  and  $\delta^{13}\text{C}$ . This owes to the high amplitude glacial – interglacial shifts in climate and environment (Fleitmann et al., 2009), making  $\delta^{18}\text{O}$  more positive and  $\delta^{13}\text{C}$  more negative (and vice versa) at the same time. During the Holocene however, the correlation is positive but quite low ( $r = 0.23$ ). This is another indication that the subtle changes in the Holocene lead to lower amplitude variations in  $\delta^{18}\text{O}$  and  $\delta^{13}\text{C}$ , complicating their relationship. For instance, when  $\delta^{13}\text{C}$  is more negative in the Holocene, it is a sign of increased spring-summer-fall precipitation (Section 2.5.2.1). On the other hand, this creates contrasting effects on  $\delta^{18}\text{O}$ , since warm season rainfall tends to be enriched in the Sofular site, whereas intense rainfall during summer and fall can be quite depleted (Fig. 2.6). Even if the climatic factors determining  $\delta^{18}\text{O}$  variations could be disentangled, the fact that the oxygen isotopic composition of the Black Sea is currently not known after 8 ka BP (Fig. 2.8a) would still hamper the interpretation of this proxy.

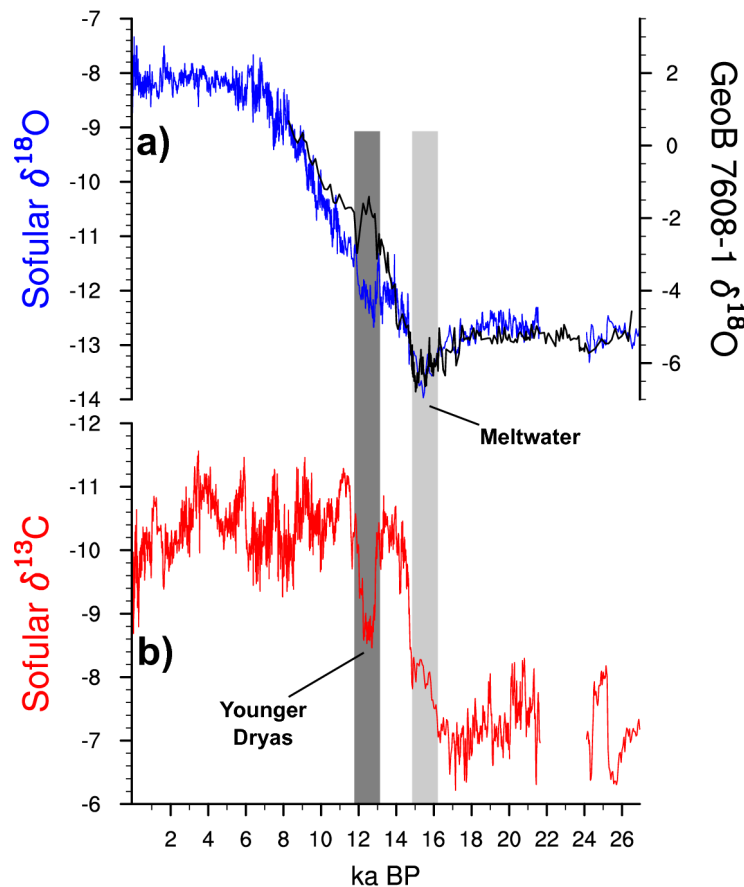


**Fig. 2.8: Sofular isotopes since approximately the Last Glacial Maximum.** a) Sofular  $\delta^{18}\text{O}$  (VPDB) record (blue) versus the  $\delta^{18}\text{O}$  record (VPDB) from the western Black Sea (core GeoB7608-1, Bahr et al., 2006). b) Sofular  $\delta^{13}\text{C}$  (VPDB). Time of glacial meltwater intrusion and the Younger Dryas are marked. 'BP' refers to before present (1950).

Therefore, at this stage, it would be premature to comment on the Holocene  $\delta^{18}\text{O}$  variations, which are much smaller compared to those during the glacial and glacial-interglacial shifts (Fleitmann et al. 2009; Badertscher et al., 2011). Future studies from



the same area, as well as a cave monitoring program will probably improve the climatic interpretation of  $\delta^{18}\text{O}$  profile in the Holocene section of the Sofular record.

### 2.5.3 Growth Rate and Diameter

The robust age model of the stalagmite So-1 (Fig. 2.3) allows us to construct a highly resolved time series of growth rates. Growth rates vary between  $\sim 0.030$  and  $0.639$  mm/year around an average of  $0.133$ , taking significantly higher values between  $\sim 9.6$  and  $5.4$  ka BP (Fig. 2.7b, gray shade). We also measured the diameter of the stalagmite So-1 on equally cut slabs. The diameter takes values between  $28$  and  $63$  mm, with a decreasing trend in the last  $5.5$  ka. The upward trend in the growth rates commencing at  $\sim 1.5$  ka BP is accompanied by the lowest diameters in the entire Holocene (Fig. 2.7b).

Growth rate and diameter (or, equilibrium diameter) in stalagmites can be used as proxies for climatic conditions (Kaufmann and Dreybrodt, 2004; Fairchild et al., 2006). Although variable Ca concentrations in drip water may blur the signal, growth rate has been related to water supply and the temperature of the dripwater (Baker et al., 1998a, Proctor et al., 2000, Genty et al., 2001, Fleitmann et al., 2004), i.e., more rainfall and warmer temperatures lead to higher growth rates. However, Genty et al. (2001) reported that thin soil cover above the cave can lead to a breakdown in the temperature dependence of the growth rates due to lack of soil  $\text{CO}_2$  or prior calcite precipitation. Greater stalagmite diameter is also indicative of higher drip rate and, thus, greater availability of water (Kaufmann, 2003). Height of drip above stalagmite must also be taken into consideration, as shorter drip heights tend to generate smaller diameters owing to the lack of splash effects (Gams, 1981).

### 2.5.4 Initial $^{234}\text{U}/^{238}\text{U}$

Using the forty one  $^{230}\text{Th}$  dates (Appendix A) within the last  $12$  ka and following the method described by Kaufman et al. (1998), we constructed a time series of  $(^{234}\text{U}/^{238}\text{U})_0$  for the Sofular Holocene record, in order to obtain an additional parameter for paleohydrological changes at our site. The values vary between  $1.80$  and  $2.10$  (Fig. 2.7c), with lower values clustering between  $\sim 9.6$  and  $4.7$  ka BP. Studies that use U isotopes in speleothems demonstrate the potential of the  $(^{234}\text{U}/^{238}\text{U})_0$  ratio to infer paleohydrology (Fairchild and Treble, 2009). Lower  $(^{234}\text{U}/^{238}\text{U})_0$  ratios are interpreted to reflect increased and heavier rainfall and resultant enhanced weathering and dissolution of the carbonate rock, which is not likely to be a source of high  $(^{234}\text{U}/^{238}\text{U})_0$  (Kaufman et al., 1998; Ayalon et al., 1999; Hellstrom and McCulloch, 2000). Moreover, the relative contribution of soil leaching is reduced when water moves faster through the soil, also resulting in a further decrease in the  $(^{234}\text{U}/^{238}\text{U})_0$  (Ayalon et al., 1999).

## 2.6 Discussion

### 2.6.1 Holocene Climate Variability on the Southern Black Sea Coast

#### 2.6.1.1 The Early Holocene: 11.6 – 9.6 ka BP

Although the growth rates and the  $(^{234}\text{U}/^{238}\text{U})_0$  imply that the first two thousand years were not the wettest of the Holocene, (Fig. 2.7b-c), the end of the Younger Dryas is marked by a rapid decrease in  $\delta^{13}\text{C}$  to one of the lowest values in the record (Fig. 2.4), implying a substantial increase in effective moisture and a fast re-vegetation with trees and shrubs. As previously discussed by Fleitmann et al. (2009), this contrasts with the pollen records from the Eastern Mediterranean (Bottema, 1995; Kotthoff et al., 2008, Fig. 2.9d), which exhibit a time lag of several hundred to thousands of years between climate and the vegetation at the onset of the Holocene. The much faster Holocene re-vegetation at the Sofular site supports the hypothesis that the Black Sea mountains were glacial refugia for temperate trees (Leroy and Arpe, 2007). Moreover, the warm, comparably more humid and summer-wet climate of the southern Black Sea coast must have been established very shortly after the Younger Dryas, and effective moisture reached levels for optimum vegetation development and soil microbial activity; despite the precipitation amount not yet reaching the highest values found in the Holocene.

#### 2.6.1.2 The 'Hypsithermal': 9.6 – 5.4 ka BP

Referring to the warm conditions in northern mid- to high latitudes, the time frame between about 9 ka BP and 5-6 ka BP is called the 'Hypsithermal' (or the 'Holocene climatic optimum', Wanner et al., 2008), when sapropel S1 was deposited in the Mediterranean (Rohling et al., 2009a). The most noticeable feature in the Holocene Sofular record is the significantly greater growth rates between ~ 9.6 and 5.4 ka BP (Fig. 2.7b, light gray shade), coincident with the 'Hypsithermal'. Though not continuously high, the mean growth rate is 0.176 mm/yr between ~ 9.6 and 5.4 ka BP (gray shades, Fig. 2.7b), with values reaching a maximum of 0.639 mm/yr. Elsewhere in the Holocene Sofular record, the growth rate is 0.094 mm/yr on average. This suggests a greater drip water supply. Taking the thin soil cover above the Sofular Cave into account and following the work of Genty et al. (2001), we claim that the high growth rates during this time frame indicate a much higher amount of precipitation. This interpretation is strongly supported by the lower  $(^{234}\text{U}/^{238}\text{U})_0$  values of ~ 1.80 to 2.00 between ~ 9.6 and 5.4 ka BP (Fig. 2.7c), implying faster movement of water through the soil and enhanced weathering of the host rock with heavy rainfall. In this regard, the period between ~ 7.5 and 6.1 ka BP (darker shade in Fig. 2.7) is particularly interesting. Along with high growth rates and increasing stalagmite diameter, this period exhibits the lowest  $(^{234}\text{U}/^{238}\text{U})_0$  values during the entire Holocene, and coincide with a relatively lighter colored fabric. This is a sign for even more intense precipitation above the cave from ~ 7.5 to 6.1 ka BP, as the contribution of soil U was the lowest owing to the shorter residence time of water in the soil and to the weathering of the host-rock. Ayalon et al. (1999) concluded the same relationship for stalagmites from Soreq Cave, in which a decrease in  $(^{234}\text{U}/^{238}\text{U})_0$  implies increased weathering of the host rock due to heavy rain events. Although we currently do not know the cause for the lighter colored fabric in the Sofular stalagmite from ~ 7.5 to 6.1 ka BP, relatively light-colored layers were previously interpreted to indicate increased rainfall

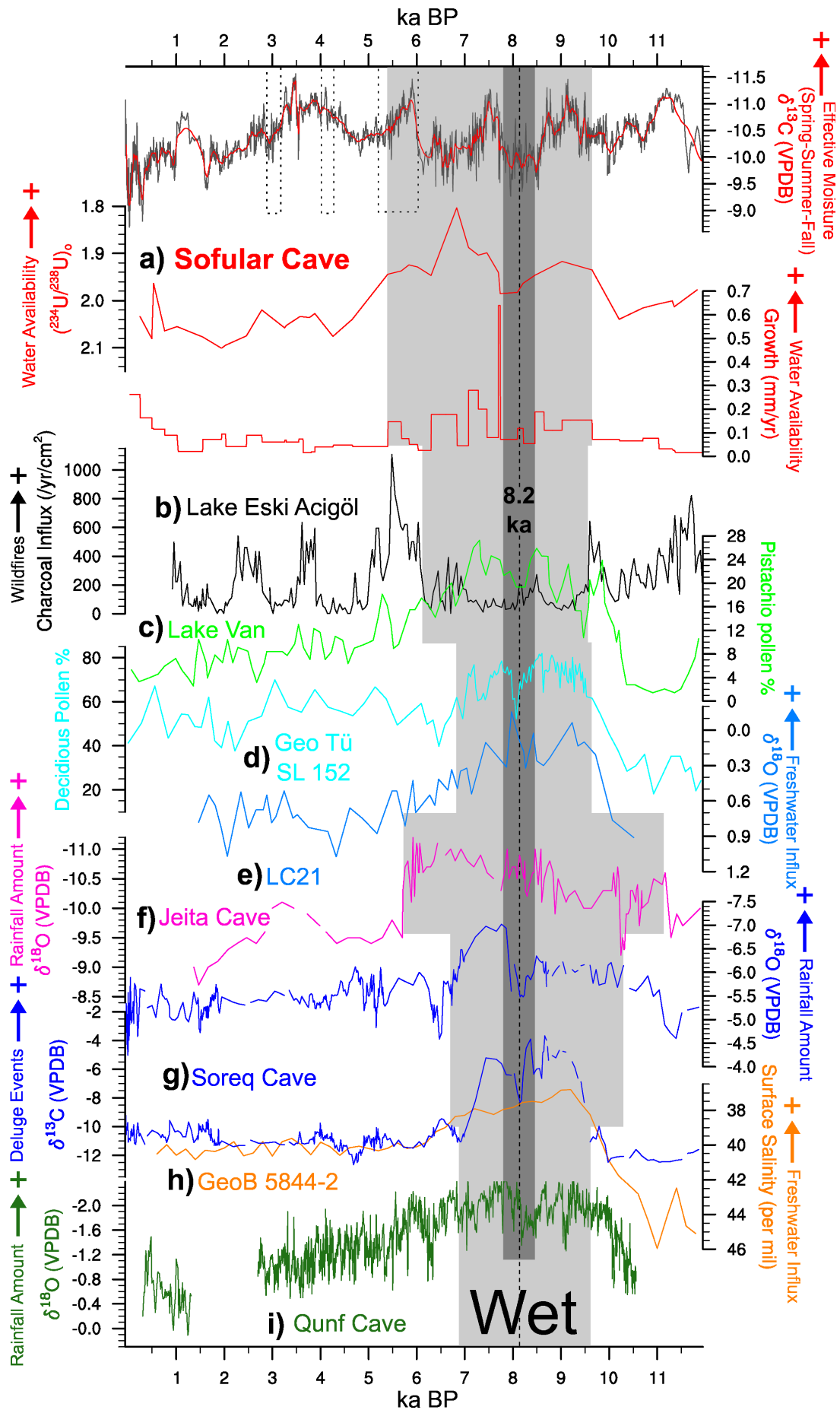
and soil humification for stalagmites from England (Baker et al., 1998b), Tasmania (Xia et al., 2001) and Belize (Webster et al., 2007). Putting together all evidences, we conclude that not only the amount of precipitation was on average higher between ~ 9.6 and 5.4 ka BP, but also individual rainfall events must have been much more intense, especially between ~ 7.5 and 6.1 ka BP.

On the other hand, our interpretation of  $\delta^{13}\text{C}$  values as a proxy for effective moisture does not support the existence of a more humid period from ~ 9.6 to 5.4 ka BP (Fig. 2.7a), not even between ~ 7.5 and 6.1 ka BP when growth rates and  $(^{234}\text{U}/^{238}\text{U})_0$  indicate the highest rainfall amount and intensity. An explanation for this discrepancy can be found in high groundwater recharge conditions resulting from excessive rainfall. Beyond a certain threshold for precipitation, very rapid flows within the soil zone are possible owing to the saturation of the soil with water (Baker et al., 1997). This will cause a lack of equilibration between seepage waters and soil  $\text{CO}_2$ , reducing the uptake of low  $\delta^{13}\text{C}$  biogenic carbon and resulting in higher  $\delta^{13}\text{C}$  values (Baker et al., 1997). The same mechanism is responsible for the elevated values of  $\delta^{13}\text{C}$  in the Soreq Cave record at times of heavier rainfall in the Holocene (Bar-Matthews et al., 1999). However, it is not clear when exactly within ~ 9.6 and 5.4 ka BP and to what extent this process increased the  $\delta^{13}\text{C}$  values in the Sofular Cave record. The time interval between ~ 7.5 and 6.1 ka BP (Fig. 2.7, dark gray shade) with the lowest  $(^{234}\text{U}/^{238}\text{U})_0$  and high growth rates is most likely to exhibit higher  $\delta^{13}\text{C}$  values because of the excessive rainfall and lack of equilibration with soil  $\text{CO}_2$ . Outside ~ 7.5 – 6.1 ka BP, higher values of  $\delta^{13}\text{C}$  can still be attributed to lower effective moisture, if other proxies (growth rates and  $(^{234}\text{U}/^{238}\text{U})_0$ ) support this interpretation. One example is the time frame around the 8.2 ka event with higher  $\delta^{13}\text{C}$  (lower moisture), when growth rates and the  $(^{234}\text{U}/^{238}\text{U})_0$  also indicate lower rainfall (Fig. 2.9a, darker gray shade). This is also when a significant response to an RCC is clearly discernable in the Holocene Sofular record; and it occurs over a longer time from ~ 8.4 to 7.8 ka BP, as suggested by Rohling and Palike (2005).

Alternative explanations can also be proposed for the higher values of  $\delta^{13}\text{C}$  within the wet period, especially for the section from ~ 7.5 to 6.1 ka BP (Fig. 2.7, dark gray shade). It has been previously shown in this article that Sofular  $\delta^{13}\text{C}$  values become more negative when spring-summer-fall precipitation increases (Fig. 2.5a), as a result of a rise in biogenic  $\text{CO}_2$  in the soil zone during growing season and the uptake of it by seepage waters in all three seasons. Therefore, a decrease in the amount of precipitation in spring and summer may well have led to elevated  $\delta^{13}\text{C}$  values. Some densely banded layers with alternating colors observed between ~ 7.5 and 6.1 ka BP, which look like annual lamination, also agree with the idea of increased seasonality. Besides, warmer winters at that time (Rossignol-Strick, 1999; Kotthoff et al., 2008) may have made an additional contribution to the enrichment of the heavy carbon isotope, by reducing the amount of late season snowfall that would normally act as an efficient source of moisture in the growing season (Fig. 2.5b).

### 2.6.1.3 Mid- to Late Holocene: 5.4 ka BP – Present

The end of the wet period in the Sofular record is characterized by a decrease in the stalagmite growth rates at ~ 5.4 ka BP (Fig. 2.7b), and an increase in  $(^{234}\text{U}/^{238}\text{U})_0$  values (Fig. 2.7c). The behavior of the  $\delta^{13}\text{C}$  curve at the beginning of this time frame provides valuable insights into the Holocene hydrological conditions in the Sofular area: Despite an



initial downward trend in the effective moisture signal (higher  $\delta^{13}\text{C}$ , Fig. 2.7a), which is compatible with lower growth rates and elevated  $(^{234}\text{U}/^{238}\text{U})_0$  values, the  $\delta^{13}\text{C}$  reaches its most negative values of the entire Holocene record at  $\sim 3.5$  ka BP. What we can infer from this is twofold: 1) Adequate moisture for maximum vegetation and soil microbial activity in the Sofular site can be provided without a substantial increase in the rainfall amount (1200 mm/yr at present), which would otherwise be reflected either in the growth rates or in  $(^{234}\text{U}/^{238}\text{U})_0$  at  $\sim 3.5$  ka BP. 2) The period between  $\sim 9.6$  and 5.4 ka with high growth rates and low  $(^{234}\text{U}/^{238}\text{U})_0$  was *excessively wet* in this area.

Past the moisture peak at  $\sim 3.5$  ka BP, the  $\delta^{13}\text{C}$  curve indicates a drying trend until the beginning of the 20<sup>th</sup> century AD. The possibility, however, that this rise in  $\delta^{13}\text{C}$  may have been due to the increased anthropogenic impact on land cover during the late Holocene, remains. The most recent  $\sim 600$  years of the record and the corresponding calcite fabric are also noteworthy. A yellowish colored texture is accompanied by increasing growth rates, the lowest diameters of the entire stalagmite and quite high  $\delta^{13}\text{C}$  values exceeding  $-9.0\%$  in the last  $\sim 250$  years, to recover back to  $-11.0\%$  only at the tip. Greater growth rates in this section, rather than indicating a rainfall increase, seem to be a compensation for the very low diameter; which may be due to the stalagmite getting closer to its drip site and to a reduction in splash energy. This is also supported by the  $(^{234}\text{U}/^{238}\text{U})_0$ , which remains high except for one value. Thus, we conclude that the last 600 years, with the exception of the 20<sup>th</sup> century, was the driest period of the Holocene in the Sofular area.

The three RCCs other than the 8.2 ka event, namely the 6.0 – 5.2, 4.2 – 4.0 and 3.1 – 2.9 ka BP events mentioned by Weninger et al. (2009) are within this time interval. However, none of these events (Fig 8a, dashed rectangles) have a consistent and convincing signature in the Sofular  $\delta^{13}\text{C}$  record. Only the 6.0 – 5.2 ka event can be regarded present, as the transition from the wetter period (Fig. 2.7, light gray shade) to present day conditions started at  $\sim 5.4$  ka BP.

## 2.6.2 Comparison with Eastern Mediterranean and Monsoon Records

In the light of our investigation on how the Sofular record should be interpreted within the Holocene, a meaningful comparison of our record can be made with other high quality paleoclimate records from the Eastern Mediterranean (Fig. 2.9). The light gray shaded

**Fig. 2.9 (see left): Eastern Mediterranean comparison.** Comparison of various paleoclimate records from the Eastern Mediterranean and Monsoon realms through the Holocene. The order of the records follows a north-south transect (geographical locations are shown in Fig. 2.1). Light gray shade with the varying width denotes the wet period in each record. The time frame around 8.2 ka BP is shown with a dashed line and a darker gray shade. Dashed rectangles beneath the top axis mark the timing of Rapid Climate Change events (Weninger et al., 2009). BP refers to before present (1950). **a)** Sofular cave  $\delta^{13}\text{C}$  (top, note descending axis), initial  $^{234}\text{U}/^{238}\text{U}$  (middle, note descending axis) and the growth rate (bottom) records (this study). **b)** Microcharcoal flux values for lake Eski Acıgöl, Central Anatolia (Turner et al., 2008) **c)** Pistachio pollen percentage from Lake Van (Wick et al., 2003). **d)** Deciduous pollen percentage from the northern Aegean Sea core GeoTü SL152 (Kotthoff et al., 2008) **e)**  $\delta^{18}\text{O}$  record (note descending axis) from the southern Aegean Sea core LC21 (Rohling et al., 2002) **f)**  $\delta^{18}\text{O}$  record (note descending axis) from the Jeita cave, Lebanon (Verheyden et al., 2008). **g)**  $\delta^{18}\text{O}$  (note descending axis) and  $\delta^{13}\text{C}$  records from the Soreq cave, Israel (Bar-Matthews, 2003, modified in Almogi-Labin et al., 2009). **h)** Sea surface salinity estimates (note descending axis) from the northern Red Sea core GeoB5844-2 (Arz et al., 2003). **i)**  $\delta^{18}\text{O}$  record (note descending axis) from the Qunf Cave, Oman (Fleitmann et al. 2007).

time frame (marked “Wet” in Fig. 2.9) overlaps most of the fast-growing part (from ~ 9.6 to 5.4 ka BP) of the Sofular record. During this period, hydrological conditions in the Eastern Mediterranean region were markedly different from those of today. At the southeastern corner of the Mediterranean Sea, the Soreq Cave depleted  $\delta^{18}\text{O}$  and enriched  $\delta^{13}\text{C}$  values (Fig. 2.9g) indicate significantly higher rainfall (Bar-Matthews et al., 1999; 2000). The  $\delta^{18}\text{O}$  depletion in Soreq Cave speleothems has also been suggested to stem from freshwater flooding from the Nile and resultant negative isotopic shift in  $\delta^{18}\text{O}$  of Mediterranean surface water (Marino et al., 2009). This effect, triggered by enhanced monsoons in North Africa (Casford et al., 2002, 2003), can be even traced in  $\delta^{18}\text{O}$  records from the southern Aegean (Fig. 2.9e) (Rohling et al., 2002). Direct effect of stronger monsoons due to orbital forcing (Liu et al., 2004) is evident in the Qunf Cave record from southern Oman (Fig. 2.9i), which exhibits depleted  $\delta^{18}\text{O}$  values during the “wet period”. This reflects the strengthening of the Indian Monsoon during the early- to mid-Holocene (Fleitmann et al., 2003; 2007). On the other hand, lower salinity values from the northern Red Sea (Fig. 2.9h, Arz et al., 2003), persistently low wildfire occurrence in Central Anatolia (Fig. 2.9b, Turner et al., 2008), increased deciduous pollen in Northern Aegean borderlands (Fig. 2.9d, Kotthoff et al., 2008) and high pistachio pollen at Lake Van area (Fig. 2.9c, Wick et al., 2003); all coincide with high growth rates and low  $(^{234}\text{U}/^{238}\text{U})_0$  in the Sofular record, which are evidence for excessive rainfall at our study site. These are strong indications of a common change in hydrological conditions that *cannot* directly or indirectly be related to Indian / North African monsoon intensification. Penetration of Indian monsoon beyond 20° N is considered highly unlikely (Tzedakis, 2007; Rohling et al., 2009a). Other marine (Kallel et al., 1997; Rossignol-Strick, 1999), lake level (Harrison et al., 1996), lake isotope (Roberts et al., 2008) and speleothem isotope (Fig. 2.9f, Verheyden et al., 2008) records suggest high precipitation in the Eastern Mediterranean area as well. Hypotheses explaining this wet period will be discussed in Section 2.6.3.2. Although high growth rates continue for the Sofular record between 6.0 and 5.4 ka BP (Fig. 2.9a) when most of the other records in Fig. 2.9 have reached their middle to late Holocene values, which is a discrepancy; timing of some shorter term events within the “wet period” are quite similar. For example, the ~ 600 year period around the 8.2 ka event is marked by relatively lower growth rates, higher  $\delta^{13}\text{C}$ , and higher  $(^{234}\text{U}/^{238}\text{U})_0$  (Fig. 2.9a), coinciding with a decrease in precipitation in the Soreq Cave site (Fig. 2.9g), decline in deciduous pollen in the Northern Aegean (Fig. 2.9d), weakening of the Indian monsoon (Fig. 2.9i) and a relative increase in wildfire intensity over the Anatolian plateau (Fig. 2.9b). Moreover, the wettest interval for the Soreq Cave record inferred from its  $\delta^{18}\text{O}$  profile (centered at ~ 7.5 ka BP) matches well with the highest growth rates in Sofular, and even with a very high level of effective moisture (Fig. 2.9a), despite the probable increase in  $\delta^{13}\text{C}$  due to non-equilibration with soil  $\text{CO}_2$ , as detailed in Section 2.6.1.2. It is interesting to note that the wildfire frequency in Central Anatolia is also very low around ~ 7.5 ka BP (Fig. 2.9b).

## **2.6.3 Wet Period during Sapropel I:**

### **2.6.3.1 Timing**

The timing (of especially the termination) of the early- to mid-Holocene wet period in the Eastern Mediterranean seems to be an issue. Fig. 2.9 reveals that the wet period in the Sofular area ended at ~ 5.4 (Fig. 2.9a) ka BP, one of the latest among all records compared. At Lake Van in Eastern Turkey, the highest amount of pistachio pollen is observed

between 9.5 and 6 ka BP (Fig. 2.9b); however, Wick et al. (2003) argue that the climatically optimum conditions at this site occurred between as 8.2 and 4.0 ka BP, using other pollen data, salinity values and  $\delta^{18}\text{O}$ . The pollen record from Lake Zeribar in Iran (Stevens et al., 2001) also indicates that the expansion of woodland started as late as  $\sim 7.0$  ka BP, yet these delays might not be directly related to climate. The Jeita Cave record from Lebanon (Fig. 2.9d, Verheyden et al., 2008) is another one with a long wet period ending at around 5.5 ka BP, which is comparable to that of Sofular, but some 1000-1500 years later than those of the records further south, such as the Soreq Cave (Fig. 2.9g; Bar-Matthews, 2003; modified in Almogi-Labin et al., 2009) and Northern Red Sea (Fig. 2.9h; Arz et al., 2003). More timing discrepancies can be inferred from Fig. 2.9, which shows that the early to mid-Holocene wet period around the Eastern Mediterranean is not perfectly synchronous among all sites. This implies the possible role of more than one climatic mechanism leading to the observed patterns, or different thresholds of each proxy record to relatively small changes in precipitation.

### 2.6.3.2 Possible Mechanisms

The early to mid-Holocene wet phase in the Eastern Mediterranean (Fig. 2.9, light gray shade) coincides with the formation of marine sapropel I between  $\sim 9.5$  and 6.5 ka BP, that is linked to increased freshwater input into the Mediterranean sea from its borderlands (Rohling et al., 1994) and also to direct precipitation over the sea itself (Kallel et al., 1997; Kotthoff et al., 2008). Sofular record exhibits some noticeably similar features with the other Eastern Mediterranean records during this period, which is significant for a number of reasons. The Sofular Cave site is influenced marginally by the Mediterranean Sea and Mediterranean-derived precipitation systems, first due to the intervening distance, and, maybe more importantly, due to its partly secluded location behind two mountain chains, namely the Taurus and the North Anatolian ranges (Fig. 2.1). Moreover, the major moisture source for Sofular area, the Black Sea, lies immediately north of it and reshapes the climate on its southern coast by modifying the air masses from north (Trewartha, 1966) and obscuring the effects of teleconnection patterns such as the North Atlantic Oscillation (Türkeş, 2003). Consequently, the Sofular  $\delta^{18}\text{O}$  profile, which was shown to accurately reflect the surface isotopic composition of the Black Sea in the Pleistocene (Fleitmann et al., 2009; Badertscher et al., 2011), continues its long term trend in the Holocene (Fig. 2.5a and Fig. 2.8), showing no signs of an isotopic pattern that could be ascribed to Mediterranean-derived moisture. Yet, the Sofular record indicates a marked increase in precipitation amount and intensity during the times of sapropel formation in the Mediterranean and marks one of the northernmost locations where a similar rise in precipitation can be deduced from paleoclimate archives.

Then what could be the climatic mechanism that led to these almost simultaneous changes in a broad area from the northern Red Sea to the Black Sea? The Sofular record allows us to go over the available hypotheses again with a new look. In a comprehensive review of the issue, Tzedakis (2007) rejects all proposed mechanisms that feature increased summer rainfall in the Eastern Mediterranean region, arguing that palynological evidence suggest the opposite. He stresses that times of sapropel deposition in the Eastern Mediterranean coincide with insolation maxima and Indian monsoon intensification, which strengthens the descending branch of the Hadley cell (Raicich et al., 2003; Ziv et al., 2004) and should lead to even more extreme summer aridity in the Eastern Mediterranean. Alternatively,

he explains the obviously wetter conditions at the time by invoking increased fall / winter precipitation, which would arise as a result of high sea surface temperatures (SSTs) in the summer persisting into the fall months. Elevated summer SSTs during times of sapropel formation reconstructed by Lourens et al. (1992) were considered to represent a summer signal under high summer insolation regimes. Indeed, a substantial increase in fall precipitation in response to higher SSTs may well have been the case for Sofular area, as recently demonstrated by Bozkurt and Sen (2009) with a modeling study. They found that, a rise of 2° C in the surface temperatures of all the seas surrounding Anatolian Peninsula causes significant increases in summer and fall precipitation over the Black Sea region in Turkey, whereas in other seasons changes are insignificant. Moreover, precipitation in this region is more likely to occur in the form of huge rainstorms during the fall, as the interaction of warm Black Sea waters with cooler air masses creates vigorous convective activity. Evidence for periods with frequent massive rain storms are present in both the modern meteorological data from Sofular area (Fig. 2.6) and the Sofular Cave records (Fig. 2.7), as well as in the Soreq Cave record (Bar-Matthews et al., 1999; Vaks et al., 2003). Besides, an increase in fall precipitation by a certain factor would be much more effective than a proportionate rise for other seasons in creating the excessive growth rates observed in the Sofular record during the wet period (Fig. 2.5); since fall is currently the wettest season in the Black Sea region (Fig. 2.2a; Türkeş, 1996). Furthermore, there seem to be annual lamination in parts of the Sofular stalagmite So-1 from ~ 7.5 to 6.1 ka BP (Fig. 2.5, dark gray shade), which corresponds with increased  $\delta^{13}\text{C}$ . This also supports an increase in the seasonality of precipitation in favor of fall and winter. While this mechanism seems apt to explain the common increase in precipitation in both Black Sea and Mediterranean regions, the issue of SSTs is problematic. An alkenone-based reconstruction for the Eastern Mediterranean (Rimbu et al., 2004) reported lower SSTs for early Holocene. Though the study does not provide seasonally resolved data, it concludes that the findings should indicate a positive mode of early Holocene NAO in winter, thus, cooler winter SSTs. This raises the doubt whether winter precipitation may actually have increased due to both low SSTs and a positive winter NAO in areas such as interior Anatolia, where an increase in only fall precipitation would not suffice to explain the observed early Holocene depletion in lake records (Roberts et al., 2008). However, a number of pollen records indicate that winters were mild and wet in northern Aegean borderlands (Wijmstra, 1990; Kotthoff, 2008) and around the Eastern Mediterranean sea (Rossignol-Strick, 1999); in contrast to the findings of Rimbu et al. (2004). Additionally, a more recent reconstruction from the core LC21 in the southern Aegean Sea (Marino et al., 2009) exhibits higher SSTs both in the winter and summer during sapropel deposition, most notably from ~ 7.6 to 7.0 ka BP (Fig. 2.10b). This is also a time of very high growth rates and low ( $^{234}\text{U}/^{238}\text{U}$ )<sub>0</sub> in the Sofular record (Fig. 2.10a), indicating excessively wet conditions. The evidence in favor of wet summers were reviewed by Rohling et al. (2009a), who also concluded that there was a change in the seasonality of precipitation in the Eastern Mediterranean borderlands during the period of sapropel deposition. Rohling and Hilgen (1991) were the first to suggest a dynamical mechanism, which they called 'Mediterranean summer depressions' scenario. As an alternative to this, Arz et al. (2003) proposed an independent, regional monsoon mechanism in the Eastern Mediterranean. Both of these hypotheses contradict the present day relationship of the Indian Monsoon with the Eastern Mediterranean summer regime, in which the intensification of the former leads to aridification in the latter (Raicich et al., 2003; Ziv et al., 2004). Additionally, none of them could be consistently simulated by climate models (Brewer et al., 2007). However, both the stability



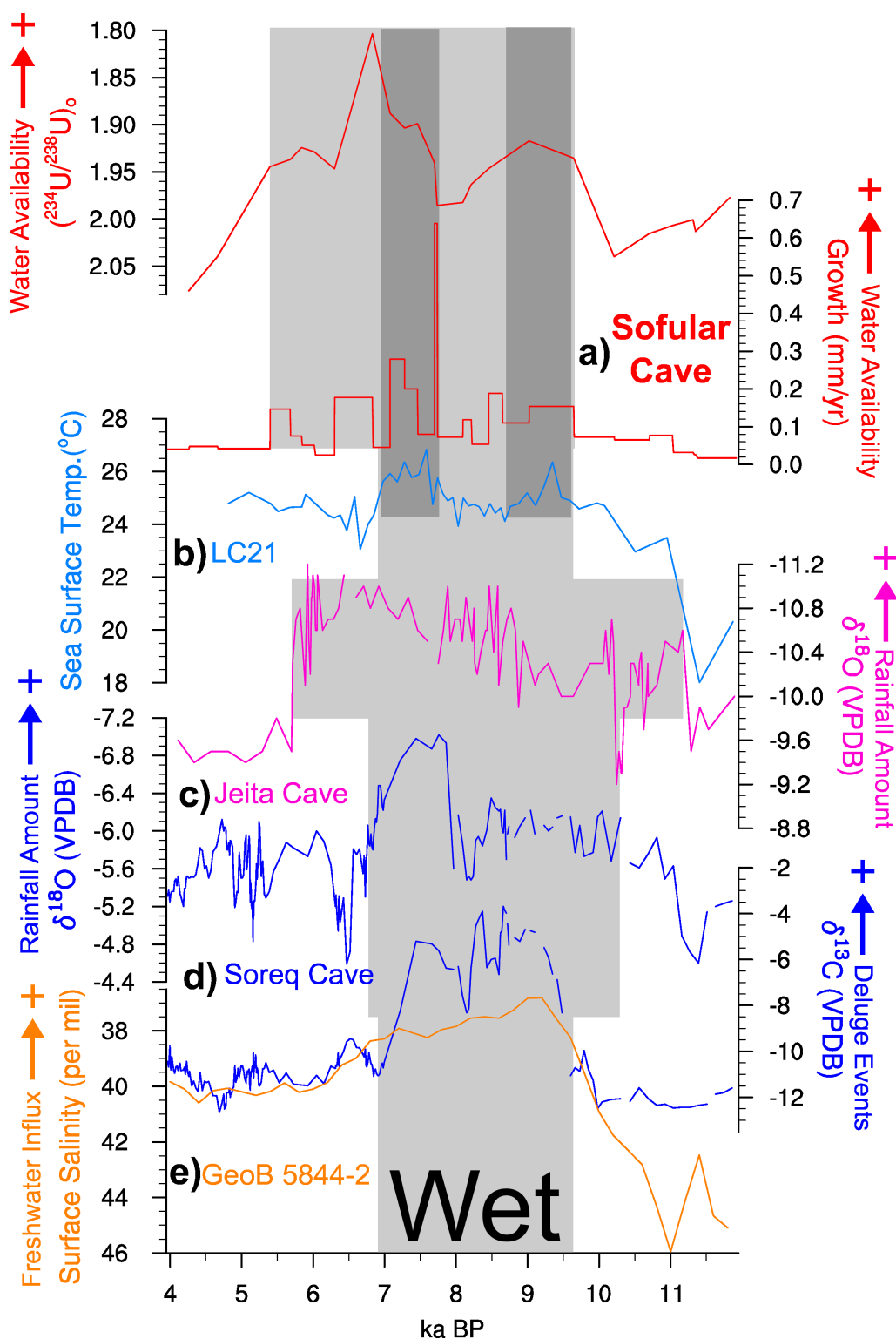


**Fig. 2.10: SSTs and Eastern Mediterranean records.** Comparison of the summer SST record (b) from the southern Aegean Sea core LC21 (Rohling et al., 2002) with various other records (geographical locations are shown in Fig. 2.1). BP refers to before present (1950). Light gray shade with the varying width denotes the wet period in each record. The two time frames when the SSTs were the highest are shown with darker gray shades. a) Sofular cave initial  $^{234}\text{U}/^{238}\text{U}$  (upper, note descending axis) and the growth rate (lower) records (this study). c)  $\delta^{18}\text{O}$  record (note descending axis) from the Jeita cave, Lebanon (Verheyden et al., 2008). d)  $\delta^{18}\text{O}$  (note descending axis) and  $\delta^{13}\text{C}$  records from the Soreq cave, Israel (Bar-Matthews, 2003, modified in Almog-Labin et al., 2009). e) Sea surface salinity estimates (note descending axis) from the northern Red Sea core GeoB5844-2 (Arz et al., 2003).

of modern-day teleconnection patterns and climate models' simulation capability of regional processes should be questioned, since insolation forcing was entirely different in the early- to mid-Holocene (Berger, 1978). Today, there are numerous areas over the Eastern Mediterranean where summer depressions still form, but these are not strong enough to overcome the descending branch of the Hadley cell, therefore cannot cause precipitation (Trigo et al, 1999). The same is valid for the 'thermal lows' of the Eastern Mediterranean land surfaces, in that they are not strong enough to lead to a persistent upper level flow from the surrounding seas, thus are short-lived and dry. One intriguing possibility is that this situation might have been different during the early to mid-Holocene, especially for the thermal lows of the land surfaces. The intense heating of the land might have led to a strengthening of the thermal lows, creating an independent monsoon-type circulation that was able to overcome the descending motion of the Hadley cell, which would make the "Mediterranean Monsoon" scenario of Arz et al. (2003) possible. There is no direct evidence in the Sofular record supporting this mechanism, yet it provides some hints when compared to the wildfire record (Turner et al., 2008) from lake Eski Acıgöl in central Anatolia (Fig. 2.9b). During the 'wet period' (light gray shade in Fig. 2.9), the Eski Acıgöl charcoal record indicates almost persistently low occurrences of wildfires, which might well be a sign of wet summers. Curiously, within the 'wet period', relatively elevated values of charcoal coincide with lower effective moisture (more positive  $\delta^{13}\text{C}$ ) in the Sofular area, and vice versa. A regional summer monsoon mechanism featuring low pressure centers over Anatolia that draw moisture from both the Black and Mediterranean seas would lead to this relationship, shifting most of the rainfall to summer for both regions simultaneously, and creating the greater growth rates and lower  $(^{234}\text{U}/^{238}\text{U})_0$  values in the Sofular record. One interesting study supporting rainy summers in Anatolia is the pollen-based temperature reconstruction of Davis et al. (2003). They found that between  $\sim 10.0$  and  $6.0$  ka BP, summer temperatures in southeastern Europe including Anatolia were the lowest in the entire Holocene, implying enhanced moisture availability, increased latent heat flux into the atmosphere and cloudy conditions. However, Bonfils et al. (2004) argue that this increase in latent heat flux was due to high winter soil moisture persisting into summer.

All in all, the Sofular record provides valuable insights into the issue of hydrological changes in the Eastern Mediterranean during the formation of Sapropel I. However, it does not allow us to present a firm solution for the *seasonality of precipitation* issue at the moment.

## 2.7 Summary and Conclusions

We present the updated Holocene profile of the Sofular Cave record from the southern coast of the Black Sea. The robust age model constructed with forty one  $^{230}\text{Th}$  dates in the Holocene allows us to construct a record consisting of  $\delta^{18}\text{O}$ ,  $\delta^{13}\text{C}$ , growth rate and  $(^{234}\text{U}/^{238}\text{U})_0$  time series with a very high mean temporal resolution of 5.4 years for the stable isotope profiles. Two more stalagmite records partially covering the Holocene with lower temporal resolution were also produced. The main conclusions are:

-  $\delta^{13}\text{C}$ , growth rates and the  $(^{234}\text{U}/^{238}\text{U})_0$  time series proved to be more useful than  $\delta^{18}\text{O}$  in understanding the hydrological conditions over the southern Black Sea coast through the Holocene; as the direct effect of climatic changes on the  $\delta^{18}\text{O}$  is masked by changes in the

$\delta^{18}\text{O}$  of Black Sea surface water. High growth rates and low  $(^{234}\text{U}/^{238}\text{U})_0$  between 9.6 and 5.4 ka BP, which coincide with the early- to mid-Holocene wet period and sapropel deposition in the Eastern Mediterranean, show that the southern Black Sea region experienced times of enhanced and more intense precipitation in concert with regional trends. However, the  $\delta^{13}\text{C}$  record does not indicate an increase in effective moisture level, probably due to water-excess related non-equilibration of seepage waters with soil  $\text{CO}_2$ , or, less likely, to a rainfall deficit in the vegetation growing season.

- Of the previously suggested climatic mechanisms for the early- to mid-Holocene wet period, there is evidence in Sofular record supporting two of the scenarios, albeit without a firm conclusion: a) The enhanced fall / winter precipitation mechanism with increased summer aridity, due to elevated summertime SSTs (Tzedakis, 2007). b) A regional summer monsoon mechanism involving the Black Sea and the Mediterranean, previously proposed by Arz et al. (2003) for the northern Red Sea involving only the Mediterranean. There are disagreements among the Eastern Mediterranean records concerning the timing of the wet period, complicating the issue even further. More high-quality paleoclimate records are needed in order to eliminate one of the scenarios, as well as to explain the timing discrepancies.

- The influence of Rapid Climate Change events (RCCs, Mayewski et al., 2004) on the southern Black Sea coast is unclear; probably due to the local effects of the Black Sea (e.g. sea effect precipitation) and the North Anatolian mountain range. Nevertheless, the long-term anomaly centered at 8.2 ka (Rohling and Palike, 2005) is present in Sofular Cave record as a decrease in rainfall.

## Acknowledgements

The authors would like to thank Frank McDermott, A.M.Celal Şengör, Daniel Rufer, Naki Akçar, Sally Lowick and the two anonymous reviewers for their constructive comments on the manuscript. Yaman Özakın is thanked for his support in the cave. This work was supported by the Swiss National Science Foundation (grant PP002-110554/1 to D. F.), the U.S. National Science Foundation (ESH 0502535 to R. L. E. and H. C.), the Gary Comer Science and Education Foundation (CP41 to R. L. E.), and Istanbul Technical University.

## 2.8 References

- Allen, J., Brandt, U., Brauer, A., Hubberten, H., Huntley, B., Keller, J., Kraml, M., Mackensen, A., Mingram, J., Negendank, J., Nowaczyk, N., Oberhansli, H., Watts, W., Wulf, S., Zolitschka, B., 1999. Rapid environmental changes in southern Europe during the last glacial period. *Nature* 400, 740-743.
- Almogi-Labin, A., Bar-Matthews, M., Shriki, D., Kolosovsky, E., Paterne, M., Schilman, B., Ayalon, A., Aizenshtat, Z., Matthews, A., 2009. Climatic variability during the last 90 ka of the southern and northern Levantine Basin as evident from marine records and speleothems. *Quaternary Sci Rev* 28, 2882-2896.
- Arz, H.W., Lamy, F., Patzold, J., Muller, P.J., Prins, M., 2003. Mediterranean moisture source for an early-Holocene humid period in the northern Red Sea. *Science* 300, 118-121.
- Ayalon, A., Bar-Matthews, M., Kaufman, A., 1999. Petrography, strontium, barium and uranium concentrations, and strontium and uranium isotope ratios in speleothems as palaeoclimatic proxies: Soreq Cave, Israel. *Holocene* 9, 715-722.

- Badertscher, S., Fleitmann, D., Cheng, H., Edwards, R.L., Göktürk, O.M., Zumbühl, A., Leuenberger, M., Tüysüz, O., 2011. Pleistocene water intrusions from the Mediterranean and Caspian seas into the Black Sea. *Nat Geosci* 4, 236-239.
- Bahr, A., Arz, H.W., Lamy, F., Wefer, G., 2006. Late glacial to Holocene paleoenvironmental evolution of the Black Sea, reconstructed with stable oxygen isotope records obtained on ostracod shells. *Earth Planet. Sci. Lett.* 241, 863-875.
- Baker, A., Ito, E., Smart, P.L., McEwan, R.F., 1997. Elevated and variable values of C-13 in speleothems in a British cave system. *Chem. Geol.* 136, 263-270.
- Baker, A., Genty, D., Dreybrodt, W., Barnes, W.L., Mockler, N.J., Grapes, J., 1998a. Testing theoretically predicted stalagmite growth rate with Recent annually laminated samples: Implications for past stalagmite deposition. *Geochim. Cosmochim. Acta* 62, 393-404.
- Baker, A., Genty, D., Smart, P.L., 1998b. High-resolution records of soil humification and paleoclimate change from variations in speleothem luminescence excitation and emission wavelengths. *Geology* 26, 903-906.
- Baldini, J.U.L., McDermott, F., Baker, A., Baldini, L.M., Matthey, D.P., Railsback, L.B., 2005. Biomass effects on stalagmite growth and isotope ratios: A 20th century analogue from Wiltshire, England. *Earth Planet. Sci. Lett.* 240, 486-494.
- Bar-Matthews, M., Ayalon, A., Kaufman, A., 1997. Late quaternary paleoclimate in the eastern Mediterranean region from stable isotope analysis of speleothems at Soreq Cave, Israel. *Quaternary Res.* 47, 155-168.
- Bar-Matthews, M., Ayalon, A., Kaufman, A., Wasserburg, G.J., 1999. The Eastern Mediterranean paleoclimate as a reflection of regional events: Soreq Cave, Israel. *Earth Planet. Sci. Lett.* 166, 85-95.
- Bar-Matthews, M., Ayalon, A., Kaufman, A., 2000. Timing and hydrological conditions of Sapropel events in the Eastern Mediterranean, as evident from speleothems, Soreq Cave, Israel. *Chem. Geol.* 169, 145-156.
- Bar-Matthews, M., Ayalon, A., Gilmour, M., Matthews, A., Hawkesworth, C.J., 2003. *Geochim. Cosmochim. Acta* 67, 3181-3199.
- Berger, A.L., 1978. Long-term variations of daily insolation and quaternary climatic changes. *J. Atmos. Sci.* 35, 2362-2367.
- Bonfils, C., de Noblet-Ducoudre, N., Guiot, J., Bartlein, P., 2004. Some mechanisms of mid-Holocene climate change in Europe, inferred from comparing PMIP models to data. *Clim. Dynam.* 23, 79-98.
- Bottema, S., 1995. The Younger Dryas in the Eastern Mediterranean. *Quaternary Sci. Rev.* 14, 883-891.
- Bozkurt, D., Şen, Ö.L., 2009. Precipitation in the Anatolian Peninsula: sensitivity to increased SSTs in the surrounding seas. *Clim. Dynam.* 36, 711-726.
- Brewer, S., Guiot, J., Torre, F., 2007. Mid-Holocene climate change in Europe: a data-model comparison. *Clim. Past* 3, 499-512.
- Casford, J.S.L., Rohling, E.J., Abu-Reid, R., Cooke, S., Fontanier, C., Leng, M., Lykousis, V., 2002. Circulation changes and nutrient concentrations in the late Quaternary Aegean Sea: A nonsteady state concept for sapropel formation. *Paleoceanography* 17, doi: 10.1029/2000PA000601.
- Casford, J.S.L., Rohling, E.J., Abu-Zied, R.H., Fontanier, C., Jorissen, F.J., Leng, M.J., Schmiedl, G., Thomson, J., 2003. A dynamic concept for eastern Mediterranean circulation and oxygenation during sapropel formation. *Palaeogeogr. Palaeoclimatol.* 190, 103-119.
- Davis, B.A.S., Brewer, S., Stevenson, A.C., Guiot, J., 2003. The temperature of Europe during the Holocene reconstructed from pollen data. *Quaternary Sci. Rev.* 22, 1701-1716.
- Earman, S., Campbell, A.R., Phillips, F.M., Newman, B.D., 2006. Isotopic exchange between snow and atmospheric water vapor: Estimation of the snowmelt component of groundwater recharge in the southwestern United States. *J. Geophys. Res-Atmos.* 111, D09302 doi: 10.1029/2005JD006470.
- Fairchild, I.J., Smith, C.L., Baker, A., Fuller, L., Spotl, C., Matthey, D., McDermott, F., 2006.

- Modification and preservation of environmental signals in speleothems. *Earth-Sci. Rev.* 75, 105-153.
- Fairchild, I.J., Treble, P.C., 2009. Trace elements in speleothems as recorders of environmental change. *Quaternary Sci. Rev.* 28, 449-468.
- Fleitmann, D., Burns, S.J., Mudelsee, M., Neff, U., Kramers, J., Mangini, A., Matter, A., 2003. Holocene forcing of the Indian monsoon recorded in a stalagmite from Southern Oman. *Science* 300, 1737-1739.
- Fleitmann, D., Burns, S.J., Neff, U., Mudelsee, M., Mangini, A., Matter, A., 2004. Palaeoclimatic interpretation of high-resolution oxygen isotope profiles derived from annually laminated speleothems from Southern Oman. *Quaternary Sci. Rev.* 23, 935-945.
- Fleitmann, D., Burns, S.J., Mangini, A., Mudelsee, M., Kramers, J., Villa, I., Neff, U., Al-Subbary, A.A., Buettner, A., Hippler, D., Matter, A., 2007. Holocene ITCZ and Indian monsoon dynamics recorded in stalagmites from Oman and Yemen (Socotra). *Quaternary Sci. Rev.* 26, 170-188.
- Fleitmann, D., Cheng, H., Badertscher, S., Edwards, R.L., Mudelsee, M., Göktürk, O.M., Fankhauser, A., Pickering, R., Raible, C.C., Matter, A., Kramers, J., Tüysüz, O., 2009. Timing and climatic impact of Greenland interstadials recorded in stalagmites from northern Turkey. *Geophys Res Lett* 36, L19707.
- Gams, I., 1981. Contribution to morphometrics of stalagmites. *Proceedings of the 8th International Congress of Speleology, Bowling Green, Kentucky*, pp. 276-278.
- Genty, D., Baker, A., Vokal, B., 2001. Intra- and inter-annual growth rate of modern stalagmites. *Chem. Geol.* 176, 191-212.
- Genty, D., Blamart, D., Ouahdi, R., Gilmour, M., Baker, A., Jouzel, J., Van-Exter, S., 2003. Precise dating of Dansgaard-Oeschger climate oscillations in western Europe from stalagmite data. *Nature* 421, 833-837.
- Genty, D., Blamart, D., Ghaleb, B., Plagnes, V., Causse, C., Bakalowicz, M., Zouari, K., Chkir, N., Hellstrom, J., Wainer, K., Bourges, F., 2006. Timing and dynamics of the last deglaciation from European and North African delta C-13 stalagmite profiles - comparison with Chinese and South Hemisphere stalagmites. *Quaternary Sci Rev* 25, 2118-2142.
- Göktürk, O.M., Bozkurt, D., Şen, O.L., Karaca, M., 2008. Quality control and homogeneity of Turkish precipitation data. *Hydrol. Process.* 22, 3210-3218.
- Harrison, S.P., Yu, G., Tarasov, P.E., 1996. Late quaternary lake-level record from northern Eurasia. *Quaternary Res.* 45, 138-159.
- Hellstrom, J., McCulloch, M., Stone, J., 1998. A detailed 31,000-year record of climate and vegetation change, from the isotope geochemistry of two New Zealand speleothems. *Quaternary Res* 50, 167-178.
- Hellstrom, J.C., McCulloch, M.T., 2000. Multi-proxy constraints on the climatic significance of trace element records from a New Zealand speleothem. *Earth Planet. Sci. Lett.* 179, 287-297.
- Jemcov, I., Petric, M., 2009. Measured precipitation vs. effective infiltration and their influence on the assessment of karst systems based on results of the time series analysis. *J. Hydrol.* 379, 304-314.
- Kallel, N., Paterne, M., Duplessy, J.C., Vergnaud-Grazzini, C., Pujol, C., Labeyrie, L., Arnold, M., Fontugne, M., Pierre, C., 1997. Enhanced rainfall in the Mediterranean region during the last sapropel event. *Oceanol. Acta* 20, 697-712.
- Kaufman, A., Wasserburg, G.J., Porcelli, D., Bar-Matthews, M., Ayalon, A., Halicz, L., 1998. U-Th isotope systematics from the Soreq Cave, Israel and climatic correlations. *Earth Planet. Sci. Lett.* 156, 141-155.
- Kaufmann, G., 2003. Stalagmite growth and palaeo-climate: the numerical perspective. *Earth Planet. Sci. Lett.* 214, 251-266.
- Kaufmann, G., Dreybrodt, W., 2004. Stalagmite growth and palaeo-climate: an inverse approach. *Earth Planet. Sci. Lett.* 224, 529-545.
- Kottek, M., Grieser, J., Beck, C., Rudolf, B., Rubel, F., 2006. World map of the Köppen-Geiger climate classification updated. *Meteorol. Z.* 15, 259-263.
- Kotthoff, U., Pross, J., Müller, U.C., Peyron, O., Schmiiedl, G., Schulz, H., Bordon, A., 2008. Climate

- dynamics in the borderlands of the Aegean Sea during formation of sapropel S1 deduced from a marine pollen record. *Quaternary Sci. Rev.* 27, 832-845.
- Leroy, S.A.G., Arpe, K., 2007. Glacial refugia for summer-green trees in Europe and south-west Asia as proposed by ECHAM3 time-slice atmospheric model simulations. *J. Biogeogr.* 34, 2115-2128.
- Liu, Z., Harrison, S.P., Kutzbach, J., Otto-Bliesner, B., 2004. Global monsoons in the mid-Holocene and oceanic feedback. *Clim. Dynam.* 22, 157-182.
- Lourens, L.J., Hilgen, F.J., Gudjonsson, L., Zachariasse, W.J., 1992. Late Pliocene to early Pleistocene astronomically forced sea-surface productivity and temperature variations in the Mediterranean. *Mar. Micropaleontol.* 19, 49-78.
- Marino, G., Rohling, E.J., Sangiorgi, F., Hayes, A., Casford, J.L., Lotter, A.F., Kucera, M., Brinkhuis, H., 2009. Early and middle Holocene in the Aegean Sea: interplay between high and low latitude climate variability. *Quaternary Sci. Rev.* 28, 3246-3262.
- Mayewski, P.A., Rohling, E.J., Stager, J.C., Karlen, W., Maasch, K.A., Meeker, L.D., Meyerson, E.A., Gasse, F., van Kreveld, S., Holmgren, K., Lee-Thorp, J., Rosqvist, G., Rack, F., Staubwasser, M., Schneider, R.R., Steig, E.J., 2004. Holocene climate variability. *Quaternary Res* 62, 243-255.
- McDermott, F., 2004. Palaeo-climate reconstruction from stable isotope variations in speleothems: a review. *Quaternary Sci. Rev.* 23, 901-918.
- PAGES, 2009. Science Plan and Implementation Strategy. IGBP Report No. 57. IGBP Secretariat, Stockholm. 67pp.
- Proctor, C.J., Baker, A., Barnes, W.L., Gilmour, R.A., 2000. A thousand year speleothem proxy record of North Atlantic climate from Scotland. *Clim. Dynam.* 16, 815-820.
- Raicich, F., Pinardi, N., Navarra, A., 2003. Teleconnections between Indian monsoon and Sahel rainfall and the Mediterranean. *Int. J. Climatol.* 23, 173-186.
- Rimbu, N., Lohmann, G., Lorenz, S.J., Kim, J.H., Schneider, R.R., 2004. Holocene climate variability as derived from alkenone sea surface temperature and coupled ocean-atmosphere model experiments. *Clim. Dynam.* 23, 215-227.
- Roberts, N., Jones, M.D., Benkaddour, A., Eastwood, W.J., Filippi, M.L., Frogley, M.R., Lamb, H.F., Leng, M.J., Reed, J.M., Stein, M., Stevens, L., Valero-Garces, B., Zanchetta, G., 2008. Stable isotope records of Late Quaternary climate and hydrology from Mediterranean lakes: the ISOMED synthesis. *Quaternary Sci. Rev.* 27, 2426-2441.
- Rohling, E.J., 1994. Review and new aspects concerning the formation of eastern Mediterranean sapropels. *Mar. Geology* 122, 1-28.
- Rohling, E.J., Mayewski, P.A., Abu-Zied, R.H., Casford, J.S.L., Hayes, A., 2002. Holocene atmosphere-ocean interactions: records from Greenland and the Aegean Sea. *Clim. Dynam.* 18, 587-593.
- Rohling, E.J., Palikey, H., 2005. Centennial-scale climate cooling with a sudden cold event around 8,200 years ago. *Nature* 434, 975-979.
- Rohling, E.J., Abu-Zied, R., Casford, J.L.S., Hayes, A., Hoogakker, B.A.A., 2009a. The marine environment: present and past. In: Woodward, J.C. (Ed.), *The physical geography of the Mediterranean*. Oxford University Press, Oxford, UK, pp. 33-67.
- Rohling, E.J., Angela, H., Mayewski, P.A., Kucera, M., 2009b. Holocene climate variability in the eastern Mediterranean, and the End of the Bronze Age. In: Bachhuber, C., Roberts, G. (Eds.), *Forces of Transformation: The End of the Bronze Age in the Mediterranean*. Oxbow Books, Oxford, UK, pp. 2-5.
- Rosignol-Strick, M., 1999. The Holocene climatic optimum and pollen records of sapropel 1 in the eastern Mediterranean, 9000-6000 BP. *Quaternary Sci. Rev.* 18, 515-530.
- Spötl, C., Fairchild, I.J., Tooth, A.F., 2005. Cave air control on dripwater geochemistry, Obir Caves (Austria): Implications for speleothem deposition in dynamically ventilated caves. *Geochim. Cosmochim. Acta* 69, 2451-2468.
- Stevens, L.R., Wright, H.E., Ito, E., 2001. Proposed changes in seasonality of climate during the Lateglacial and Holocene at Lake Zeribar, Iran. *Holocene* 11, 747-755.

- Thornthwaite, C.W., 1948. An approach toward a rational classification of climate. *Geographical Review* 38, 55-94.
- Trewartha, G.T., 1981. *The earth's problem climates*. Univ. Wis. Press, Madison, Wisconsin, USA, 371 pp.
- Trigo, I.F., Davies, T.D., Bigg, G.R., 1999. Objective climatology of cyclones in the Mediterranean region. *J Climate* 12, 1685-1696.
- Türkeş, M., 1996. Spatial and temporal analysis of annual rainfall variations in Turkey. *Int. J. Climatol.* 16, 1057-1076.
- Türkeş, M., Erlat, E., 2003. Precipitation changes and variability in turkey linked to the North Atlantic oscillation during the period 1930-2000. *Int. J. Climatol.* 23, 1771-1796.
- Turner, R., Roberts, N., Jones, M.D., 2008. Climatic pacing of Mediterranean fire histories from lake sedimentary microcharcoal. *Global Planet. Change* 63, 317-324.
- Tzedakis, P.C., 2007. Seven ambiguities in the Mediterranean palaeoenvironmental narrative. *Quaternary Sci. Rev.* 26, 2042-2066.
- Vaks, A., Bar-Matthews, M., Ayalon, A., Schilman, B., Gilmour, M., Hawkesworth, C.J., Frumkin, A., Kaufman, A., Matthews, A., 2003. Paleoclimate reconstruction based on the timing of speleothem growth and oxygen and carbon isotope composition in a cave located in the rain shadow in Israel. *Quaternary Res.* 59, 182-193.
- Verheyden, S., Nader, F.H., Cheng, H.J., Edwards, L.R., Swennen, R., 2008. Paleoclimate reconstruction in the Levant region from the geochemistry of a Holocene stalagmite from the Jeita Cave, Lebanon. *Quaternary Res.* 70, 368-381.
- Wanner, H., Beer, J., Butikofer, J., Crowley, T.J., Cubasch, U., Fluckiger, J., Goosse, H., Grosjean, M., Joos, F., Kaplan, J.O., Kuttel, M., Muller, S.A., Prentice, I.C., Solomina, O., Stocker, T.F., Tarasov, P., Wagner, M., Widmann, M., 2008. Mid- to Late Holocene climate change: an overview. *Quaternary Sci. Rev.* 27, 1791-1828.
- Webster, J.W., Brook, G.A., Railsback, L.B., Cheng, H., Edwards, R.L., Alexander, C., Reeder, P.P., 2007. Stalagmite evidence from Belize indicating significant droughts at the time of Preclassic Abandonment, the Maya Hiatus, and the Classic Maya collapse. *Palaeogeogr. Palaeoclimatol.* 250, 1-17.
- Weninger, B., Clare, L., Rohling, E.L., Bar-Yosef, O., Böhrer, U., Budja, M., Bundschuh, M., Feurdean, A., Gebel, H.G., Jöris, O., Linstädter, J., Mayewski, P., Mühlenbruch, T., Reingruber, A., Rollefson, G., Schyle, D., Thissen, L., Todorova, H., Zielhofer, C., 2009. The Impact of Rapid Climate Change on prehistoric societies during the Holocene in the Eastern Mediterranean. *Documenta Praehistorica* 36, 7-59.
- Wick, L., Lemcke, G., Sturm, M., 2003. Evidence of Lateglacial and Holocene climatic change and human impact in eastern Anatolia: high-resolution pollen, charcoal, isotopic and geochemical records from the laminated sediments of Lake Van, Turkey. *Holocene* 13, 665-675.
- Wijmstra, T.A., Young, R., Witte, H.J.L., 1990. An evaluation of the climatic conditions during the late Quaternary in northern Greece by means of multivariate-analysis of palynological data and comparison with recent phytosociological and climatic data. *Geol. Mijnbouw* 69, 243-251.
- Xia, Q.K., Zhao, J.X., Collerson, K.D., 2001. Early-Mid Holocene climatic variations in Tasmania, Australia: multi-proxy records in a stalagmite from Lynds Cave. *Earth Planet. Sci. Lett.* 194, 177-187.
- Ziv, B., Saaroni, H., Alpert, P., 2004. The factors governing the summer regime of the eastern Mediterranean. *Int. J. Climatol.* 24, 1859-1871.





---

**CHAPTER 3****LATE HOLOCENE WINTER TEMPERATURES  
IN THE EASTERN MEDITERRANEAN  
AND THEIR RELATION TO CULTURAL CHANGES:  
THE KOCAIN CAVE RECORD\***

O.M.Göktürk<sup>1,2</sup>, D.Fleitmann<sup>1,2</sup>, S.Badertscher<sup>1,2</sup>  
H.Cheng<sup>3,4</sup>, R.L.Edwards<sup>4</sup>, J.Kramers<sup>1</sup>, O.Tüysüz<sup>5</sup>

1: Institute of Geological Sciences, University of Bern, Bern, Switzerland.

2: Oeschger Centre for Climate Change Research, University of Bern, Bern, Switzerland.

3: Institute of Global Environmental Change, Xi'an Jiaotong University, Xi'an, Shaanxi, China.

4: Department of Geology and Geophysics, University of Minnesota-Twin Cities, Minneapolis, Minnesota, USA.

5: Eurasia Institute of Earth Sciences, Istanbul Technical University, Istanbul, Turkey.

**3.1 Abstract**

Based on the  $\delta^{13}\text{C}$  profile of a stalagmite from the Kocain Cave in southern Turkey, we present a new proxy record of winter temperatures for the Eastern Mediterranean, covering the last ~5700 years with a high temporal resolution (2.3 years on average). In this region, highly resolved paleoclimate records for the cold season are almost non-existent. Comparison of the recent part of the record with meteorological observations reveals that, stalagmite  $\delta^{13}\text{C}$  at this site has a slow (decadal) response to the amount of snowfall above the cave, which correlates well with average winter temperatures. Cold periods in the rest of the record coincide with widespread glacier advances, especially with the ones in the Alps during the Bronze Age – Iron Age transition (from ~1000 BC on) and the late Little Ice Age (~1600 to 1850 AD). This further supports the interpretation of  $\delta^{13}\text{C}$  as a temperature proxy. Although the winters during the Medieval Climate Anomaly were not continuously warm in the Eastern Mediterranean, winter warmth in the modern era was matched or exceeded several times in the last ~5700 years, especially during the time of Minoan civilization in Crete (~2700 to 1200 BC). Moreover, we provide evidence for the argued role of winter cold and drought in the events leading to the unrest in the 16<sup>th</sup> century Anatolia, during the Ottoman rule. The Kocain Cave record brings insights into several climatically-induced historical changes in the Eastern Mediterranean, and has the potential to be a key record for the region, which has a long and rich human history.

\* To be submitted to *Earth and Planetary Science Letters*

## 3.2 Introduction

In the second half of the Holocene which covers roughly the last 6000 years, boundary conditions of the global climate system (e.g. orbital parameters, ice sheet extent) have not changed much (Wanner et al., 2008). Understanding the regional variability of climate over this period is of particular importance for assessing the significance of current and future climate change, as the same boundary conditions will be valid in the next few centuries. Moreover, numerous culturally disruptive climatic deteriorations occurred during the late Holocene (deMenocal, 2001). Several of these 'events', such as the proposed widespread drought at ~4.2 ka BP (Weiss et al., 1993; Staubwasser and Weiss, 2006) and the 'Rapid Climate Change's (RCCs, Mayewski et al., 2004) probably had profound influences on the ancient Eastern Mediterranean civilizations (Weiss et al., 1993; Weninger et al., 2009). Construction of highly resolved proxy records that can reveal regional responses to larger scale climate forcings is therefore crucial (PAGES, 2009), especially for the Eastern Mediterranean, where the effects of global warming can be critical for modern societies (IPCC, 2007).

Paleoclimate records covering the late Holocene (especially the last 1000 to 1500 year period) are actually large in number and widely distributed (Wanner et al., 2008), owing primarily to the abundance of tree proxies. For example, in the global temperature reconstruction of Mann et al. (2009), all proxy records for the Mediterranean basin (except one documentary) are either ring widths or maximum latewood densities of trees. However, despite their almost perfect dating and annual resolution, tree proxies are largely insensitive to temperature variations in the cold season (Hughes, 2002; Mangini et al., 2007). In this respect, speleothems are a feasible option to fill the gap, as they can record various aspects of climate such as mean annual temperature and rainfall variability, provided that the study site and the sample is chosen carefully (McDermott, 2004).

In this paper, we present a new high resolution stalagmite record from the Kocain Cave in southern Turkey (near Antalya), covering the last ~5700 years. Thanks to the strong seasonality of precipitation in this area (favoring winter) and the characteristics of the cave site, calcite  $\delta^{13}\text{C}$  respond to winter temperatures on a decadal scale. We hypothesize that this occurs through the response of the soil-bedrock-cave system to variations in snowfall amount above the cave, and we provide evidence for this hypothesis by comparing the most recent part of our record with local meteorological observations. Further comparison with periods of global glacier advances reveals that our interpretation is probably correct and  $\delta^{13}\text{C}$  is a good approximation of winter temperatures. This is the first study to show this unique response of stalagmite  $\delta^{13}\text{C}$  to climatic conditions above a cave, making the Kocain Cave record a potential key record for the late Holocene winter climate and cultural history in the Eastern Mediterranean. We demonstrate this over some important issues of the late Holocene climatic and cultural changes; such as the hypothesis of a persistent positive winter North Atlantic Oscillation (NAO) during Medieval time (Mann et al., 2009; Trouet et al., 2009) or the possible role of climate in the events leading to Bronze Age collapse at ~1150 BC (Weninger et al., 2009).

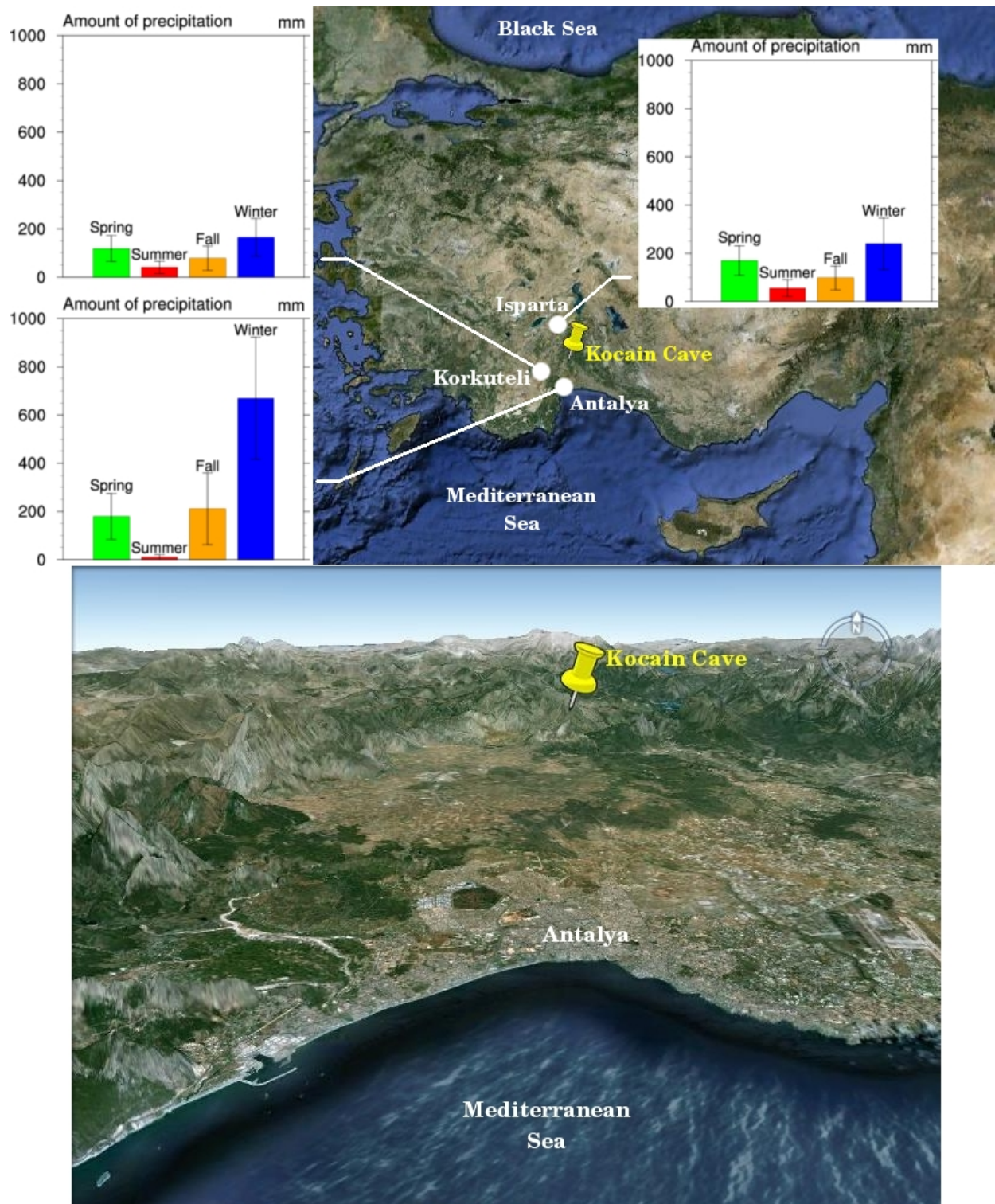


**Fig. 3.1: Upper:** Location of Kocain Cave and the nearby three meteorological stations; along with their seasonal distribution of precipitation. Meteorological data were obtained from the State Meteorological Service of Turkey. **Lower:** Location of Kocain Cave in an inclined view from the south, with respect to Antalya city center and the Mediterranean Sea (the bay of Antalya).

### 3.3 Kocain Cave: Climatic and Environmental Setting

Kocain Cave (entrance: 37°13'57" N, 30°42'42" E, 870 m asl) is located in southern Turkey, 38 km north (beeline) of Antalya city center (Fig. 3.1). As its name implies (“BigCave” in Turkish), the cave is a huge hole inside a mountain named İndağı (“CaveMountain”). In fact, it is the largest cave in Turkey in terms of opening width (70 m) and gallery size (36000 m<sup>2</sup>) (Tay Project, 2011). It has a horizontal length of 633 m and a ceiling height of up to 80 m (BÜMAK, 2011). Accordingly, Kocain Cave had been inhabited on and off since prehistoric times, until it was forgotten during the Ottoman period (Tay Project, 2011). The terrain above the cave is a moderately steep, exposed slope that is covered -albeit somewhat sparsely- by typical Mediterranean vegetation, consisting mainly of evergreen shrubs (Fig. 3.S1 and 3.S2). Because of this terrain, human impact on the land above the cave is highly unlikely. There is currently no human settlement nearby.

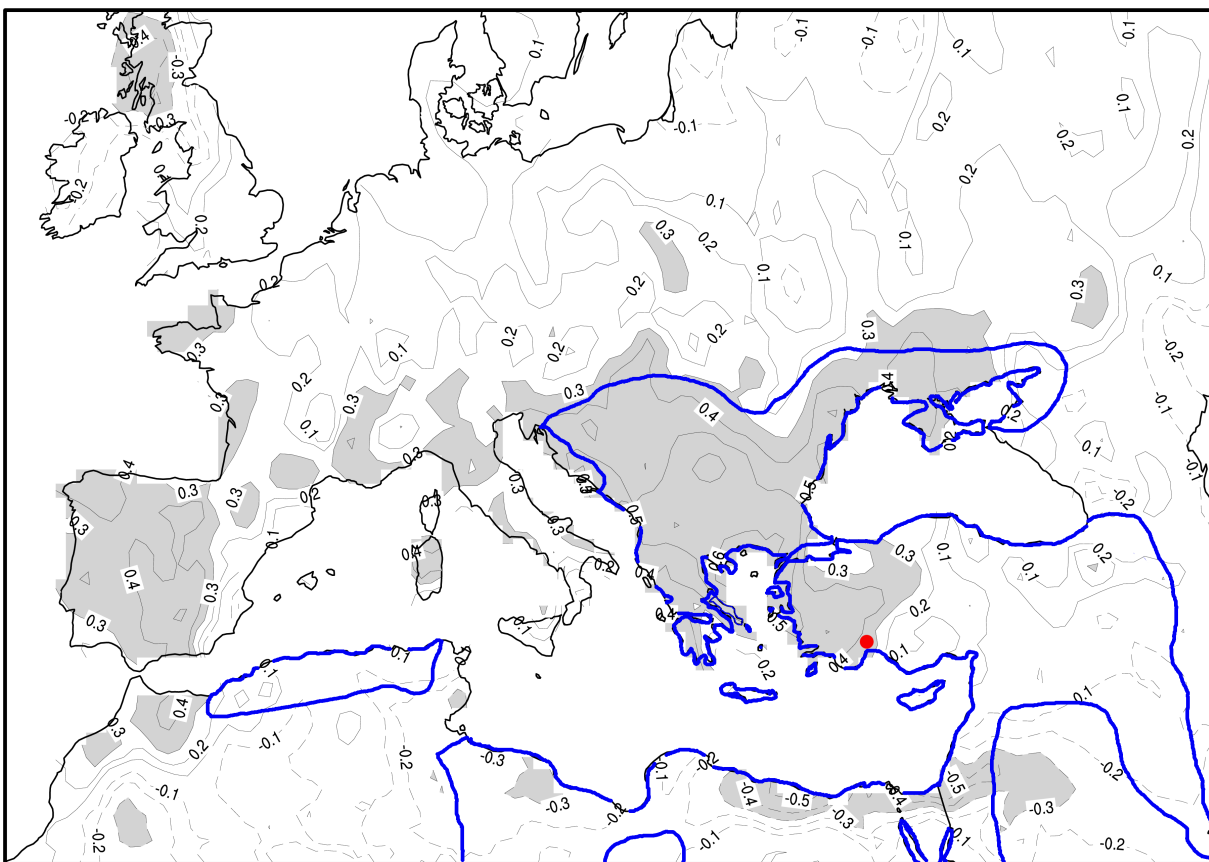


**Fig. 3.2:** Correlation coefficients of Antalya's (red dot) winter (DJF) temperatures with gridded winter/spring (DJFMAM) precipitation time series (CRU 2.1, Mitchell and Jones, 2005). Areas where the correlations are statistically significant (95%) are shaded gray. Negative correlations are shown by dashed lines. Approximate borders of the Ottoman Empire at 1566 AD (their apogee; Shaw, 1976) are shown by blue contours.

Coastal Antalya area has a typical Mediterranean climate with hot, dry summers and mild, rainy winters. According to the Turkish Meteorological Service's observations in Antalya city center dating back to 1930, the mean temperature of the coldest month (January) is 9.7° C, and the most (~65%) of total precipitation occurs in winter (DJF), reaching a seasonal total of ~670 mm on average (Fig. 3.1). However, this last value is very variable ( $\sigma = 500$  mm), implying the large year to year asymmetry of the Mediterranean

winter rainfall. The interior plateau features a markedly different climate. For instance, just 100 km (beeline) from Antalya center and at an elevation of 1035 m asl (Fig. 3.1), Isparta has a coldest month (January) average temperature of 1.7° C, and a mean DJF precipitation of only 230 mm, almost one third of that of Antalya. This is a direct consequence of the Taurus mountain range, which forms a barrier between the coastal and the interior part of this region. (Fig. 3.1).

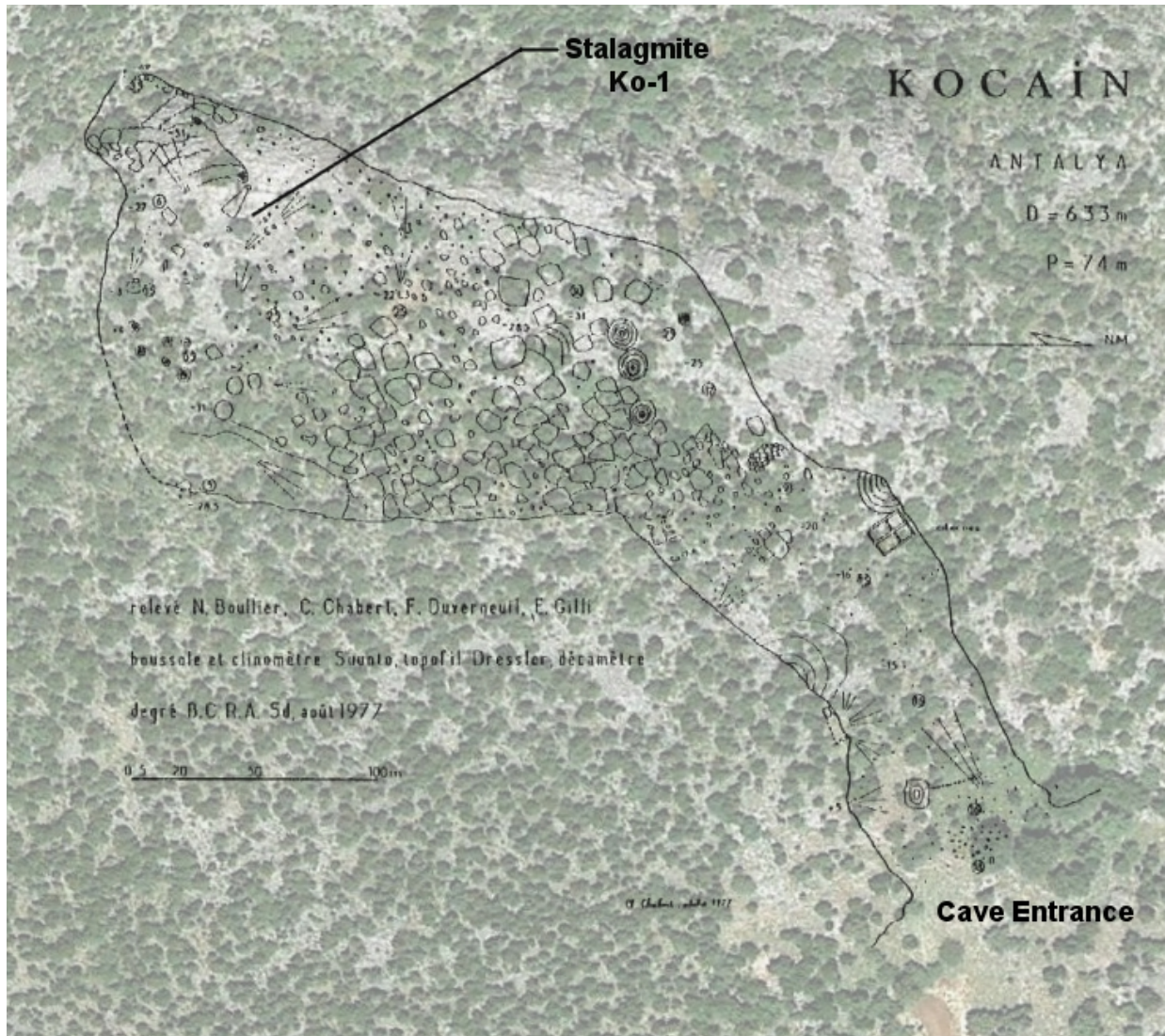


**Fig. 3.S1:** Plan of the Kocain Cave shown on top of the terrain above it. The approximate location of stalagmite Ko-1 in the cave is marked. The plan was retrieved from the web site of Boğaziçi University Caving Club (BÜMAK, 2011). Terrain image is from GoogleEarth.

Since there is no station in the immediate vicinity of the Kocain Cave possessing a long meteorological record and the topography of this region is quite complex, exact location of the cave site is critical for correctly assessing its climate characteristics. The cave is located on the first series of heights that mark the end of the Antalya Travertine Plateau (Fig. 3.1). There is no higher hill that could hinder the southerly moist air coming from the Mediterranean to reach the cave site. Rain-out due to the distance from the shore is probably compensated by uplift of moist air masses against the hills. Therefore we assume

that, precipitation-wise, the Kocain Cave has the characteristics of the Antalya meteorological station. Temperature must also vary in tandem with Antalya, although being lower owing to the altitude.

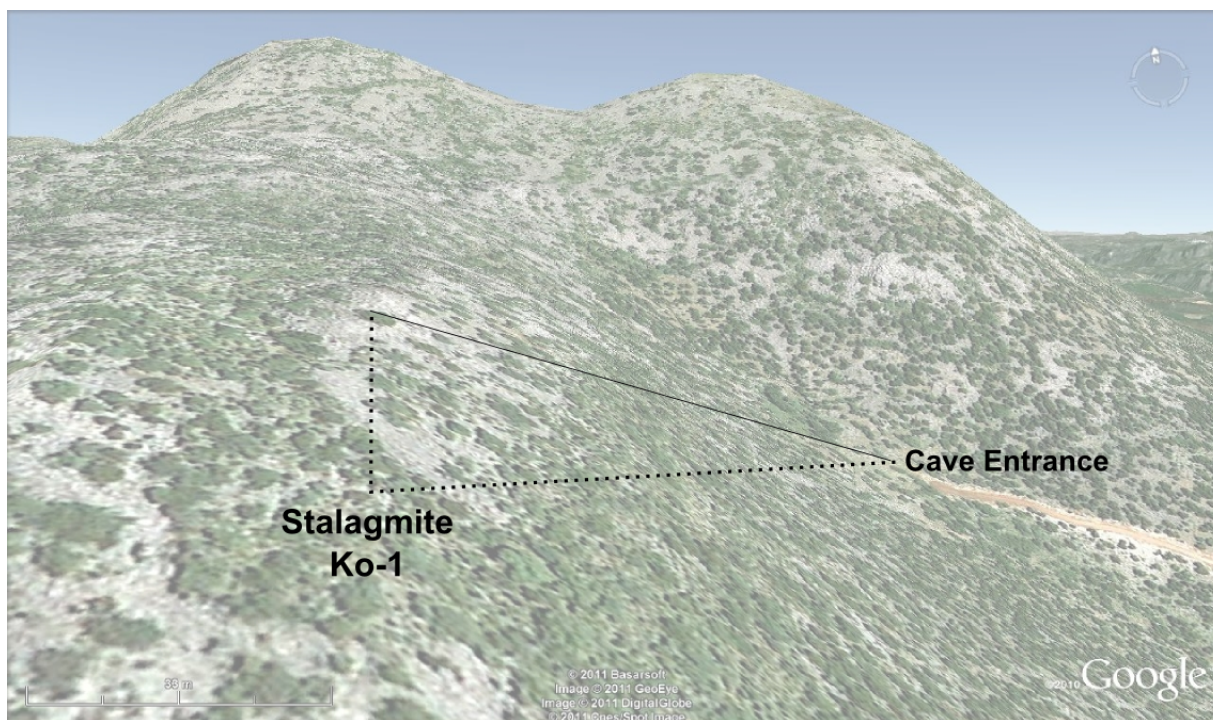


**Fig. 3.S2:** The slope under which the Kocain Cave resides. Dashed lines mark the position of stalagmite Ko-1 in the cave with respect to the overlying terrain and the cave entrance. Image is from GoogleEarth.

Winter is the key season for our paleoclimatic interpretations, as it is the main hydrological season at the cave site. Located in the Eastern Mediterranean, winter climate in Antalya is controlled by the main Eurasian climatic patterns, namely the North Atlantic Oscillation (NAO; Hurrell, 1995) and the North Sea – Caspian pattern (NCP, Krichak et al., 2002). Very broadly, positive (negative) modes of both patterns lead to cooler (warmer) and drier (wetter) conditions in southern Turkey (Krichak et al., 2002; Kutiel et al., 2002; Türkeş and Erlat, 2003; Türkeş and Erlat, 2009), though correlations are not high ( $r < 0.5$ ). Accordingly, winter temperature and precipitation time series show significant positive correlations as well. In Fig. 3.2, correlation coefficients between Antalya's winter temperature series and the gridded winter/spring precipitation series (Mitchell and Jones, 2005) are shown. As a winter temperature proxy (Section 3.5.2.1.) is presented, the intention of this figure is to assess the representativeness of Antalya's winter temperatures for precipitation in Mediterranean borderlands.

### 3.4 Material and Methods

The  $^{230}\text{Th}$  dated Kocain Cave stable isotope ( $\delta^{13}\text{C}$  and  $\delta^{18}\text{O}$ ) record is based on a 32 cm long stalagmite, Ko-1. The stalagmite was collected almost at the end of the 633 m long Kocain Cave, in August 2005. Above the cave section where the stalagmite was located, the terrain (960 m asl) is partially barren. Calcite samples were taken every 0.1 mm and 0.2 mm within the upper 17.5 cm and lower 14.5 cm portions of Ko-1, respectively. This was done using a digitally controlled micromill through continuous trenches along the growth axis of

the stalagmite. Stable isotope ( $\delta^{13}\text{C}$  and  $\delta^{18}\text{O}$ ) content of the resulting samples were measured at the Institute of Geological Sciences, University of Bern (Switzerland); on a Finnigan Delta V Advantage mass spectrometer equipped with an automated carbonate preparation system (Gas Bench-II). Larger quantity calcite samples were obtained by a dental drill for  $^{230}\text{Th}$  dating.  $^{230}\text{Th}$  measurements were performed on multi-collector inductively coupled plasma mass spectrometers at the Minnesota Isotope Laboratory, University of Minnesota, USA (MC-ICP-MS, Thermo-Finnigan-Neptune); and at the Institute of Geological Sciences, University of Bern, Switzerland (Nu Instruments MC-ICP-

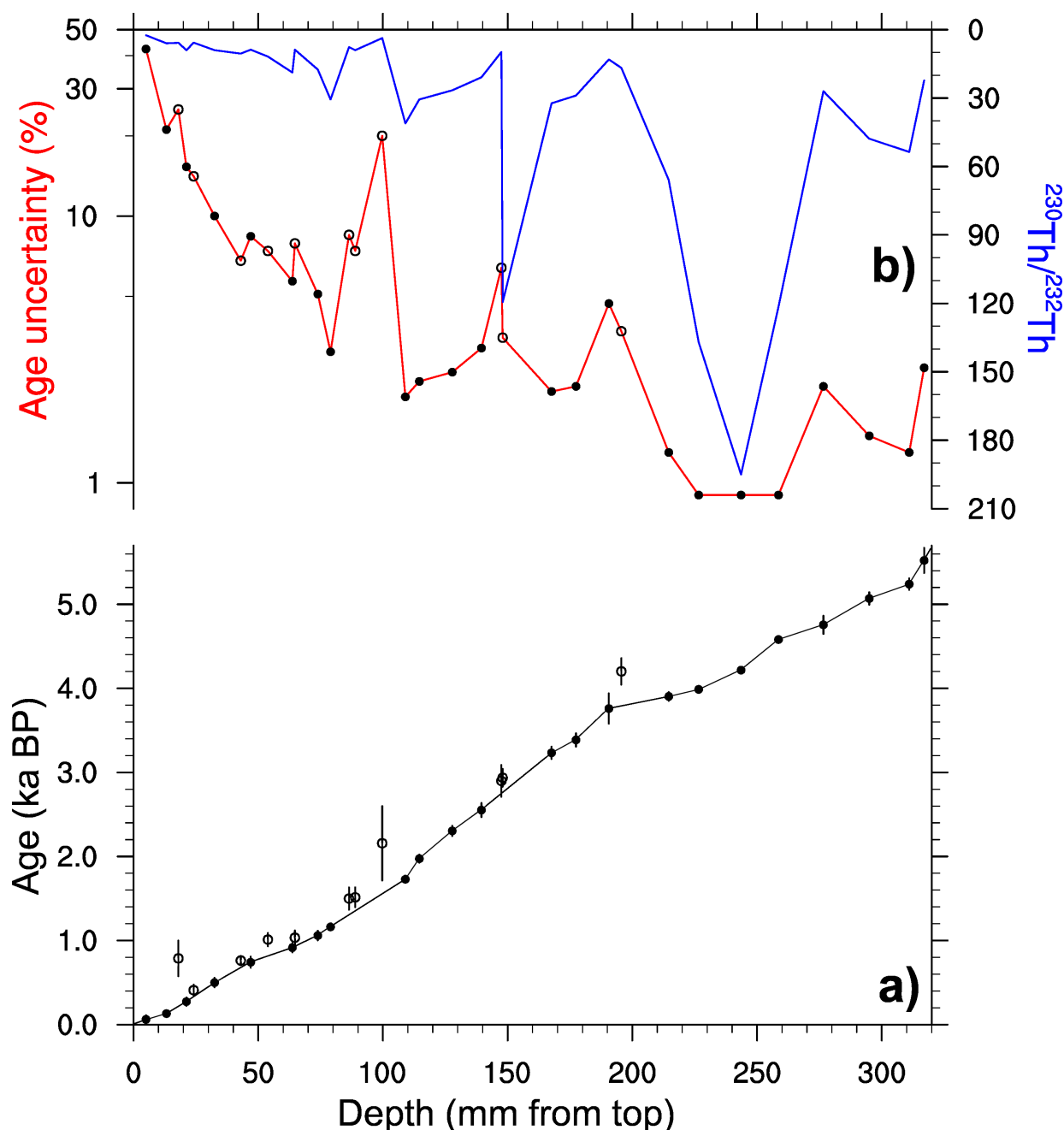


**Fig. 3.3:** Chronology of the stalagmite Ko-1. **a)** Age versus depth plot.  $^{230}\text{Th}$  dates used in the construction of the age model are marked with full circles, whereas hollow circles show the discarded dates. Absolute age uncertainties are designated with bars on each  $^{230}\text{Th}$  date. BP stands for “Before Present”, where Present is defined as 1950 AD. **b)** Age uncertainties on each  $^{230}\text{Th}$  date as percentages (red curve) and the corresponding  $^{230}\text{Th}/^{232}\text{Th}$  ratio (blue curve). Uncertainties of discarded  $^{230}\text{Th}$  dates are marked by a hollow circle.

MS). Further details on stable isotope analyses and  $^{230}\text{Th}$  dating method are provided by Fleitmann et al. (2009) and Badertscher et al. (2011).

### 3.5 Results and Discussion

#### 3.5.1 Chronology and Growth Rates

The age-depth plot for stalagmite Ko-1 is given in Fig. 3.3a. The age model is based on linear interpolation through 23 stratigraphically ordered  $^{230}\text{Th}$  dates, out of 34 measured. Chronological uncertainties for  $^{230}\text{Th}$  dates are between 0.9% and 42.3% (Fig. 3.3b) around an average of 7.2%. Low  $^{230}\text{Th}/^{232}\text{Th}$  (Fig. 3.3b) implying detrital contamination (Richards and Dorale, 2003), along with the low  $^{238}\text{U}$  contents of around ~100 ppb is the most probable cause for the observed large uncertainties (See Appendix A for tabulated results of  $^{230}\text{Th}$  dating on stalagmite Ko-1).

Stalagmite Ko-1 grew with no detectable hiatus from ~5.5 ka BP (~3500 BC) on and was actively growing before being sampled in 2005. This is also evident from the slope of the age-depth line after the youngest  $^{230}\text{Th}$  date of 61 years BP at 5 mm depth (Fig. 3.3a), which indicates a continuing growth consistent with the lower parts of the stalagmite. ('BP' stands for 'Before Present', where present is defined as 1950 AD).

Growth rates between successive  $^{230}\text{Th}$  dates were also calculated. Values range between ~0.02 and ~0.17 mm/yr, with an average of ~0.07 mm/yr (Fig. 3.4c). Compared to other moist Mediterranean sites where rates of 0.30 – 0.40 mm/yr or greater are common (Fairchild et al., 2006), the growth of our stalagmite is very slow. A plausible explanation for this can be found in the presence of a partially barren, steep, and thus run-off prone terrain (Dunne et al., 1991) above that section of the Kocain Cave, from which our stalagmite was sampled (Figs. S1 and S2). Sparse vegetation keeps the soil  $p\text{CO}_2$  low, leading to lower amounts of dissolved  $\text{CaCO}_3$  in drip waters and in turn low calcite deposition in the cave (Baldini et al., 2005). Moreover, enhanced run-off reduces infiltration and drip rates, directly limiting stalagmite growth.

#### 3.5.2 Stable Isotope Profiles and Their Interpretation

A total of 2476 stable isotope ( $\delta^{13}\text{C}$  and  $\delta^{18}\text{O}$ ) measurements were performed, resulting in an average temporal resolution of 2.3 years.

##### 3.5.2.1 $\delta^{13}\text{C}$

In temperate regions where C3-type vegetation is dominant, as in the site of Kocain Cave, speleothem  $\delta^{13}\text{C}$  values are typically found to be in the range of -14 to -6‰ (McDermott, 2004). However, the  $\delta^{13}\text{C}$  profile in the Kocain record vary between ~-9.0 and -2.5‰ (Fig. 3.4b), around an average of -5.8‰. Low vegetation cover and ineffective infiltration, both of which gave rise to the observed low growth rates (Section 3.5.1, this paper) should be major factors for the higher than expected calcite  $\delta^{13}\text{C}$  as well. Little biogenic carbon in the overlying soil and enhanced  $\text{CO}_2$  degassing due to low drip rates in the cave cause a general enrichment of heavy carbon isotope in speleothems (Baker et al., 1997; Baldini et al., 2005), and this is also valid for the Kocain Cave.



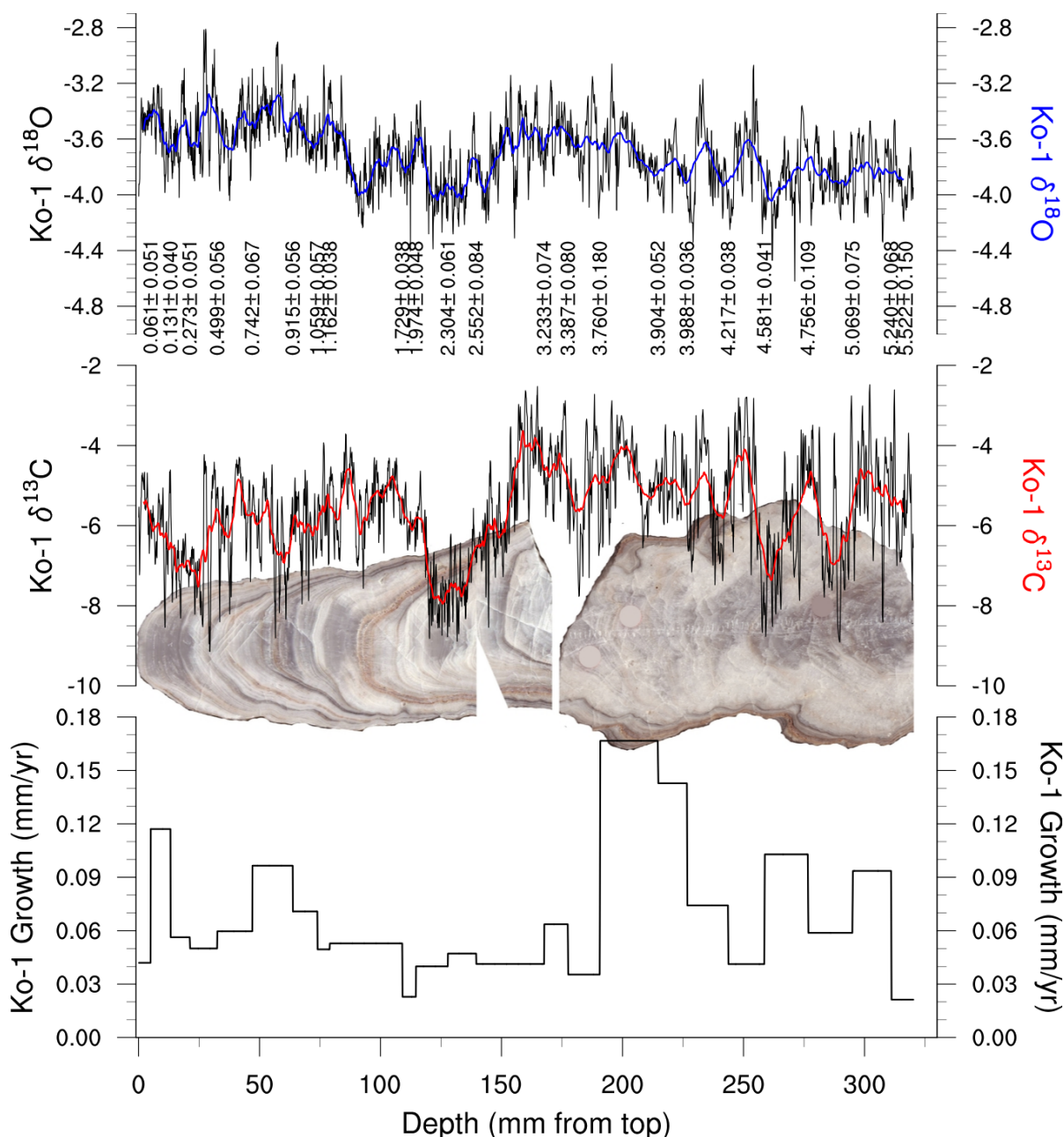


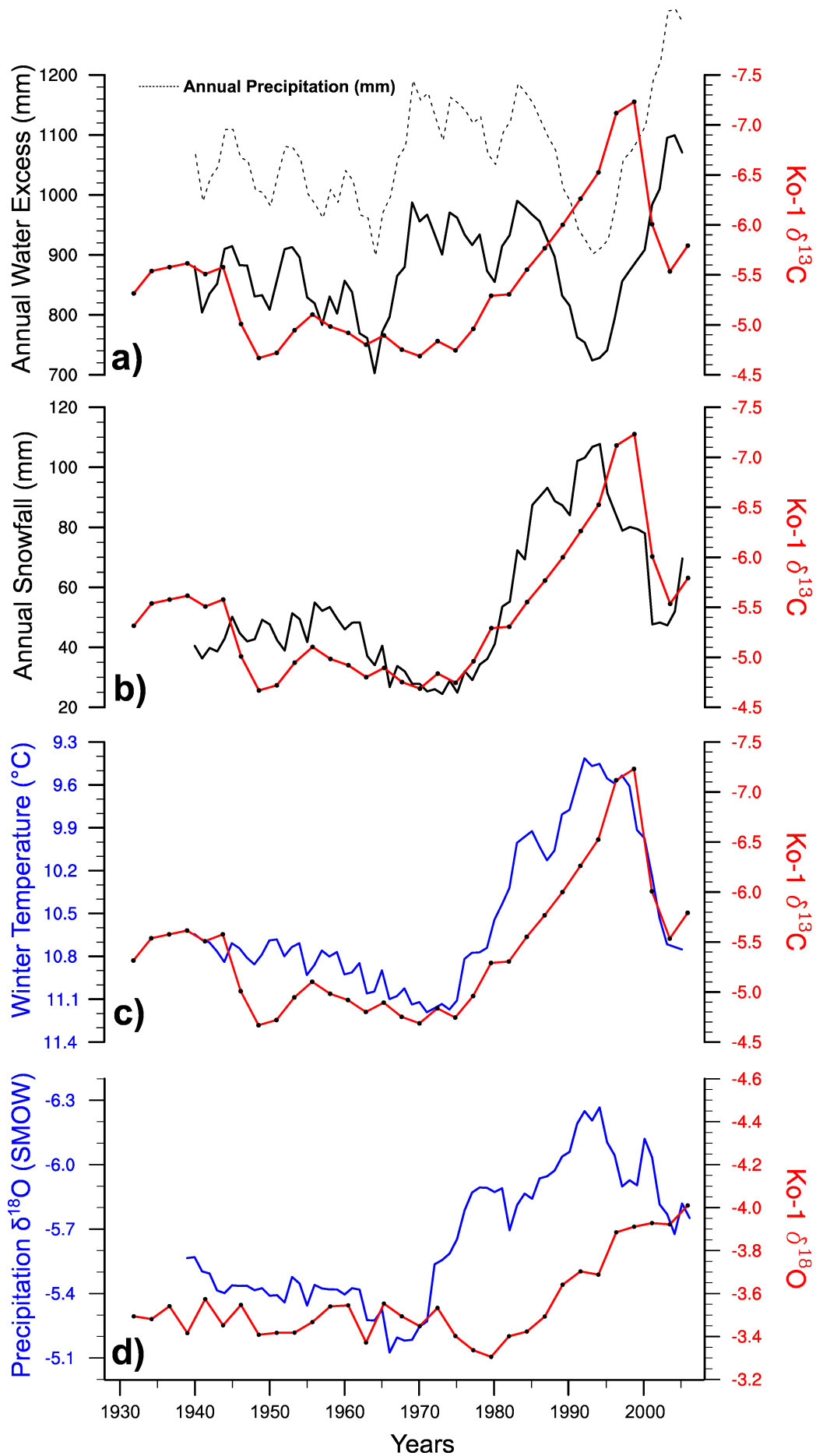
**Fig. 3.4:** Parameters of the Kocain Cave record on a depth scale along with an image of the stalagmite Ko-1. **a)**  $\delta^{18}\text{O}$  (VPDB). **b)**  $\delta^{13}\text{C}$  (VPDB). In each plot, black curve is the raw values, whereas the blue/red curves are 43-point running averages, corresponding approximately to centennial means. Numbers between plots **a** and **b** are the  $^{230}\text{Th}$  dates (ka BP) used in the age model and their associated uncertainties. BP stands for “Before Present”, where Present is defined as 1950 AD. **c)** Growth rates of the stalagmite calculated using the  $^{230}\text{Th}$  dates shown in this plot.

As the density of vegetation can be assumed quasi-constant on short time scales, amount and timing of actual infiltration should be the main climatic factors controlling  $\delta^{13}\text{C}$  variations in our record. Therefore, we compared the most recent section of the  $\delta^{13}\text{C}$  profile with various parameters derived from the precipitation amounts measured at the Antalya meteorological station. Fig. 3.5a shows the comparison of  $\delta^{13}\text{C}$  and the annual ‘water excess’, calculated according to the formula of Thornthwaite (1948). Clearly, there is no response from  $\delta^{13}\text{C}$  to the variations in total amount of precipitation that can potentially

recharge the groundwater. This also supports the assumption of very low actual infiltration into the aquifer feeding stalagmite Ko-1 (Section 3.5.1). An almost uniform difference between the excess water and bulk precipitation (Fig. 3.5a, dashed line) reflects the seasonal invariability of precipitation. There is also no correspondence of more negative  $\delta^{13}\text{C}$  values with the excess water amount during spring and summer (not shown), which rules out the possible importance of precipitation falling in the vegetation growing season (Baker et al., 1997).

At this point, one promising approach is to consider the impact of snowfall on groundwater recharge. It has been shown that snowmelt's contribution to recharge may well exceed the proportion of snow in average annual precipitation (Maule et al., 1994; Earman et al., 2006 and references therein). That is, a shift from rain to snow can cause significantly increased recharge (Earman et al., 2006). Snowmelt is also effective at rewetting soils (Fairchild et al., 2006), and especially at replenishing the water deep in the soil (Gazis and Feng, 2004), which can enhance the uptake of the lower  $\delta^{13}\text{C}$  soil  $\text{CO}_2$ . Moreover, slow and delayed infiltration of snowmelt (Bakalowicz et al., 2008) may shift the timing of soil wetting to the vegetation growing season, which will further increase the lower  $\delta^{13}\text{C}$  biogenic carbon in groundwater. At a cave site such as Kocain, where run off is apparently substantial, these factors should have even more influence. Therefore, we estimated the annual snowfall amounts above the Kocain Cave. Daily snowfall amounts were calculated according to the method of Pipes and Quick (1977) outlined by Kienzle (2008), using daily mean temperature and rainfall measured in Antalya station. The environmental lapse rate value of 6.5 K/km was incorporated to estimate the temperature difference between Antalya meteorological station (51 m asl) and Kocain Cave site (960 m asl). Indeed, Fig. 3.5b reveals that the stalagmite Ko-1  $\delta^{13}\text{C}$  values are chiefly controlled by variations in snowfall. The shift of  $\delta^{13}\text{C}$  to more negative values in the cold and snowy 1980s (Fig. 3.5b-c) is particularly convincing, as this decade is one of the driest periods in Antalya's meteorological record (Fig. 3.5a). This means that even if the total amount of precipitation decreases, the above mentioned factors lead to a more negative  $\delta^{13}\text{C}$  owing to colder conditions and increased snowfall. The low frequency variability of  $\delta^{13}\text{C}$  and the fact that it best correlates with a smoothed climate signal (average snowfall amount of the preceding 10 years, Fig. 3.5b) are indicative of storage and mixing effects in the karst aquifer (Baker et al. 2007) and a  $\delta^{13}\text{C}$  response to decadal climate trends. Low drip and stalagmite growth rates, as well as the ~80 m thick bedrock above the section of the Kocain Cave where stalagmite Ko-1 was sampled (Fig. 3.S2) are all consistent with these observations.

**Fig. 3.5 (see right):** Comparison of the most recent section of stalagmite Ko-1 stable isotope profiles (red curves, note descending axes!) with various parameters derived from the meteorological and GNIP precipitation isotope (IAEA/WMO, 2006) records of Antalya station. For meteorological and GNIP records plotted, every value is the average value of the preceding 10 years including that year (see main text for further explanation). Kocain Cave stable isotope profiles are shown with red lines with black dots on, representing each data point. **a)** Annual water excess (full black line) calculated by the method of Thorntwaite (1948) versus Kocain  $\delta^{13}\text{C}$ . Negative monthly water excess values were taken as zero. Annual gross (bulk) precipitation amount is shown with a dashed line. **b)** Annual snowfall above the cave versus Kocain  $\delta^{13}\text{C}$ . See Section 3.5.2.1 for the details of the calculation. **c)** Winter (DJF) temperature (note descending axis!) versus Kocain  $\delta^{13}\text{C}$ . **d)** GNIP precipitation  $\delta^{18}\text{O}$  (note descending axis!) versus Kocain Cave  $\delta^{18}\text{O}$ . In the calculation of annual average values, monthly precipitation  $\delta^{18}\text{O}$  was weighted by monthly water excess (Thorntwaite, 1948). Missing monthly  $\delta^{18}\text{O}$  values were estimated using the long term mean  $\delta^{18}\text{O}$  value for that month and the temperature deviation from the monthly long term mean temperature. A +0.6‰ change in  $\delta^{18}\text{O}$  was assumed for every 1.0 °C monthly temperature increase (Rozanski et al., 1993). All meteorological data were obtained from the State Meteorological Service of Turkey.



Possible influence of cave air circulation on stalagmite  $\delta^{13}\text{C}$  is probably negligible, since colder winters were shown to cause an enrichment of  $\delta^{13}\text{C}$  through flushing of low  $p\text{CO}_2$  into the cave (Spötl et al., 2005), which is opposite to what is observed in our record (Fig. 3.5c). One discrepancy is the lack of any consistent correlation between growth rates and  $\delta^{13}\text{C}$  in the last 5.5 ka (Fig. 3.4b-c). Enhanced snowmelt infiltration should normally cause more negative  $\delta^{13}\text{C}$  as well as higher growth rates, but this does not seem to be the case. However, it should be noted that the factors leading to faster stalagmite growth, namely higher temperatures and increased drip rates (Genty et al., 2001; Baker et al., 1998), have competing sources in our context; since increased drip rates are associated with snowfall and colder conditions.

To sum up, we argue that the Ko-1  $\delta^{13}\text{C}$  record can be used as a winter temperature proxy, since it matches well both with winter temperature and snowfall amount in the last 65 years, consistent with cave site characteristics. Snowmelt is the major contributor of groundwater recharge above the Kocain Cave. It also increases the amount of lower  $\delta^{13}\text{C}$  soil  $\text{CO}_2$  in the percolating waters via slow infiltration that can be delayed into vegetation growing season.

### 3.5.2.2 $\delta^{18}\text{O}$

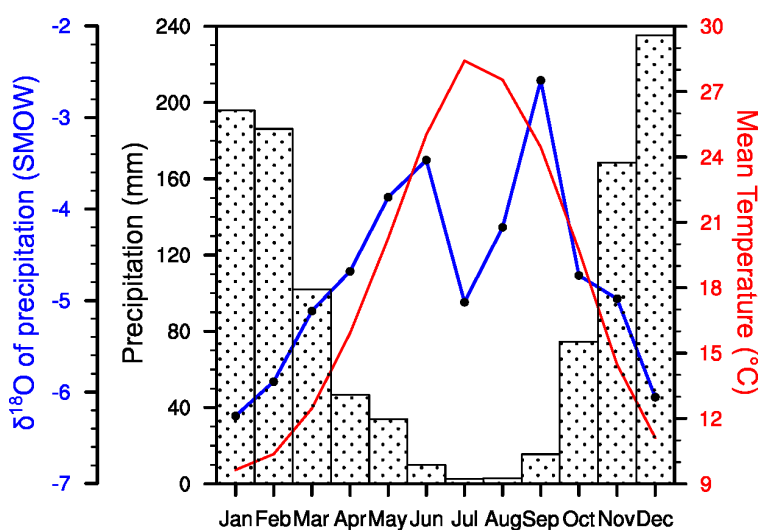


**Fig. 3.6:** Long term monthly mean temperatures (red curve) and precipitation (bars) for the station of Antalya, in relation with  $\delta^{18}\text{O}$  values in precipitation (blue curve; IAEA/WMO, 2006). Meteorological data were obtained from the State Meteorological Service of Turkey.

$\delta^{18}\text{O}$  values in stalagmite Ko-1 range from  $\sim -4.6$  to  $-2.8\text{‰}$  (Fig. 3.4b) with a mean of  $-3.7\text{‰}$ , showing much less variability than that of  $\delta^{13}\text{C}$ . A statistically significant (above 99% level), although not so high correlation ( $r^2 = 0.18$ ,  $r = 0.42$ ) between  $\delta^{18}\text{O}$  and  $\delta^{13}\text{C}$ , as well as the greater range of variability of  $\delta^{13}\text{C}$  than  $\delta^{18}\text{O}$  suggest that, fluctuations in the two proxies are interrelated and disequilibrium fractionation probably plays a role in isotopic variations (Baker et al., 2007). It is very difficult though to check possible kinetic effects by applying a lateral 'Hendy test' (Hendy, 1971) on stalagmite Ko-1, as the overall growth rate is very

low and sampling within a single growth layer is virtually impossible. Nevertheless, covariation of  $\delta^{18}\text{O}$  and  $\delta^{13}\text{C}$  in Ko-1 should mainly be climate-controlled, since the amount of  $\text{CO}_2$  degassing in the cave (thus the degree of kinetic fractionation) is associated with drip rates (Fairchild et al., 2006 and references therein), which we attribute to changes in snowfall amount and winter temperature (Section 3.5.2.1). Several other authors (e.g. Lachniet et al., 2004; Fleitmann et al., 2004) also interpreted this isotopic covariation in terms of climate; and as long as there is no aim of reconstructing temperatures or rainfall precisely, it is regarded a reasonable assumption (Fairchild et al., 2006). The inference that

snowmelt is the major part of infiltrating precipitation (Section 3.5.2.1.) may seem contradictory with the high stalagmite  $\delta^{18}\text{O}$  values ( $\sim -4.6$  to  $-2.8\text{‰}$ ), compared to those observed at other Mediterranean sites such as the Soreq Cave (Bar-Matthews et al., 2003). However, snow is known to become isotopically enriched until it melts (Taylor et al., 2001; Unnikrishna et al., 2002; Earman et al., 2006; Koeniger et al., 2008; Lee et al., 2010), reportedly reaching a composition similar to that of rain at the same site (Earman et al., 2006). Considering also the kinetic fractionation which leads to higher  $\delta^{18}\text{O}$ , measured values in stalagmite Ko-1 are not too distant from the minimum monthly  $\delta^{18}\text{O}$  values of  $\sim -6.0$  measured in precipitation in Antalya (Fig. 3.6). Although  $\delta^{18}\text{O}$  and  $\delta^{13}\text{C}$  are moderately correlated throughout the record, their trends over longer time intervals are not always similar (Fig. 3.4a-b). For instance, in the last 25 years, one can observe a low amplitude yet persistent decline in  $\delta^{18}\text{O}$  (Fig. 3.5d) despite recovering winter temperatures and increasing  $\delta^{13}\text{C}$  in the last 10 years of the record (Fig. 3.5c). Therefore, other factors such as seasonality of precipitation, the 'amount effect' or the changing isotopic composition of vapor source (McDermott, 2004) must also be taken into account. Although precipitation is highly seasonal in this region (65% in DJF, 92% in NDJFM) and infiltration is apparently limited to winter months (Section 3.5.2.1), we compared  $\delta^{18}\text{O}$  with the mentioned meteorological parameters to rule out any possible relationship. As expected, none of these comparisons (not shown) reveal a correlation of  $\delta^{18}\text{O}$  either with the seasonality of precipitation or the amount of rainfall. Furthermore, mentioned downtrend in Ko-1  $\delta^{18}\text{O}$  is not corroborated by the precipitation  $\delta^{18}\text{O}$  data set of Antalya (Fig. 3.5d). Thus, it is unclear at the moment what determines Kocain  $\delta^{18}\text{O}$  when it does not follow  $\delta^{13}\text{C}$ . Longer term trends in  $\delta^{18}\text{O}$  may be partly attributed to changes in the isotopic composition of the Eastern Mediterranean sea, as this is the major moisture source for the area. The influence of changes in the isotopic composition of Mediterranean Sea has been demonstrated by Bar-Matthews et al. (2003) for the Soreq Cave in Israel, and recently by Badertscher et al. (2011) for the Sofular Cave near the Black Sea coast. Unfortunately, reconstructions of oxygen isotopic composition for the Eastern Mediterranean sea that cover middle to late Holocene (Fontugne and Calvert, 1992; Kuhnt et al., 2008) are too coarsely resolved to be meaningfully compared with Ko-1  $\delta^{18}\text{O}$ , also are far away to be representative for Kocain Cave site.

Future studies concerning the Kocain Cave should focus on deciphering the evolution of water  $\delta^{18}\text{O}$  until it reaches the stalagmite (e.g. cave monitoring along with precipitation and snowpack isotope measurements); so that a more robust interpretation of Kocain  $\delta^{18}\text{O}$  can be made. For the time being, we will stick to  $\delta^{13}\text{C}$  for our paleoclimatic interpretations.

### **3.5.3 Implications for Late Holocene Climate and Cultural Changes in the Eastern Mediterranean**

Winter temperature variability at Kocain Cave site since  $\sim 3700$  BC, inferred from the  $\delta^{13}\text{C}$  profile of stalagmite Ko-1, is given in Fig. 3.7. Some of the important implications of this new record concerning regional and global climate dynamics, as well as cultural changes, are elaborated on below.

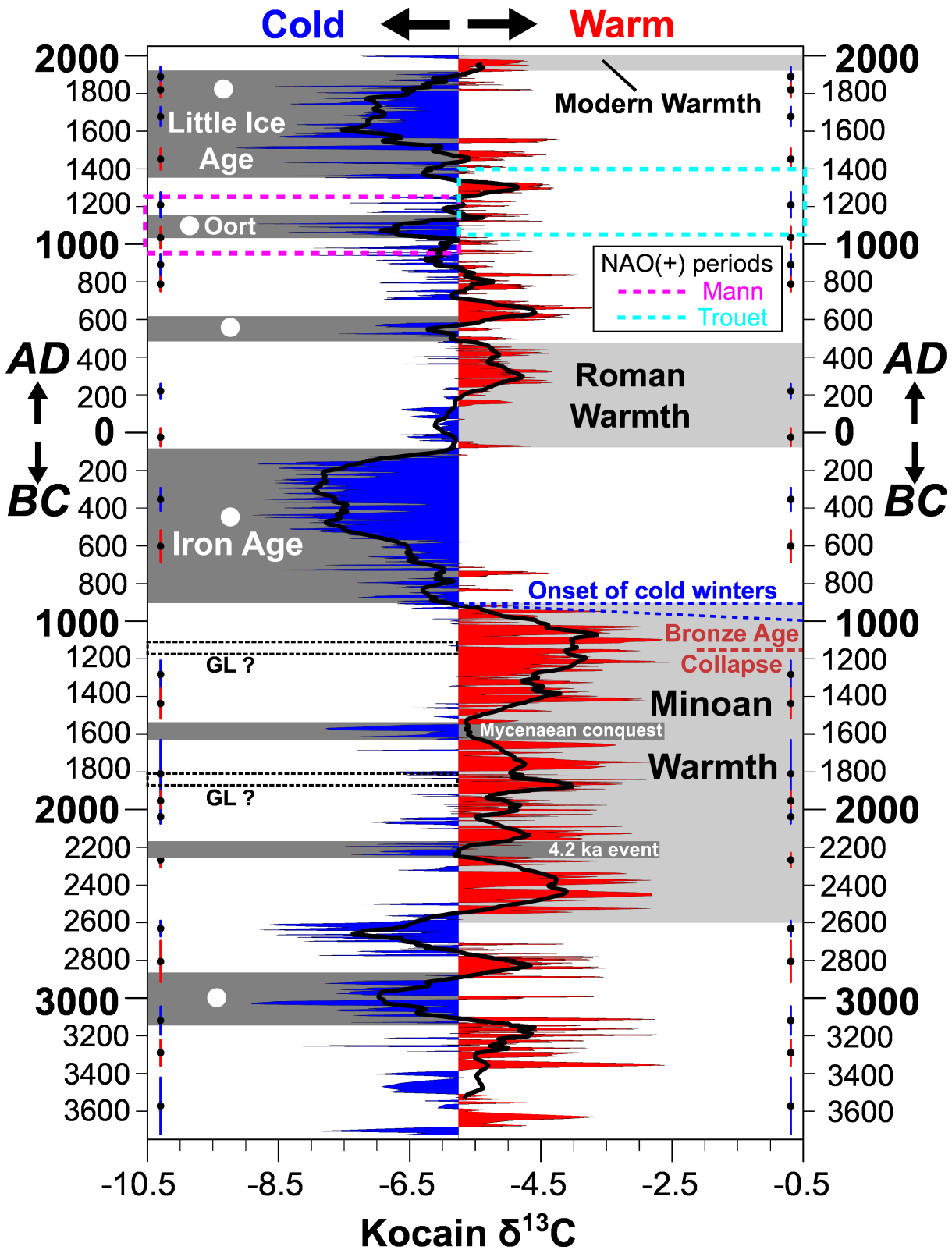


**Fig. 3.7:** The Kocain Cave  $\delta^{13}\text{C}$  record on a time scale. Values (blue/red fillings) are shown as deviations (negative/positive) from the mean value of  $\delta^{13}\text{C}$  in the entire record. Thick black line is a 43 point running mean, corresponding to 100 years on average. All cold intervals mentioned in the text are shaded dark gray. White full circles mark the timing of widespread glacial advances (Wanner et al., 2008). Distinct warm periods mentioned in the text are shaded with light gray. Hypothesized intervals of positive NAO during the Medieval Warm Period are marked by violet (Mann et al., 2009) and cyan (Trouet et al., 2009) dashed rectangles. Age control points and their associated uncertainties are shown by black dots and alternating blue/red bars over each dot, to avoid confusion.

### 3.5.3.1 Synchronicity of Cold Periods with Global Glacier Advances

In their review of the mid to late-Holocene climate changes, Wanner et al. (2008) define seven distinct periods of widespread glacier advances (marked “GL” in Fig. 3.7), which occurred quasi-simultaneously in both hemispheres. Four of those, namely the ones at the Little Ice Age (LIA), the Oort solar minimum, the Iron Age and around 3000 BC, coincide with the coldest periods in the Kocain record, whereas the time between 500 – 600 AD exhibits a series of short term cooling events and is on average only slightly cold. The remaining two glacier advances around 1850 BC and 1150 BC, for which no global or regional mechanism was proposed so far (Wanner et al., 2008), seem to occur during warm intervals in the our record (Fig. 3.7, periods centered at full white circles). Nonetheless, the most prominent and well determined glacier advances (Wanner et al., 2008) show an unambiguous synchronicity with the cold periods in Kocain Cave record (Fig. 3.7). Advances in the Alpine glaciers (Holzhauser et al., 2005) during the Bronze Age – Iron Age transition (from ~1000 BC on) and the late Little Ice Age (~1600 to 1850 AD) are obvious in Fig. 3.8e, and these are accompanied by cooling trends (lower  $\delta^{13}\text{C}$ ) in the Kocain Cave record. This does not only justify our interpretation of stalagmite  $\delta^{13}\text{C}$  as a proxy for winter temperature at this site, but also reveals that inferred temperature declines in the mentioned periods were not confined to the Eastern Mediterranean; also probably not to a single season; as mid and high latitude glaciers need low summer temperatures to grow (Oerlemans, 2005; Steiner et al., 2008). Orbitally induced reduction of insolation (for the event around ~3000 BC, Bond et al., 2001) and a decrease in solar activity (van Geel et al., 2000; Holzhauser et al., 2005), as well as an increase in volcanic eruptions (Wanner et al., 2008) remain the most likely causes for these global cooling phenomena.

### 3.5.3.2 Minoan Warm Period, 4.2 ka BP Event and the Bronze Age Collapse

Between ~2600 and 900 BC, a prolonged period of warm winters in the Eastern Mediterranean can be deduced from the Kocain Cave record (Fig. 3.7), punctuated by only short term (max. ~100 years) coolings. This is when several eminent Bronze Age civilizations flourished in and around Anatolia (Drews, 1993), one of them being the Minoans' in Crete (hence the name Minoan warm period). The first of the two relatively long cold interruptions taking place in this interval (Fig. 3.7, darker gray shades) is coincident with the 4.2 ka BP (~2200 BC) event, which is regarded as a fundamental cause for the collapse of the Akkadian empire, arguably due to aridification in northern Mesopotamia (Weiss et al., 1993). Various dynamical scenarios have been proposed to explain the inferred aridity, including a North Atlantic teleconnection (Mayewski and White, 2002) and a complex regional monsoon (Staubwasser and Weiss, 2006). Although the cooling signal is fairly robust in the Kocain Cave record, there is no means to suggest that this cold spell must be related to a widespread aridification in the Eastern Mediterranean, as present day correlations of winter temperatures in Antalya with precipitation in the neighboring regions are weak (Fig. 3.2). However, we argue that winter cold by itself could have been a critical factor leading to societal collapse in the northern Mesopotamia at the time. This is supported by the timing of the warm spell in the Kocain record (~2580 to 2260 BC), which matches very well with the expansion of the ancient city Tell Leilan in today's northeastern Syria (Weiss et al., 1993). Besides sufficient rainfall, persistent mild winters must have allowed Tell Leilan people to build a large city, where collection, storage and redistribution are possible (Weiss et al., 1993). After ~300 years of

ongoing winter warmth (apparently warmer than today), an ~80 years cold spell starting at ~2260 BC did probably lead to a breakdown of the central authority in Tell Leilan within a few decades. One should note that, due to continentality and snow cover, temperatures can fall well below freezing in northeastern Syria and especially in southeastern Turkey, but only during cold winters. The second and longer (~100 years)

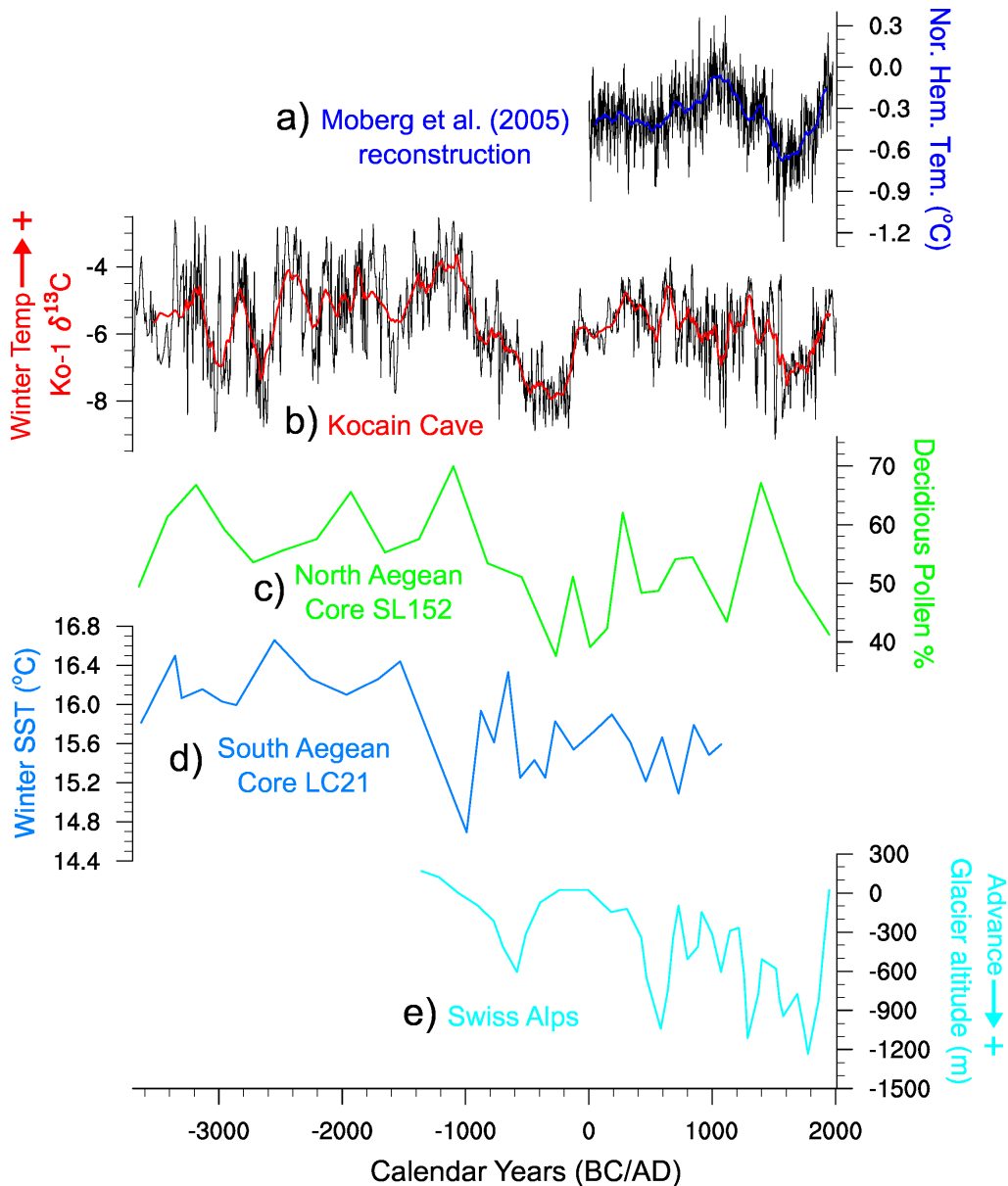


**Fig. 3.8:** Comparison of the Kocain Cave record with various paleoclimate records. **a)** Northern hemisphere temperature reconstructed by Moberg et al. (2005) expressed as anomalies from 1961-90 average. Black line shows raw data, whereas blue line is 100-yr running average. **b)** The Kocain Cave  $\delta^{13}\text{C}$  record. Black line is raw data, whereas red line is 43-point running mean, corresponding to 100 years on average. **c)** Deciduous pollen percentage from the core SL152 in the northern Aegean Sea (Kotthoff et al., 2008a) **d)** Reconstructed winter sea surface temperatures from the core LC21 in the southern Aegean sea. Data digitized from Rohling et al. (2009). **e)** Glacier dynamics record from the Swiss Alps (Holzhauser et al., 2005), expressed as the difference of the glacier altitude from that of today.



cold spell during the Minoan warm period centered at ~1600 BC (Fig. 3.7) coincides with the well-known eruption of the Santorini volcano (Friedrich et al., 2006). While attributing this cooling to the eruption is not trivial; it is interesting to note that Minoan civilization in Crete endured some hardship around this time, which caused an easier Mycenaean conquest of Crete (Antonopoulos, 1992). Sudden onset of colder winters that were independent from the volcanic event, might have been one of the natural factors; according to the Kocain record.

From an archaeological point of view, the most important event of the 2<sup>nd</sup> millennium BC is the transition from the Bronze Age to the Iron Age from ~1200 BC on, commencing with the destruction or disintegration of numerous ancient civilizations in and around Anatolia including the Hittite empire and the 'palatial' Mycenae (Drews, 1993). Rohling et al. (2009) suggested a linkage with the 'Rapid Climate Change' (RCC) that occurred between 1500 and 500 BC (Mayewski et al., 2004), characterized by a winter sea surface temperature drop of 2 °C in the southeastern Aegean from 1500 to 1000 BC (Fig. 3.8d). Yet, attribution of these events to climate change remains problematic, as other non-climatic factors may have played significant roles (Weninger et al., 2009). With its high temporal resolution, the Kocain record can bring insights into the issue. A gradual drop in winter temperatures is observed from ~1000 to ~500 BC (Fig. 3.7), which agrees well both with the broad timing of the RCC given by Mayewski et al. (2004) and the narrower interval of 1050 – 980 BC by Weninger et al. (2009). However, even when age uncertainties are taken into account, the onset of colder than normal winters in the Kocain record occurs no earlier than 1000 BC, which is still late relative to the abandonment of Troy at 1050 BC (Weninger et al., 2009) and the sudden destruction of many Bronze Age cities such as Hattusa and Ugarit between 1200 and 1150 BC (Drews, 1993). Moreover, the deciduous pollen record from a northern Aegean sea core (Kotthoff et al., 2008a) does *not* exhibit a drop either, the opposite of which was interpreted for the same record as the effect of the 8.2 ka BP cooling (Kotthoff et al., 2008b). Thus, the influence of a cold RCC on these historical events remains doubtful. On the other hand, recent evidence suggests that drought, which is not necessarily associated with cooling, could well have led to the Bronze Age collapse. Kaniewski et al. (2010) reported very dry conditions in Syria between ~1200 and 850 BC. Tsonis et al. (2010) linked the gradual decline of the Minoan civilization in Crete with drought as well, due to abnormally strong El Nino events starting around 1450 BC and lasting for several centuries. Although they found that this is probably a local response of Crete's winter precipitation to very strong El Nino events, coincidence of the proposed drought interval with very warm conditions in the Kocain record strengthens their hypothesis. El Nino / Southern Oscillation explains ~30% of the variation in global annual mean surface temperatures over the period 1867 – 1988 AD (Jones, 1989). The period between 1450 and 1250 BC was also found to be warm in central Europe (Tinner et al., 2003), for instance the Great Aletsch glacier in the Alps was 1000 m shorter than today (Holzhauser et al., 2005). This also implies a larger scale, El Nino-like influence on temperatures, rather than a NAO-like control, as the NAO effects temperatures in the Alps and the Eastern Mediterranean in opposite directions (Türkeş and Erlat, 2009).

### 3.5.3.3 Roman Warm Period and Medieval Climate Anomaly

After a long epoch of cold and snowy winters in the Kocain record between ~900 BC and ~100 BC (Fig. 3.7), temperatures started to recover and then peaked at ~300 AD. This is

the so called Roman Warm Period (RWP), though its timing exhibits discrepancies compared to other parts of the North Atlantic. For example, Desprat et al. (2003) reported the onset of the RWP as 250 BC in Iberia, when harsh winters still prevailed in the Eastern Mediterranean according to the Kocain Cave record. Again, Patterson et al. (2010) detected the highest temperature in Iceland at ~130 BC, which is the peak of a rise that started at ~230 BC. Moreover, in our record, despite the recovery in temperatures from ~100 BC on, winters seem generally cooler than today before ~200 AD.

One of the hot topics concerning the climate of the last 2000 years is the causes of warm temperatures in some parts of the globe during Medieval time. Bradley et al. (2003) argued that the concept of the 'Medieval Warm Period' was almost exclusively articulated on historical anecdotes and paleoclimate data from western Europe, therefore the term 'Medieval Climate Anomaly' (MCA) is preferred here. Recently, Medieval winter warmth in western Europe was explained with a tendency to La Nina-like conditions in the tropical Pacific (Mann et al., 2009) and a persistent positive mode of the NAO (Mann et al., 2009; Trouet et al., 2009). Because winter temperatures in Turkey have statistically significant negative correlations with the winter NAO index (Türkeş and Erlat, 2009), i.e. NAO(+) should be associated with generally cooler temperatures in Turkey, we can test this hypothesis using the Kocain record. First of all, rather than a distinct warm period as constructed by Moberg et al. (2005) for the northern hemisphere (Fig. 3.8a), we observe an alternating pattern of warm and cold times between 800 and 1400 BC with a cooler than normal period average (Fig. 3.7 and Fig. 3.8b). This implies that the idea of a generally NAO(+) during the Medieval times may have merit. Indeed, during most of the MCA defined by Mann et al. (2009) (dashed violet rectangle in Fig. 3.7), the Kocain record indicates low winter temperatures. However, this is only partly valid for the persistent NAO(+) period of Trouet et al. (2009) (dashed cyan rectangle in Fig. 3.7), as we observe a very warm period of ~100 years centered at 1300 AD. Having said these, it must be stressed that explaining much of the variation in our record with the NAO index is not possible. Although the relationship between Turkey's winter temperatures and the NAO is obvious, the correlation coefficients are weak ( $r < 0.5$ ; Türkeş and Erlat, 2009), and other teleconnections such as the North Sea – Caspian pattern have significant influence on Turkey's winter temperature regime as well (Kutiel et al., 2002). Finally, the most distinct cold interval in our record within the MCA coincides with the Oort solar minimum and glacier advances in the Alps (Wanner et al., 2008), which implies a rather widespread cooling at the time, possibly independent of the NAO and related to a decrease in solar insolation.

### **3.5.3.4 Little Ice Age and the Decline of the Ottoman Empire**

The first part of the Little Ice Age (LIA) in Anatolia, occurring between the late 14<sup>th</sup> and late 16<sup>th</sup> centuries AD in the Kocain record (Fig. 3.7), is characterized by fluctuating winter temperatures from warm to very cold (Fig. 3.7). After the last warm spell centered at 1550 AD, a period of persistently cold decades is inferred up until the 20<sup>th</sup> century, interrupted only briefly in the 19<sup>th</sup> century. In this sense, our record contradicts the notion of a generally negative NAO during the LIA (Shindell et al., 2001; Mann et al., 2009), as NAO(-) should be associated with warm and rainy winters in southern Turkey (Türkeş and Erlat, 2009). On the other hand, it has also been shown that NAO(+) might have dominated parts of the LIA (Nesje et al., 2008). Thus, a large scale winter temperature decline in Europe

and the Eastern Mediterranean, which should only partly be associated with the changes in the NAO, seems more plausible according to the Kocain Cave record. This is also in line with the findings of Xoplaki et al. (2001) for the Balkans and Greece.

The Kocain Cave record is a key natural archive for confirming the role of climate change in shaping the history of the Ottoman empire, as we provide the first high resolution winter temperature proxy record for Turkey. White (2008) has compiled the most extensive historical information about the effects of the LIA on the Ottoman lands, concluding that cold and drought led to huge famines, and in turn an uprising in Anatolia called the 'Celali Rebellion', which matches very closely with the timing of the most sustained and severe cold period in the Kocain record from ~1560 AD on. Moreover, the retreat in the demographic and territorial expansion of the Ottoman empire began by the 18<sup>th</sup> century AD (White, 2008). One very interesting note regarding the geographical extent of the climatic deterioration in the mentioned time frame is, that the worst drought occurred in the lands surrounding the Aegean sea (White, 2008 and references therein). Confirming this, we report that the highest positive correlation coefficients of Antalya's winter temperature with winter/spring precipitation are observed in the borderlands of the Aegean (Fig. 3.2), mostly as a characterization of winter climate in this area. Therefore, drought must have been associated with cold during the LIA. A modern analogue for this is the winter of 1991-92, which was the coldest and driest in the Aegean region of Turkey over the last 70 years. This also coincides with the third highest winter NAO index of the last century and the aftermath of the Pinatubo eruption.

### 3.5.3.5 The Degree of Warmth in the Modern Era

One can clearly infer from Fig. 3.7 that the winter warmth in southern Turkey during the 20<sup>th</sup> century was not exceptional when compared to the entire Kocain record spanning the last ~5700 years; the Minoan warm period stands out as the warmest. However, it should be noted that our temperature proxy,  $\delta^{13}\text{C}$ , is not sensitive to changes in summer temperature, as hydrological processes in the Antalya area during summer practically cease. This is also confirmed by a lack of response from the  $\delta^{13}\text{C}$  to the sharp increase in summer temperatures from 1995 AD (not shown). According to numerous studies (e.g. IPCC, 2007 and references therein; Kuglitsch et al., 2010), summer heat waves are a major threat of anthropogenic global warming to the Eastern Mediterranean.

## 3.6 Summary and Conclusions

We presented a new high resolution proxy record for winter temperatures in southern Turkey, covering the last ~5700 years. This record is based on the  $\delta^{13}\text{C}$  profile of a stalagmite from the Kocain Cave near Antalya. During the time of meteorological observations,  $\delta^{13}\text{C}$  values in this stalagmite match variations in the amount of decadal snowfall, which closely follows decadal winter temperatures. It is shown, for the first time, that stalagmite  $\delta^{13}\text{C}$  can have more negative values as a response to increased snowfall, rather than to increased rainfall above the cave; this is most probably due to preferential infiltration and higher soil wetting ability of snowmelt. Our main conclusions concerning the climate of the last 5700 years and its relationship with cultural changes are as follows (see also Fig. 3.7):

- There is a good agreement between periods of major cold in the Kocain Cave record and widespread glacier advances; which independently confirms our interpretation of stalagmite  $\delta^{13}\text{C}$  as a snowfall and winter temperature proxy.
- Winter warmth in southern Turkey during the 20<sup>th</sup> century AD is matched and exceeded several times in the last ~5700 years, especially during the time of the Minoan civilization in Crete between ~2400 and 1100 BC.
- While a persistent positive NAO during the Medieval Climate Anomaly is only partially supported by the Kocain record, our results contradict the idea of generally negative NAO during the Little Ice Age.
- Both cold and warm extremes can lead to societal crisis or collapse, as implied by the Kocain Cave record. This record provides strong evidence for the previously hypothesized influence of extreme cold and drought on the uprisings in the 16<sup>th</sup> century AD Ottoman empire. The 4.2 ka BP event in northern Mesopotamia may primarily be a cold event, rather than widespread aridification. Large-scale extremes not encountered in the instrumental era may have led to climatic patterns and regional responses that are unknown today, especially in the case of Bronze Age collapse in the Eastern Mediterranean. The time around the Bronze Age collapse is the warmest in the entire Kocain record.
- Our hypotheses, specifically the one linking  $\delta^{13}\text{C}$  to snowfall will be further tested in the future through analysis of new stalagmites from Kocain Cave, as well as monitoring studies in the cave and its environment.

### 3.7 References

- Antonopoulos, J., 1992. The great Minoan eruption of Thera volcano and the ensuing tsunami in the Greek archipelago. *Nat. Hazards* 5, 153-168.
- Badertscher, S., Fleitmann, D., Cheng, H., Edwards, R.L., Gokturk, O.M., Zumbuhl, A., Leuenberger, M., Tuysuz, O., 2011. Pleistocene water intrusions from the Mediterranean and Caspian seas into the Black Sea. *Nat Geosci* 4, 236-239.
- Bakalowicz, M., El Hakim, M., El-Hajj, A., 2008. Karst groundwater resources in the countries of eastern Mediterranean: the example of Lebanon. *Environ Geol* 54, 597-604.
- Baker, A., Ito, E., Smart, P.L., McEwan, R.F., 1997. Elevated and variable values of C-13 in speleothems in a British cave system. *Chem Geol* 136, 263-270.
- Baker, A., Genty, D., Dreybrodt, W., Barnes, W.L., Mockler, N.J., Grapes, J., 1998. Testing theoretically predicted stalagmite growth rate with Recent annually laminated samples: Implications for past stalagmite deposition. *Geochim Cosmochim Acta* 62, 393-404.
- Baker, A., Asrat, A., Fairchild, I.J., Leng, M.J., Wynn, P.M., Bryant, C., Genty, D., Umer, M., 2007. Analysis of the climate signal contained within delta O-18 and growth rate parameters in two Ethiopian stalagmites. *Geochim Cosmochim Acta* 71, 2975-2988.
- Baldini, J.U.L., McDermott, F., Baker, A., Baldini, L.M., Matthey, D.P., Railsback, L.B., 2005. Biomass effects on stalagmite growth and isotope ratios: A 20th century analogue from Wiltshire, England. *Earth Planet Sci Lett* 240, 486-494.
- Bar-Matthews, M., Ayalon, A., Gilmour, M., Matthews, A., Hawkesworth, C.J., 2003. Sea-land oxygen isotopic relationships from planktonic foraminifera and speleothems in the Eastern Mediterranean region and their implication for paleorainfall during interglacial intervals. *Geochim Cosmochim Acta* 67, 3181-3199.

- Bond, G., Kromer, B., Beer, J., Muscheler, R., Evans, M., Showers, W., Hoffmann, S., Lotti-Bond, R., Hajdas, I., Bonani, G., 2001. Persistent solar influence on north Atlantic climate during the Holocene. *Science* 294, 2130-2136.
- Bradley, R.S., Hughes, M.K., Diaz, H.F., 2003. Climate in Medieval Time. *Science* 302, 404-405.
- BÜMAK, 2011. Boğaziçi University Speleology Club, archive of cave maps. <http://www.bumak.boun.edu.tr/haritalar/562.jpg> (Accessed on: 10.01.2011).
- deMenocal, P.B., 2001. Cultural responses to climate change during the Late Holocene. *Science* 292, 667-673.
- Desprat, S., Goni, M.F.S., Loutre, M.F., 2003. Revealing climatic variability of the last three millennia in northwestern Iberia using pollen influx data. *Earth Planet Sci Lett* 213, 63-78.
- Drews, R., 1993. The end of the Bronze Age: Changes in warfare and the catastrophe ca. 1200 B.C., Princeton University Press, Princeton, NJ.
- Dunne, T., Zhang, W.H., Aubry, B.F., 1991. Effects of rainfall, vegetation, and microtopography on infiltration and runoff. *Water Resour Res* 27, 2271-2285.
- Earman, S., Campbell, A.R., Phillips, F., Newman, B.D., 2006. Isotopic exchange between snow and atmospheric water vapor: Estimation of the snowmelt component of groundwater recharge in the southwestern United States. *J Geophys Res-Atmos* 111, D09302 doi: 10.1029/2005JD006470.
- Fairchild, I.J., Smith, C.L., Baker, A., Fuller, L., Spotl, C., Matthey, D., McDermott, F., 2006. Modification and preservation of environmental signals in speleothems. *Earth-Sci Rev* 75, 105-153.
- Fleitmann, D., Burns, S.J., Neff, U., Mudelsee, M., Mangini, A., Matter, A., 2004. Palaeoclimatic interpretation of high-resolution oxygen isotope profiles derived from annually laminated speleothems from Southern Oman. *Quaternary Sci Rev* 23, 935-945.
- Fleitmann, D., Cheng, H., Badertscher, S., Edwards, R.L., Mudelsee, M., Göktürk, O.M., Fankhauser, A., Pickering, R., Raible, C.C., Matter, A., Kramers, J., Tuysuz, O., 2009. Timing and climatic impact of Greenland interstadials recorded in stalagmites from northern Turkey. *Geophys Res Lett* 36, L19707.
- Fontugne, M.R., Calvert, S.E., 1992. Late Pleistocene variability of the carbon isotopic composition of organic matter in the eastern Mediterranean: monitor of changes in carbon sources and atmospheric CO<sub>2</sub> concentrations. *Paleoceanography* 7, 1-20.
- Friedrich, W.L., Kromer, B., Friedrich, M., Heinemeier, J., Pfeiffer, T., Talamo, S., 2006. Santorini eruption radiocarbon dated to 1627-1600 BC. *Science* 312, 548-548.
- Gazis, C., Feng, X.H., 2004. A stable isotope study of soil water: evidence for mixing and preferential flow paths. *Geoderma* 119, 97-111.
- Genty, D., Baker, A., Vokal, B., 2001. Intra- and inter-annual growth rate of modern stalagmites. *Chem Geol* 176, 191-212.
- Hendy, C.H., 1971. Isotopic geochemistry of speleothems: I. Calculation of effects of different modes of formation on isotopic composition of speleothems and their applicability as palaeoclimatic indicators. *Geochim Cosmochim Acta* 35, 801-824.
- Holzhauser, H., Magny, M., Zumbühl, H.J., 2005. Glacier and lake-level variations in west-central Europe over the last 3500 years. *Holocene* 15, 789-801.
- Hughes, M.K., 2002. Dendrochronology in climatology: The state of the art. *Dendrochronologia* 20, 95-116.
- Hurrell, J.W., 1995. Decadal trends in the North-Atlantic Oscillation - regional temperatures and precipitation. *Science* 269, 676-679.
- IAEA/WMO, 2006. Global Network of Isotopes in Precipitation. The GNIP Database. Accessible at: <http://www.iaea.org/water>.
- IPCC, 2007: Climate Change 2007: The Physical Science Basis. Contribution of Working Group I to the Fourth Assessment Report of the Intergovernmental Panel on Climate Change, in: Solomon, S., Qin, D., Manning, M., Chen, Z., Marquis, M., Averyt, K.B., Tignor, M., Miller, H.L. (Eds.), Cambridge University Press, Cambridge, United Kingdom and New York, NY, USA.
- Jones, P.D., 1989. The influence of ENSO on global temperatures. *Clim Monit* 17, 80-89.

- Kaniewski, D., Paulissen, E., Van Campo, E., Weiss, H., Otto, T., Bretschneider, J., Van Lerberghe, K., 2010. Late second-early first millennium BC abrupt climate changes in coastal Syria and their possible significance for the history of the Eastern Mediterranean. *Quaternary Res* 74, 207-215.
- Kienzle, S.W., 2008. A new temperature based method to separate rain and snow. *Hydrol Process* 22, 5067-5085.
- Koeniger, P., Hubbart, J.A., Link, T., Marshall, J.D., 2008. Isotopic variation of snow cover and streamflow in response to changes in canopy structure in a snow-dominated mountain catchment. *Hydrol Process* 22, 557-566.
- Kotthoff, U., Muller, U.C., Pross, J., Schmiedl, G., Lawson, I.T., van de Schootbrugge, B., Schulz, H., 2008a. Lateglacial and Holocene vegetation dynamics in the Aegean region: an integrated view based on pollen data from marine and terrestrial archives. *Holocene* 18, 1019-1032.
- Kotthoff, U., Pross, J., Muller, U., Peyron, O., Schmiedl, G., Schulz, H., Bordon, A., 2008b. Climate dynamics in the borderlands of the Aegean Sea during formation of sapropel S1 deduced from a marine pollen record. *Quaternary Sci Rev* 27, 832-845.
- Krichak, S., Kishcha, P., Alpert, P., 2002. Decadal trends of main Eurasian oscillations and the Eastern Mediterranean precipitation. *Theor Appl Climatol* 72, 209-220.
- Kuglitsch, F., Toreti, A., Xoplaki, E., Della-Marta, P., Zerefos, C., Turkes, M., Luterbacher, J., 2010. Heat wave changes in the eastern Mediterranean since 1960. *Geophys Res Lett* 37, L04802.
- Kuhnt, T., Schmiedl, G., Ehrmann, W., Hamann, Y., Andersen, N., 2008. Stable isotopic composition of Holocene benthic foraminifers from the Eastern Mediterranean Sea: Past changes in productivity and deep water oxygenation. *Palaeogeogr Palaeoclimatol* 268, 106-115.
- Kutiel, H., Maheras, P., Turkes, M., Paz, S., 2002. North Sea Caspian Pattern (NCP) - an upper level atmospheric teleconnection affecting the eastern Mediterranean - implications on the regional climate. *Theor Appl Climatol* 72, 173-192.
- Lachniet, M.S., Burns, S.J., Piperno, D.R., Asmerom, Y., Polyak, V.J., Moy, C.M., Christenson, K., 2004. A 1500-year El Nino/Southern Oscillation and rainfall history for the Isthmus of Panama from speleothem calcite. *J Geophys Res-Atmos* 109, D20117.
- Lee, J., Feng, X., Faiia, A.M., Posmentier, E.S., Kirchner, J.W., Osterhuber, R., Taylor, S., 2010. Isotopic evolution of a seasonal snowcover and its melt by isotopic exchange between liquid water and ice. *Chem Geol* 270, 126-134.
- Mangini, A., Verdes, P., Spötl, C., Scholz, D., Vollweiler, N., Kromer, B., 2007. Persistent influence of the North Atlantic hydrography on central European winter temperature during the last 9000 years. *Geophys Res Lett* 34, L02704.
- Mann, M.E., Zhang, Z.H., Rutherford, S., Bradley, R.S., Hughes, M.K., Shindell, D., Ammann, C., Faluvegi, G., Ni, F.B., 2009. Global Signatures and Dynamical Origins of the Little Ice Age and Medieval Climate Anomaly. *Science* 326, 1256-1260.
- Maule, C.P., Chanasyk, D.S., Muehlenbach, K., 1994. Isotopic determination of snow-water contribution to soil-water and groundwater. *J Hydrol* 155, 73-91.
- Mayewski, P.A., White, F., 2002. *The ice chronicles: The quest to understand global climate change*, University Press of England, Hanover.
- Mayewski, P.A., Rohling, E.J., Stager, J.C., Karlen, W., Maasch, K., Meeker, L.D., Meyerson, E.A., Gasse, F., van Kreveld, S., Holmgren, K., Lee-Thorp, J., Rosqvist, G., Rack, F., Staubwasser, M., Schneider, R.R., Steig, E.J., 2004. Holocene climate variability. *Quaternary Res* 62, 243-255.
- Moberg, A., Sonechkin, D.M., Holmgren, K., Datsenko, N.M., Karlen, W., 2005. Highly variable Northern Hemisphere temperatures reconstructed from low- and high-resolution proxy data. *Nature* 433, 613-617.
- McDermott, F., 2004. Palaeo-climate reconstruction from stable isotope variations in speleothems: a review. *Quaternary Sci Rev* 23, 901-918.
- Mitchell, T.D., Jones, P.D., 2005. An improved method of constructing a database of monthly climate observations and associated high-resolution grids. *Int J Climatol* 25, 693-712.
- Nesje, A., Dahl, S.O., Thun, T., Nordli, O., 2008. The 'Little Ice Age' glacial expansion in western Scandinavia: summer temperature or winter precipitation?. *Clim Dynam* 30, 789-801.

- Oerlemans, J., 2005. Extracting a climate signal from 169 glacier records. *Science* 308, 675-677.
- PAGES, 2009. Science Plan and Implementation Strategy. IGBP Report No. 57. IGBP Secretariat, Stockholm. 67pp.
- Patterson, W.P., Dietrich, K.A., Holmden, C., Andrews, J.T., 2010. Two millennia of North Atlantic seasonality and implications for Norse colonies. *Proc Nat Acad Sci Usa* 107, 5306-5310.
- Pipes, A., Quick, M.C., 1977. UBC watershed model users guide. Department of Civil Engineering, University of British Columbia.
- Richards, D.A., Dorale, J.A., 2003. Uranium-series chronology and environmental applications of speleothems. *Reviews in Mineralogy and Geochemistry* 52, 407-460.
- Rohling, E.J., Angela, H., Mayewski, P.A., Kucera, M., 2009. Holocene climate variability in the eastern Mediterranean, and the End of the Bronze Age, in: Bachhuber, C., Roberts, G. (Eds.), *Holocene climate variability in the eastern Mediterranean, and the End of the Bronze Age*. Oxbow Books, Oxford, UK, pp. 2-5.
- Rozanski, K., Araguas-Araguas, L., Gonfiantini, R., 1993. Isotopic patterns in modern global precipitation, in: Swart, P.K., Lohmann, K.C., McKenzie, J., Savin, S. (Eds.), *Isotopic patterns in modern global precipitation*. American Geophysical Union, Washington, DC, pp. 1-36.
- Shaw, S.J., 1976. *History of the Ottoman Empire and Modern Turkey, Volume 1, Empire of the Gazis: The Rise and Decline of the Ottoman Empire, 1280-1808*. Cambridge University Press, Cambridge, UK.
- Shindell, D.T., Schmidt, G.A., Mann, M.E., Rind, D., Waple, A., 2001. Solar forcing of regional climate change during the maunder minimum. *Science* 294, 2149-2152.
- Spötl, C., Fairchild, I.J., Tooth, A.F., 2005. Cave air control on dripwater geochemistry, Obir Caves (Austria): Implications for speleothem deposition in dynamically ventilated caves. *Geochim Cosmochim Acta* 69, 2451-2468.
- Staubwasser, M., Weiss, H., 2006. Holocene climate and cultural evolution in late prehistoric-early historic West Asia - Introduction. *Quaternary Res* 66, 372-387.
- Steiner, D., Pauling, A., Nussbaumer, S.U., Nesje, A., Luterbacher, J., Wanner, H., Zumbühl, H.J., 2008. Sensitivity of European glaciers to precipitation and temperature - two case studies. *Climatic Change* 90, 413-441.
- TAY Project: The Archaeological Settlements of Turkey.  
[http://www.tayproject.org/TAYmaster\\_fm\\$Retrieve?YerlesmeNo=11392&html=masterengdetail.html&layout=web](http://www.tayproject.org/TAYmaster_fm$Retrieve?YerlesmeNo=11392&html=masterengdetail.html&layout=web) (Accessed on: 01.03.2011).
- Taylor, S., Feng, X.H., Kirchner, J.W., Osterhuber, R., Klaue, B., Renshaw, C.E., 2001. Isotopic evolution of a seasonal snowpack and its melt. *Water Resour Res* 37, 759-769.
- Thorntwaite, C.W., 1948. An approach toward a rational classification of climate. *Geographical Review* 38, 55-94.
- Tinner, W., Lotter, A.F., Ammann, B., Conedera, M., Hubschmid, P., van Leeuwen, J.F.N., Wehrli, M., 2003. Climatic change and contemporaneous land-use phases north and south of the Alps 2300 BC to 800 AD. *Quaternary Sci Rev* 22, 1447-1460.
- Trouet, V., Esper, J., Graham, N.E., Baker, A., Scourse, J.D., Frank, D.C., 2009. Persistent Positive North Atlantic Oscillation Mode Dominated the Medieval Climate Anomaly. *Science* 324, 78-80.
- Tsonis, A.A., Swanson, K.L., Sugihara, G., Tsonis, P.A., 2010. Climate change and the demise of Minoan civilization. *Clim Past* 6, 525-530.
- Türkeş, M., Erlat, E., 2003. Precipitation changes and variability in turkey linked to the North Atlantic oscillation during the period 1930-2000. *Int J Climatol* 23, 1771-1796.
- Türkeş, M., Erlat, E., 2009. Winter mean temperature variability in Turkey associated with the North Atlantic Oscillation. *Meteorol Atmos Phys* 105, 211-225.
- Unnikrishna, P.V., McDonnell, J.J., Kendall, C., 2002. Isotope variations in a Sierra Nevada snowpack and their relation to meltwater. *J Hydrol* 260, 38-57.
- van Geel, B., Heusser, C.J., Renssen, H., Schuurmans, C.J.E., 2000. Climatic change in Chile at around 2700 BP and global evidence for solar forcing: a hypothesis. *Holocene* 10, 659-664.
- Wanner, H., Beer, J., Butikofer, J., Crowley, T.J., Cubasch, U., Fluckiger, J., Goosse, H., Grosjean, M., Joos, F., Kaplan, J.O., Kuttel, M., Muller, S.A., Prentice, I.C., Solomina, O., Stocker, T.F.,

- Tarasov, P., Wagner, M., Widmann, M., 2008. Mid- to Late Holocene climate change: an overview. *Quaternary Sci Rev* 27, 1791-1828.
- Weiss, H., Courty, M.A., Wetterstrom, W., Guichard, F., Senior, L., Meadow, R., Curnow, A., 1993. The genesis and collapse of 3rd millennium north Mesopotamian civilization. *Science* 261, 995-1004.
- Weninger, B., Clare, L., Rohling, E.J., Bar-Yosef, O., Böhner, U., Budja, M., Bundschuh, M., Feurdean, A., Gebel, H.G., Jöris, O., Linstadter, J., Mayewski, P., Mühlenbruch, T., Reingruber, A., Rollefson, G., Schyle, D., Thissen, L., Todorova, H., Zielhofer, C., 2009. The Impact of Rapid Climate Change on prehistoric societies during the Holocene in the Eastern Mediterranean. *Documenta Praehistorica* 36, 7-59.
- White, S., 2008. Ecology, climate, and crisis in the Ottoman Near East. PhD thesis, Columbia University.
- Xoplaki, E., Maheras, P., Luterbacher, J., 2001. Variability of climate in Meridional Balkans during the periods 1675-1715 and 1780-1830 and its impact on human life. *Climatic Change* 48, 581-615.







---

## CHAPTER 4

### DECIPHERING THE CLIMATE SIGNAL: A NEW LATE HOLOCENE STALAGMITE RECORD FROM THE SOUTHEAST BALKAN\*

O.M.Göktürk<sup>1,2</sup>, D.Fleitmann<sup>1,2</sup>, H.Cheng<sup>3,4</sup>, S.Badertscher<sup>1,2</sup>, R.L.Edwards<sup>4</sup>, O.Tüysüz<sup>5</sup>

1: Institute of Geological Sciences, University of Bern, Bern, Switzerland.

2: Oeschger Centre for Climate Change Research, University of Bern, Bern, Switzerland.

3: Institute of Global Environmental Change, Xi'an Jiaotong University, Xi'an, Shaanxi, China.

4: Department of Geology and Geophysics, University of Minnesota-Twin Cities, Minneapolis, Minnesota, USA.

5: Eurasia Institute of Earth Sciences, Istanbul Technical University, Istanbul, Turkey.

#### 4.1 Abstract

Based on the high resolution measurements of stable oxygen and carbon isotopes ( $\delta^{18}\text{O}$  and  $\delta^{13}\text{C}$ ) on a stalagmite from the Uzuntarla Cave in northwestern Turkey, a new paleoclimate proxy record for the southeast Balkan region covering the last ~4.1 ka is presented. The recent part of this record correlates well with the parameters derived from the available meteorological records.  $\delta^{18}\text{O}$  varies according to the 'temperature effect', i.e. both a general temperature increase and a shift of the rainfall season to warmer times of the year lead to more positive values of  $\delta^{18}\text{O}$ . Though less obvious,  $\delta^{13}\text{C}$  has also a climate sensitivity, which occurs through vegetation and soil microbial activity responding to the changes in 'water excess', as well as to extreme summer heat. Each Uzuntarla proxy is apparently controlled by more than one climatic variable, yet analyzing them alongside other records from the region gives valuable hints about past changes. One of the conclusions is that the contributing climatic factor to the collapse of civilizations at the end of the Bronze Age should be drought, induced by very warm conditions, and not by cooling as previously proposed. Moreover, during the late Holocene in the Eastern Mediterranean, cooler periods may have consistently shifted the seasonality of precipitation to warmer times of the year.

\* To be revised and submitted to *The Holocene*

## 4.2 Introduction

The ultimate goal of obtaining climate proxy records from natural archives is to reconstruct a main aspect of past climate, such as temperature or precipitation. However, this is usually not possible, as proxies respond to multiple factors that can be independent from each other. It has been shown, for example, that tree growth in high latitudes is controlled not only by -often reconstructed- summer temperature but also snowfall and melt timing (Vaganov et al., 1999), which are unrelated to the former. Independent parameters operate simultaneously to determine variations also in speleothem proxy records (McDermott, 2004; Fairchild et al., 2006; Fairchild and Treble, 2009; Lachniet, 2009), e.g. it is not trivial to know whether an increase in  $\delta^{18}\text{O}$  of atmospheric precipitation (hence, speleothem calcite) is due either to an overall temperature increase or to a significant shift of rainfall period to the warmer time of the year. Still, a multi-proxy approach, as well as utilizing other paleoclimate records can help disentangle the signature of a specific variable. For instance, Lauritzen and Lundberg (1999) attempted to extract a temperature time series from the  $\delta^{18}\text{O}$  record of a Norwegian stalagmite, by using independent temperature estimates at given points in time.

In this study, we present a new paleoclimate proxy record covering the last ~4100 years, based on stable isotopic composition ( $\delta^{18}\text{O}$  and  $\delta^{13}\text{C}$ ) of a stalagmite from the Uzuntarla Cave in the southeast Balkan region (extreme northwest Turkey). Owing both to the difficulties of proxy interpretation mentioned above and to the regional complexity of climate in Turkey (Türkeş et al., 1996; Kutiel et al., 2002), there is a need for a greater number of highly resolved records to better understand and characterize past climate in this area, as well as in the greater Eastern Mediterranean region. It will be shown that, with the aid of available paleoclimate records, both  $\delta^{18}\text{O}$  and  $\delta^{13}\text{C}$  can be interpreted in a non-simplistic, yet effective way to deduce meaningful conclusions concerning past climate. Turkey is a key area for studying Holocene climate also from a historical perspective, as the Eastern Mediterranean region hosted numerous ancient civilizations.

## 4.3 Uzuntarla Cave: Climatic and Environmental Setting

Uzuntarla Cave (41°35'09" N, 27°56'.35" E, ~200 m asl) is situated where the Balkan peninsula becomes narrower in between Black, Marmara and the Aegean seas (Fig. 4.1). This region is called Thrace, part of which is today in northwestern Turkey. According to the updated Köppen-Geiger climate classification (Kottek et al., 2006), a warm temperate climate prevails here. The precipitation maximum is in winter, but along with spring and fall, the warm to hot summers feature some rain too (Fig. 4.1), which led to another definition of the climate in this region as “Marmara Transition” (Türkeş, 1996) to emphasize its difference from the typical Mediterranean climate. More subtle characteristics such as the amount of rainfall and the degree of summer heat or winter cold are determined by local conditions, which can vary considerably due to topography and to the position with respect to the water masses surrounding the area. For example, in Kırklareli (Fig. 4.1), mean temperature of the coldest month (January) is 3.1°C, whereas this value is 5.5°C in Kandilli – a station located on the Bosphorus in Istanbul. The Black Sea and the Sea of Marmara moderate and humidify the oncoming air masses, creating the significantly higher fall and winter precipitation values in Kandilli compared to those of Kırklareli and Çorlu (Fig. 4.1, lower panel). Despite being closer to those stations to its



**Fig. 4.1:** Location of the Uzuntarla Cave and the three nearby meteorological stations (circle: Kırklareli, star: Çorlu, triangle: Kandilli), along with their average seasonal precipitation amounts in the lower part of the figure. Colors denote seasons (green: spring, red: summer, orange: fall, blue: winter).

south and west, Uzuntarla Cave resembles Kandilli in terms of its proximity to the Black Sea (14 km). Thus, the precipitation amount could be more than those of Kırklareli and Çorlu stations. Anecdotal evidence from the region, as well as the obvious change in vegetation cover towards the Black Sea coast of Thrace (Fig. 4.1) supports the idea that the cave site is more humid than the interior. The terrain above the cave is densely vegetated with trees and shrubs.

Winter climate in western Turkey is influenced by the two main Eurasian climatic patterns, namely the North Atlantic Oscillation (NAO) and the North Sea – Caspian pattern (NCP). Positive (negative) modes of both patterns lead to drier (wetter) than normal conditions in western Turkey (Krichak et al., 2002; Türkeş and Erlat, 2003), but individual effects of these teleconnections are not large, as also evident from the correlations coefficients ( $r < 0.5$ ) between station time series and pattern indices. Influence of the NCP on winter temperatures in Thrace region is much more pronounced than that of the NAO (Kutiel et al., 2002; Türkeş and Erlat, 2009); with its positive (negative) mode associated with cooler (warmer) than normal winters. Summer teleconnections are not clearly defined, though it was proposed that weaker Indian monsoon leads to wetter than normal summers in the Eastern Mediterranean region (Ziv et al., 2004).

#### 4.4 Material and Methods

Stable isotope ( $\delta^{13}\text{C}$  and  $\delta^{18}\text{O}$ ) analysis and  $^{230}\text{Th}$  dating were performed on the first 79.5 cm section of an almost 1 m long stalagmite, collected from the Uzuntarla Cave in August 2005 and named U-1. For the stable isotopes, calcite samples were drilled at every 0.5 mm. This was done using a digitally controlled micromill through continuous trenches along the growth axis of the stalagmite. The  $\delta^{13}\text{C}$  and  $\delta^{18}\text{O}$  of the resulting samples were measured at the Institute of Geological Sciences, University of Bern, Switzerland; on a Finnigan Delta V Advantage mass spectrometer equipped with an automated carbonate preparation system (Gas Bench-II). Larger quantity calcite samples were obtained by a dental drill for  $^{230}\text{Th}$  dating.  $^{230}\text{Th}$  measurements were performed on a multi-collector inductively coupled plasma mass spectrometer at the Minnesota Isotope Laboratory, University of Minnesota, USA (MC-ICP-MS, Thermo-Finnigan-Neptune). Further details on stable isotope analyses and  $^{230}\text{Th}$  dating method are provided by Fleitmann et al. (2009) and Badertscher et al. (2011).

#### 4.5 Results and Discussion

##### 4.5.1 Chronology

The age model of the stalagmite U-1 is based on linear interpolation through 12 stratigraphically ordered  $^{230}\text{Th}$  dates, out of 14 measured (Fig. 4.2b). Chronological uncertainties for the  $^{230}\text{Th}$  dates used in the age model vary between 3.1% and 31.6% (Fig. 4.2a) around an average of 11.5%. The observed large uncertainties are probably caused by low  $^{230}\text{Th}/^{232}\text{Th}$  (Fig. 4.2a), implying detrital contamination in the speleothem calcite (Richards and Dorale, 2003). The analyzed section of stalagmite U-1 grew continuously from ~4.1 ka BP until the sampling date, which is evident from the uniform slope of the age model through the two youngest  $^{230}\text{Th}$  dates until the tip of the stalagmite (Fig. 4.2b).

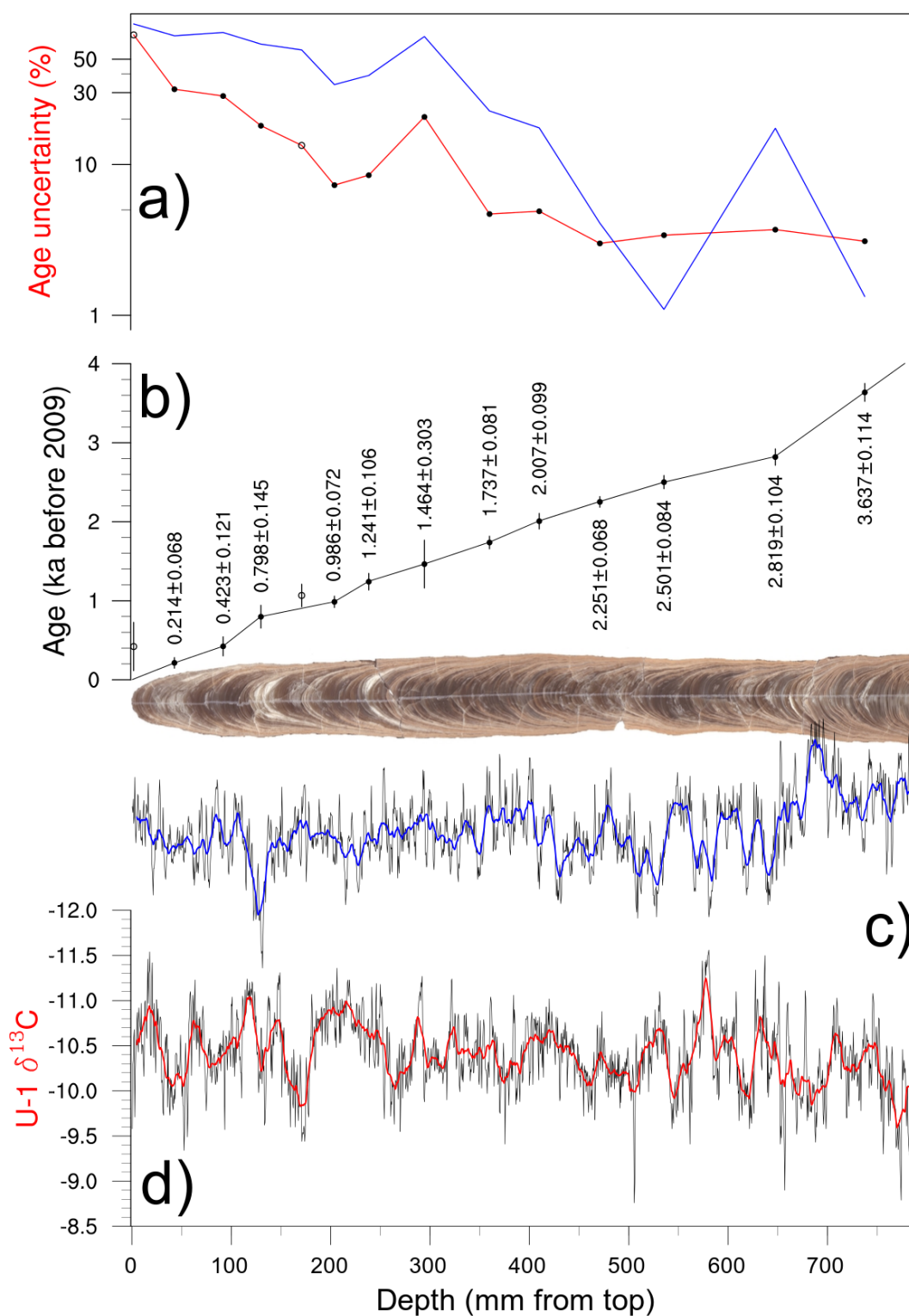


**Fig. 4.2:** Age model and the stable isotope profile of the stalagmite U-1 on a depth scale, along with an image of the stalagmite. **a)** % age uncertainties (red line) of the  $^{230}\text{Th}$  dates (black circles) and the  $^{230}\text{Th}/^{232}\text{Th}$  ratios (blue line). Hollow black circles mark the discarded dates. **b)**  $^{230}\text{Th}$  dates and their associated uncertainties. Black line shows the age model. **c)**  $\delta^{18}\text{O}$  (VPDB). Blue line is a 20-point running average. **d)**  $\delta^{13}\text{C}$  (VPDB). Red line is a 20-point running average.

The mean growth rate is 0.23 mm/yr, ranging from 0.11 to 0.39 mm/yr.

## 4.5.2 Stable Isotope Profiles and Their Interpretation

1586 stable isotope ( $\delta^{13}\text{C}$  and  $\delta^{18}\text{O}$ ) measurements on stalagmite U-1 resulted in a mean temporal resolution of 2.6 years for the last ~4100 years. There is a statistically significant (95%) but weak correlation ( $r = 0.35$ ,  $r^2 = 0.12$ ) between  $\delta^{13}\text{C}$  and  $\delta^{18}\text{O}$  time series.

### 4.5.2.1 $\delta^{18}\text{O}$

$\delta^{18}\text{O}$  values in stalagmite U-1 range from ~-8.0 to -5.9‰ (VPDB)(Fig. 4.2c) with a mean of -6.8‰. This narrow range of variability is in clear contrast to the much larger glacial-interglacial shifts, as, for example, in the Sofular Cave record (Fleitmann et al., 2009). It is therefore harder to attribute the Holocene variations in  $\delta^{18}\text{O}$  to a specific factor. Nevertheless, in mid to high latitudes, temperature is the primary climatic control on  $\delta^{18}\text{O}$  in precipitation (Dansgaard, 1964), hence in speleothems (McDermott, 2004; Lachniet, 2009). Seasonality of precipitation also has an effect via temperature, as warm season precipitation tends to have higher  $\delta^{18}\text{O}$  (Denton et al., 2005). With a variable amount of rainfall observed in all seasons (Fig. 4.1), stalagmite  $\delta^{18}\text{O}$  in Uzuntarla Cave should be controlled by changes both in temperature and the seasonality of precipitation. There is unfortunately no precipitation isotope measurement available from the area to confirm this assumption.

It is now becoming clear that an attempt to calibrate stable isotopes against meteorological records is essential to reach meaningful interpretations (Baker et al., 2011; Jex et al., 2011), even if there is no precise age control within the instrumental era. In Fig. 4.3, annual temperatures of the three nearby stations (locations given in Fig. 4.1) are compared with the most recent part of stalagmite U-1's  $\delta^{18}\text{O}$  record. To account for the seasonal variations in precipitation and resulting isotopic shifts, monthly temperatures were weighted with monthly water excess values (Thorntwaite, 1948) to calculate annual average temperatures. That is,

$$T_{\text{annual}} = [ (T_{\text{jan}} * W_{\text{jan}}) + (T_{\text{feb}} * W_{\text{feb}}) + \dots + (T_{\text{dec}} * W_{\text{dec}}) ] / W_{\text{annual}}$$

where  $T$  is the average temperature and  $W$  is the total water excess of the denoted time frame. This way, the months during which precipitation was too low to contribute to stalagmite formation are excluded from the calculation of mean temperature. An even better approach would be to use daily temperatures weighted by the precipitation value of that day (Kohn and Welker, 2005) but the climate data from this area do not have sufficient temporal resolution to allow that.

In Fig. 4.3a-b, one can observe that the isotopic variation of precipitation in the Thrace region (Çorlu and Kırklareli stations) is well registered in the Uzuntarla  $\delta^{18}\text{O}$  record, and this variation is controlled by temperature. One problem is the brevity of these meteorological records. The record from Kandilli station (Fig. 4.3c) is much longer – in fact it is the longest meteorological record in Turkey (Göktürk et al., 2008). However, it does not correlate well with U-1's  $\delta^{18}\text{O}$  record despite its humid character similar to the cave site, implying that the other two stations are more representative for the precipitation



variability at Uzuntarla. Nevertheless, the high  $\delta^{18}\text{O}$  values in the record around 1870 AD (Fig. 4.3c) coincides with the high (precipitation weighted) temperatures in Kandilli; as a response to some of the highest annual temperatures measured in this station during last 150 years (not shown). Since temperature variations are much more regionally coherent than those of precipitation, Uzuntarla  $\delta^{18}\text{O}$  should be expected to respond to significant fluctuations in Kandilli's temperature record. All in all, the Uzuntarla  $\delta^{18}\text{O}$  record is interpreted as a mixed proxy of temperature and seasonality of precipitation.

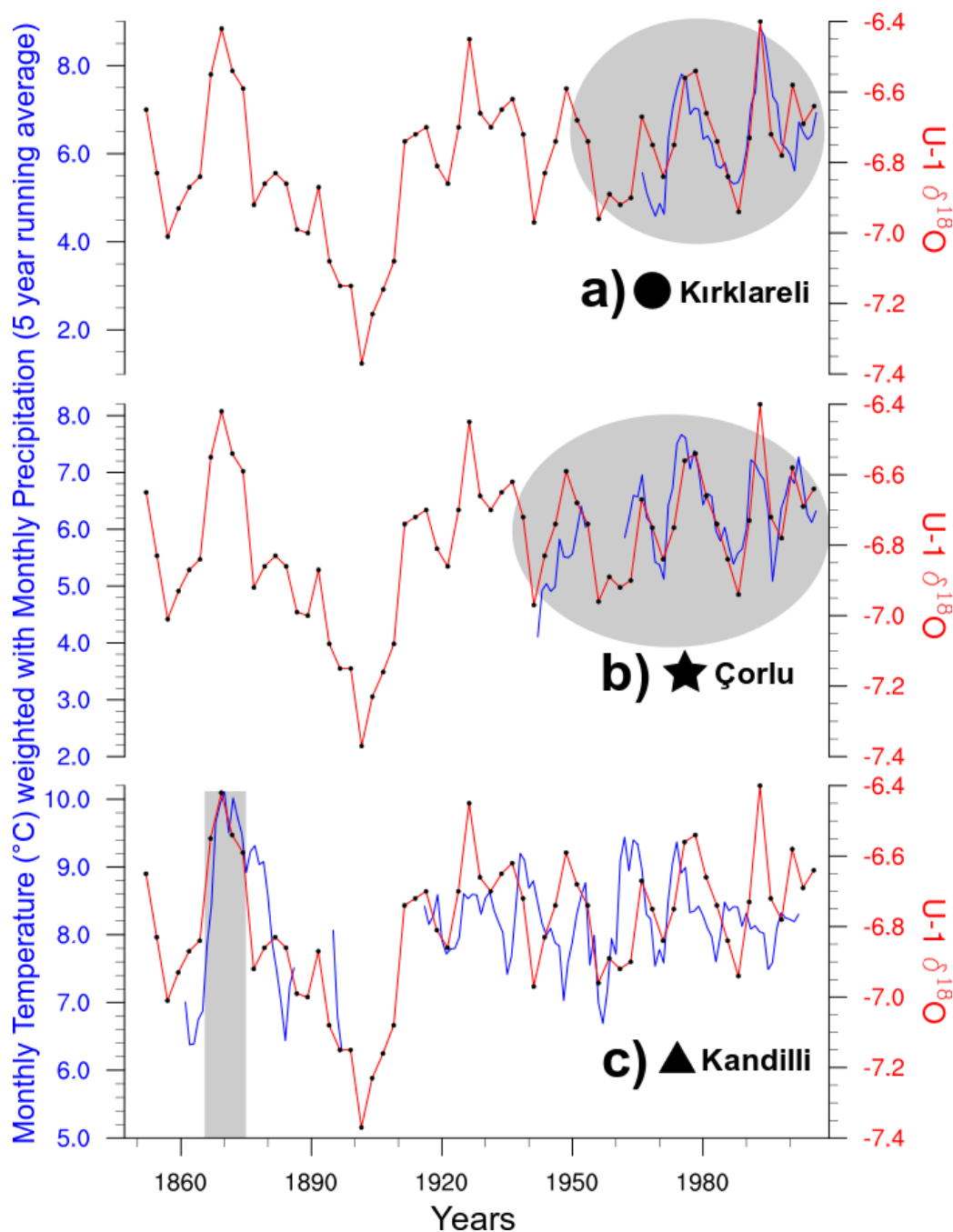


**Fig. 4.3:** Comparison of the Uzuntarla  $\delta^{18}\text{O}$  record (red curves with black dots representing data points) with the precipitation weighted monthly temperatures of **a)** Kırklareli, **b)** Çorlu and **c)** Kandilli stations (see Fig. 4.1 for locations). For meteorological records plotted, every value is the average value of the preceding 5 years including that year.

4.5.2.2  $\delta^{13}\text{C}$ 

$\delta^{13}\text{C}$  values in stalagmite U-1 vary between  $\sim -11.6$  and  $-8.8\text{‰}$  (Fig. 4.2d), around a mean of  $-10.4\text{‰}$ . This limited range of variability in  $\delta^{13}\text{C}$ , as well as the not-so-high correlation ( $r = 0.35$ ) of  $\delta^{13}\text{C}$  with  $\delta^{18}\text{O}$  suggest that kinetic fractionation played only a marginal role during the deposition of this stalagmite (Hendy, 1971; Baker et al., 2007). Variations in stalagmite  $\delta^{13}\text{C}$  is influenced by numerous processes, some of which can be related to climatic variables through their effect on vegetation and soil microbial activity (McDermott, 2004; Fairchild et al., 2006). Accordingly, lower  $\delta^{13}\text{C}$  is usually associated with abundant rainfall and moderate temperatures (e.g. Hellstrom et al., 1998; Genty et al., 2006; Fleitmann et al., 2009), though it has also been shown that rainfall above a certain threshold can lead to the opposite (Bar-Matthews et al., 2000; Göktürk et al., 2011).

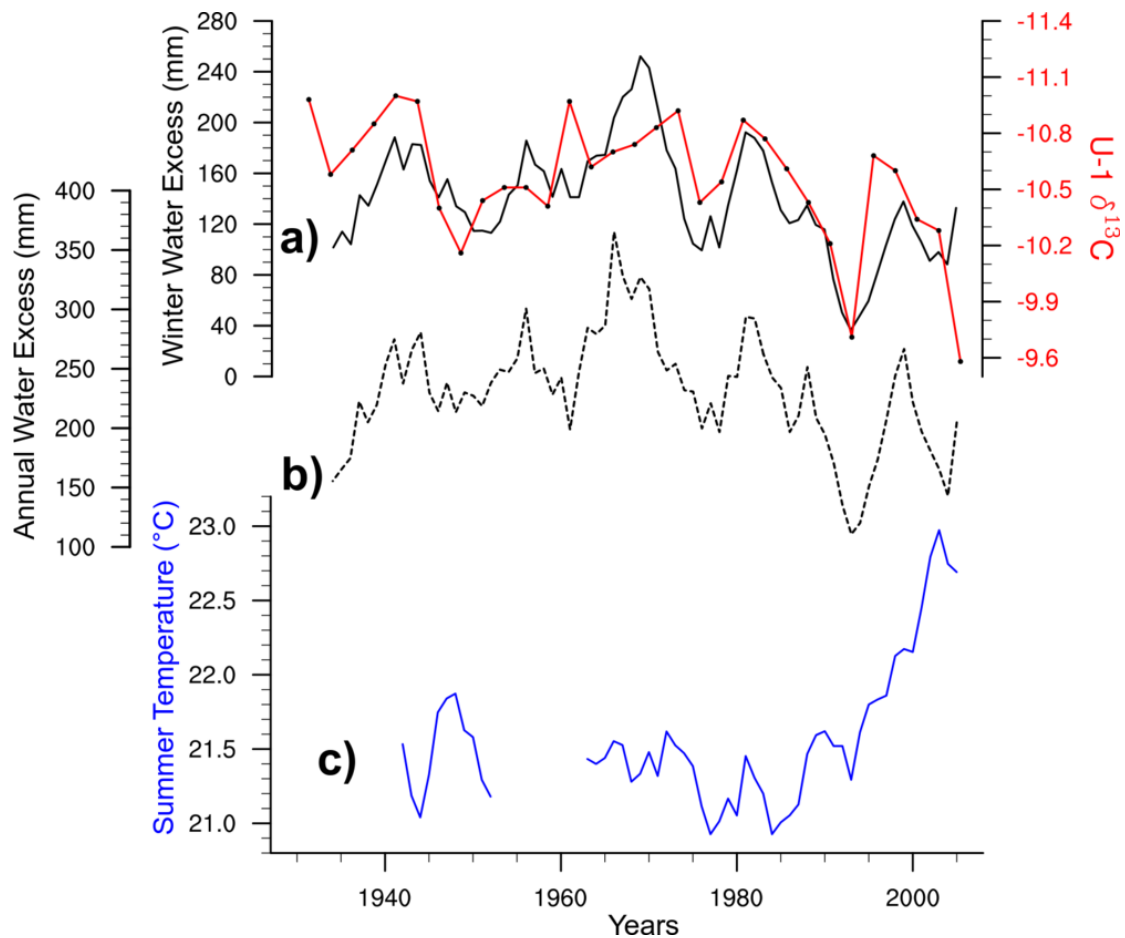


**Fig. 4.4:** Comparison of the Uzuntarla  $\delta^{13}\text{C}$  record (red line through black dots that mark data points) with **a)** the winter (DJF) water excess record (full black line) of Kırklareli, **b)** the annual water excess record (dashed black line) of Kırklareli, **c)** summer temperature (blue line) in Çorlu. For meteorological records plotted, every value is the average value of the preceding 5 years including that year. Water excess values were calculated with Thornthwaite (1948) method. See Fig. 4.1 for station locations and Section 4.5.2.2 in the text for further explanation.

In Fig. 4.4, the most recent part of the Uzuntarla  $\delta^{13}\text{C}$  is compared with the meteorological records from the region. Though not impressive,  $\delta^{13}\text{C}$  has an obvious response to the variations in water excess (Fig. 4.4a and b) in Kırklareli station (Fig. 4.1). This parameter, being in the range of  $\sim 110$  to  $360$  mm annually (Fig. 4.4b), can well be a limiting factor for

vegetation and soil microbial activity in this area, despite the indications that the cave site is probably more humid than the Kırklareli station (Section 4.3). The drying trend in this region starting at ~1970 AD (Fig. 4.4b) is especially well captured by the Uzuntarla  $\delta^{13}\text{C}$  record. Another interesting observation is that the most positive  $\delta^{13}\text{C}$  value of the last century coincides with the very hot summers of the 2000s (Fig. 4.4c; Kuglitsch et al., 2010), although annual water excess at that time is not the lowest. This may be a response of stalagmite  $\delta^{13}\text{C}$  to the decline in vegetation activity due to extreme heat (Arnone et al., 2008).

To sum up, while  $\delta^{13}\text{C}$  in Uzuntarla Cave record cannot be interpreted to perfectly reflect a certain climatic variable, it can be shown to have a climate sensitivity.  $\delta^{13}\text{C}$  responds to changes in water excess and summer temperature, becoming higher in times of aridity and very hot summers at the Uzuntarla Cave site.

### 4.5.3 Implications for Past Climate

In order to deconvolute the mixed climatic signal obtained from the stable isotopes of the Uzuntarla Cave, the  $\delta^{13}\text{C}$  record of the Kocain Cave is utilized. This record (Fig. 4.5b) was shown to reflect winter temperatures in southwestern Turkey through snowfall variations above the cave. As temperature is a regionally coherent climatic variable, Kocain  $\delta^{13}\text{C}$  can be reasonably assumed to provide the winter temperature signal for the entire western Turkey. A record of deciduous pollen percentage from a core in the northern Aegean Sea (Kotthoff et al., 2008), despite its much lower temporal resolution (Fig. 4.5c), supports the general trends in the Kocain Cave record during the last ~4.1 ka. The interpretation of Uzuntarla Cave record will be made following a time sequence, using the warm/cold epochs (Fig. 4.5) determined from the analysis of Kocain Cave record.

#### 4.5.3.1 Minoan Warm Period and the Bronze Age Collapse

According to the Kocain Cave record, the warmest winters in the last ~4.1 ka in the Eastern Mediterranean coincided with the time of Minoan Civilization in Crete, between ~2700 and 1100 BC (Fig. 4.5b). Simultaneously, the Uzuntarla record exhibits its highest  $\delta^{18}\text{O}$  values (Fig. 4.5a, lower part), which implies, following the interpretation of Uzuntarla  $\delta^{18}\text{O}$  (Section 4.5.2.1), that the substantial winter warming could have also been accompanied by summer rainfall in the southeast Balkan region. However, Uzuntarla  $\delta^{13}\text{C}$  within this time are generally higher than the remaining parts of the record (Fig. 4.5a, upper part, note descending y axis!), showing that water excess values were low and summers were probably hot and dry. This is especially so around the time of Bronze Age collapse (~1200 BC, Drews, 1993; yellow shade in Fig. 4.5); with warm winters, hot summers and low water excess values. Moreover, at the time around ~1200 BC, when the most positive  $\delta^{18}\text{O}$  values are observed in the Uzuntarla record, the stalagmite U-1 has a low rate of growth apparent from the slope of the age model (Fig. 4.2b), with yellowish brown colored growth layers, which coincided with a drying trend in an earlier study (Göktürk et al., 2011). It can be concluded that, if there is any climatic cause for the collapse of civilizations at the end of the Bronze Age (Drews, 1993; Weninger et al., 2009), this should be drought, induced by very high temperatures throughout the year, and *not* a Rapid Climate Change (cooling) event (Mayewski et al., 2004; Rohling et al., 2009). A dynamical explanation for the possible drought is still to be sought, as today's warm

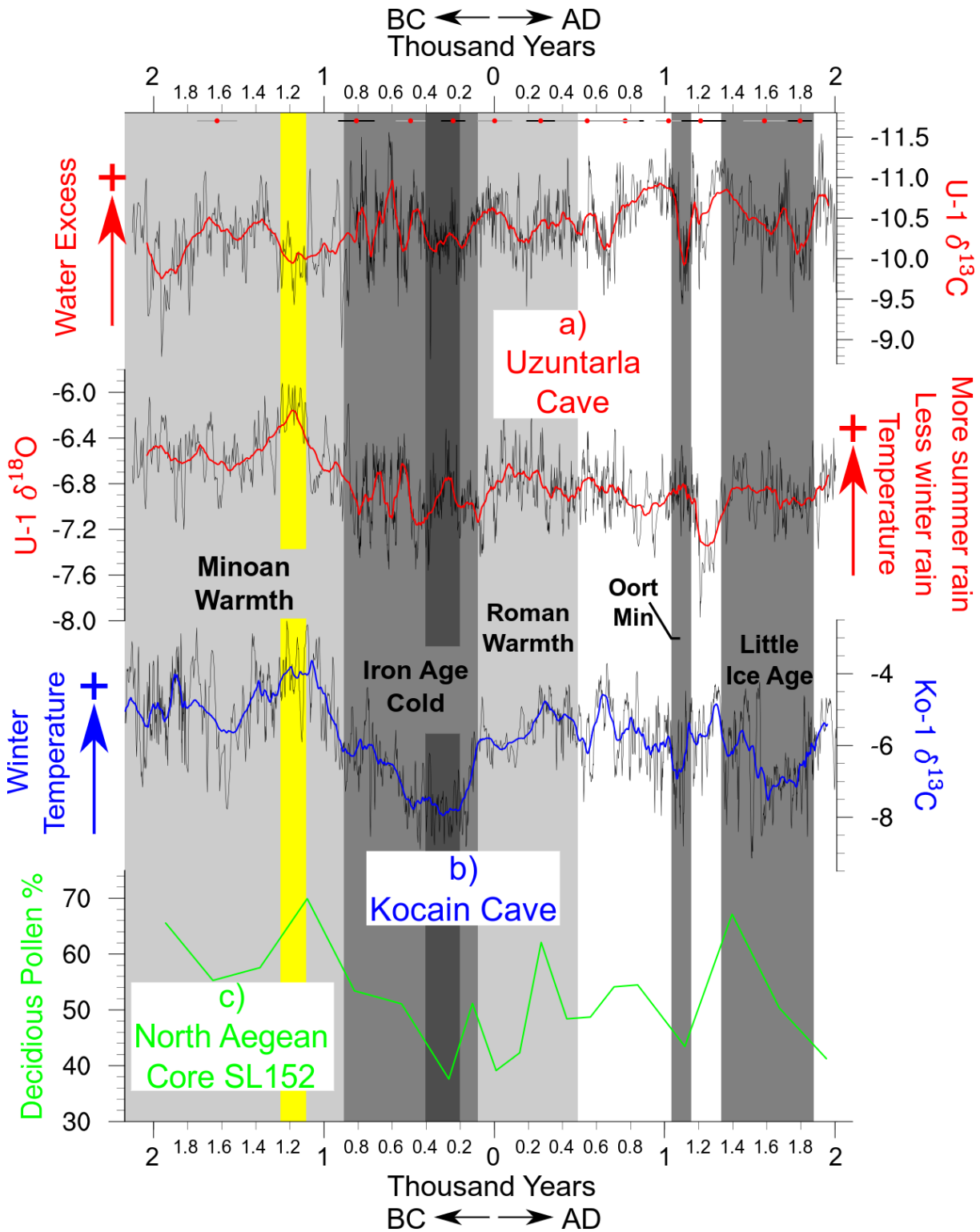


**Fig. 4.5:** Comparison of a) Uzuntarla Cave record ( $\delta^{13}C$  and  $\delta^{18}O$ , red curves are 38-year running means) with b)  $\delta^{13}C$  record (blue line is the 43-year running mean) from the Kocain Cave in southern Turkey (Göktürk et al., in prep.) and c) deciduous pollen percentage from the core SL152 (Kotthoff et al., 2008) in the Northern Aegean Sea. Warm and cold epochs were determined according to the Kocain Cave record.  $^{230}Th$  dates measured on stalagmite U-1 are shown along the top time axis (red dots) with their uncertainties. The approximate time of the Bronze Age collapse is shown with a yellow shade, whereas the darkest gray shade marks the coldest time within the Iron Age cold period.

winters in the Eastern Mediterranean are usually rainy as a response to the negative phase of both the NAO (Türkeş and Erlat, 2009) and the NCP (Krichak et al., 2002). One possibility is the influence of a series of unusually strong El Nino events (Tsonis et al., 2010; Göktürk et al., in prep.), effects of which may be unknown due to a lack of similar events in the instrumental era. Finally, the mismatch between the Uzuntarla and Kocain Cave records in the timing of the warmest period (Fig. 4.5) is probably due to the large dating (~100 years) uncertainties.

#### 4.5.3.2 Iron Age cold and Roman warm periods

Following the Minoan warmth, the Kocain Cave record indicates cooler winters in the Eastern Mediterranean between ~900 and 100 BC (Fig. 4.5b), when the global glacier advances of the Iron Age have occurred (Wanner et al., 2008). The Uzuntarla record (Fig. 4.5a) follows suit,  $\delta^{18}\text{O}$  suggesting a drop in temperatures along with  $\delta^{13}\text{C}$  indicating an increase in water excess and cooler summers. However, instead of attaining its lowest values when the winter cold culminates in the Kocain Cave record from ~400 to 200 BC (darkest gray shade in Fig. 4.5), Uzuntarla  $\delta^{18}\text{O}$  is relatively higher. This could be due to the blurring of cooling signal by a shift in the seasonality of precipitation to the warmer times of the year, as warm season rainfall has a more positive  $\delta^{18}\text{O}$  signature (Denton et al., 2005; Lachniet, 2009). Truly cold winters in the Eastern Mediterranean were shown to be associated with a lack of precipitation (Göktürk et al., 2011), especially around the Aegean Sea including Thrace region (Göktürk et al., in prep.). Accordingly, this coldest and winter-dry period of the last 4.1 ka was probably a time when both the NAO and the NCP were at their positive modes during winter.  $\delta^{13}\text{C}$  indicates a decrease in the water excess as well.

During the Roman warm period, Uzuntarla  $\delta^{18}\text{O}$  is, on average, somewhat higher than it was during the Iron Age. Apparently, the rise in  $\delta^{18}\text{O}$  due to temperature increase was partly compensated by enhanced winter precipitation – a mechanism opposite to the one during the Iron Age. The relatively stable course of Uzuntarla  $\delta^{18}\text{O}$  after the Minoan warm period implies that this modulation/compensation mechanism for  $\delta^{18}\text{O}$  operated until today.

#### 4.5.3.3 The Oort Minimum and the Little Ice Age

The Oort solar minimum and the Little Ice Age (LIA), which coincide with widespread glacier advances (Wanner et al., 2008) and do appear as prominent cooling signals in the Kocain record (Fig. 4.5b), are characterized by only slightly lower  $\delta^{18}\text{O}$  in Uzuntarla when compared to the Roman warm period; most probably arising from the shift of seasonality explained in Section 4.5.3.2. On the other hand,  $\delta^{13}\text{C}$  clearly increases (Fig. 4.5a, upper part, note descending axis!) both during the Oort minimum and the LIA, which can safely be interpreted to happen as a response to the reduction in water excess, as during the Iron Age cold period.

Between ~1200 and 1300 AD, there is a 'curious' period of consistently low  $\delta^{18}\text{O}$  values in Uzuntarla, starting with the lowest  $\delta^{18}\text{O}$  of the entire record. Accompanying this, the growth layers of the stalagmite U-1 have a very light coloring. The cause(s) for these observations is currently unknown.

## 4.6 Summary and Conclusions

In this paper, a new, highly resolved (2.6 years on average) paleoclimate proxy record covering the last ~4.1 ka was presented. The record is based on the stable isotopes ( $\delta^{18}\text{O}$  and  $\delta^{13}\text{C}$ ) of a stalagmite from the Uzuntarla Cave located in southeastern Balkan region (northwestern Turkey). Both proxies were shown to respond to more than one climatic variable, which makes their paleoclimatic interpretation difficult. Yet, reasonable conclusions can be inferred by taking other records and also regional climate characteristics into account.

- $\delta^{18}\text{O}$  in the Uzuntarla record displays a clear 'temperature effect', responding both to temperature variations and the seasonality of precipitation.
- $\delta^{13}\text{C}$  is, to some extent, a proxy for water excess, but is also influenced by summer heat.
- Using the Kocain Cave record (Göktürk et al., in prep.),  $\delta^{18}\text{O}$  and  $\delta^{13}\text{C}$  can be interpreted more clearly during the last 4.1 ka.
- The decline in the Uzuntarla  $\delta^{18}\text{O}$  as a response to cooler periods is often compensated by a shift in the seasonality of precipitation, blurring both signals. Yet, this is in good agreement with the regional climate characteristics.
- In the Eastern Mediterranean, the warm period coinciding with the Minoan civilization in Crete, seems to be warmer than any time within the last 4.1 ka, including the 20<sup>th</sup> century.
- If influenced by any climatic factor, the Bronze Age collapse must have been triggered by a widespread drought, and not by a cooling event.

## 4.7 References

- Arnone, J.A., Verburg, P.S.J., Johnson, D.W., Larsen, J.D., Jasoni, R.L., Lucchesi, A.J., Batts, C.M., von Nagy, C., Coulombe, W.G., Schorran, D.E., Buck, P.E., Braswell, B.H., Coleman, J.S., Sherry, R.A., Wallace, L.L., Luo, Y.Q., Schimel, D.S., 2008. Prolonged suppression of ecosystem carbon dioxide uptake after an anomalously warm year. *Nature* 455, 383-386.
- Baker, A., Asrat, A., Fairchild, I.J., Leng, M.J., Wynn, P.M., Bryant, C., Genty, D., Umer, M., 2007. Analysis of the climate signal contained within delta O-18 and growth rate parameters in two Ethiopian stalagmites. *Geochim Cosmochim Acta* 71, 2975-2988.
- Baker, A., Wilson, R., Fairchild, I.J., Franke, J., Spötl, C., Matthey, D., Trouet, V., Fuller, L., 2011. High resolution d18O and d13C records from an annually laminated Scottish stalagmite and relationship with last millennium climate. *Global and Planetary Change* In Press, doi:10.1016/j.gloplacha.2010.12.007.
- Bar-Matthews, M., Ayalon, A., Kaufman, A., 2000. Timing and hydrological conditions of Sapropel events in the Eastern Mediterranean, as evident from speleothems, Soreq cave, Israel. *Chem Geol* 169, 145-156.
- Dansgaard, W., 1964. Stable isotopes in precipitation. *Tellus* 16, 438-468.
- Denton, G.H., Alley, R.B., Comer, G.C., Broecker, W.S., 2005. The role of seasonality in abrupt climate change. *Quaternary Sci Rev* 24, 1159-1182.
- Drews, R., 1993. *The End of the Bronze Age: Changes in Warfare and the Catastrophe ca. 1200 B.C.*, Princeton University Press, Princeton, NJ.
- Fairchild, I.J., Smith, C.L., Baker, A., Fuller, L., Spötl, C., Matthey, D., McDermott, F., 2006. Modification and preservation of environmental signals in speleothems. *Earth-Sci Rev* 75, 105-153.

- Fairchild, I., Treble, P., 2009. Trace elements in speleothems as recorders of environmental change. *Quaternary Sci Rev* 28, 449-468.
- Fleitmann, D., Cheng, H., Badertscher, S., Edwards, R.L., Mudelsee, M., Göktürk, O.M., Fankhauser, A., Pickering, R., Raible, C.C., Matter, A., Kramers, J., Tüysüz, O., 2009. Timing and climatic impact of Greenland interstadials recorded in stalagmites from northern Turkey. *Geophys Res Lett* 36, L19707.
- Genty, D., Blamart, D., Ghaleb, B., Plagnes, V., Causse, C., Bakalowicz, M., Zouari, K., Chkir, N., Hellstrom, J., Wainer, K., Bourges, F., 2006. Timing and dynamics of the last deglaciation from European and North African delta C-13 stalagmite profiles - comparison with Chinese and South Hemisphere stalagmites. *Quaternary Sci Rev* 25, 2118-2142.
- Göktürk, O.M., Bozkurt, D., Şen, Ö., Karaca, M., 2008. Quality control and homogeneity of Turkish precipitation data. *Hydrol Process* 22, 3210-3218.
- Göktürk, O.M., Fleitmann, D., Badertscher, S., Cheng, H., Edwards, R.L., Leuenberger, M., Fankhauser, A., Tüysüz, O., Kramers, J., 2011. Climate on the southern Black Sea coast during the Holocene: Implications from the Sofular Cave record. *Quaternary Science Reviews* (accepted).
- Göktürk, O.M., Fleitmann, D., Badertscher, S., Cheng, H., Edwards, R.L., Kramers, J., Tüysüz, O. (in prep.). Late Holocene winter temperatures in the Eastern Mediterranean and their relation to cultural changes: The Kocain Cave record.
- Hellstrom, J., McCulloch, M., Stone, J., 1998. A detailed 31,000-year record of climate and vegetation change, from the isotope geochemistry of two New Zealand speleothems. *Quaternary Res* 50, 167-178.
- Hendy, C.H., 1971. Isotopic geochemistry of speleothems: I. Calculation of effects of different modes of formation on isotopic composition of speleothems and their applicability as palaeoclimatic indicators. *Geochim Cosmochim Acta* 35, 801-824.
- Jex, C.N., Baker, A., Eden, J.M., Eastwood, W.J., Fairchild, I.J., Leng, M.J., Thomas, L., Sloane, H.J., 2011. A 500 yr speleothem-derived reconstruction of late autumn-winter precipitation, North East Turkey. *Quaternary Research* In Press, doi:10.1016/j.yqres.2011.01.005.
- Kohn, M.J., Welker, J.M., 2005. On the temperature correlation of delta O-18 in modern precipitation. *Earth Planet Sci Lett* 231, 87-96.
- Kottek, M., Grieser, J., Beck, C., Rudolf, B., Rubel, F., 2006. World map of the Köppen-Geiger climate classification updated. *Meteorol Z* 15, 259-263.
- Kotthoff, U., Müller, U.C., Pross, J., Schmiedl, G., Lawson, I.T., van de Schootbrugge, B., Schulz, H., 2008. Lateglacial and Holocene vegetation dynamics in the Aegean region: an integrated view based on pollen data from marine and terrestrial archives. *Holocene* 18, 1019-1032.
- Krichak, S., Kishcha, P., Alpert, P., 2002. Decadal trends of main Eurasian oscillations and the Eastern Mediterranean precipitation. *Theor Appl Climatol* 72, 209-220.
- Kuglitsch, F., Toreti, A., Xoplaki, E., Della-Marta, P., Zerefos, C., Türkeş, M., Luterbacher, J., 2010. Heat wave changes in the eastern Mediterranean since 1960. *Geophys Res Lett* 37, L04802.
- Kutiel, H., Maheras, P., Turkes, M., Paz, S., 2002. North Sea Caspian Pattern (NCP) - an upper level atmospheric teleconnection affecting the eastern Mediterranean - implications on the regional climate. *Theor Appl Climatol* 72, 173-192.
- Lachniet, M., 2009. Climatic and environmental controls on speleothem oxygen-isotope values. *Quaternary Sci Rev* 28, 412-432.
- Lauritzen, S.E., Lundberg, J., 1999. Calibration of the speleothem delta function: an absolute temperature record for the Holocene in northern Norway. *Holocene* 9, 659-669.
- Mayewski, P.A., Rohling, E.J., Stager, J.C., Karlen, W., Maasch, K., Meeker, L.D., Meyerson, E.A., Gasse, F., van Kreveld, S., Holmgren, K., Lee-Thorp, J., Rosqvist, G., Rack, F., Staubwasser, M., Schneider, R.R., Steig, E.J., 2004. Holocene climate variability. *Quaternary Res* 62, 243-255.
- McDermott, F., 2004. Palaeo-climate reconstruction from stable isotope variations in speleothems: a review. *Quaternary Sci Rev* 23, 901-918.
- Richards, D.A., Dorale, J.A., 2003. Uranium-series chronology and environmental applications of speleothems. *Reviews in Mineralogy and Geochemistry* 52, 407-460.

- Rohling, E.J., Angela, H., Mayewski, P.A., Kucera, M., 2009. Holocene climate variability in the eastern Mediterranean, and the End of the Bronze Age, in: Bachhuber, C., Roberts, G. (Eds.), *Forces of Transformation: The End of the Bronze Age in the Mediterranean*, Oxbow Books, Oxford, UK, pp. 2-5.
- Thornthwaite, C.W., 1948. An approach toward a rational classification of climate. *Geographical Review* 38, 55-94.
- Tsonis, A.A., Swanson, K.L., Sugihara, G., Tsonis, P.A., 2010. Climate change and the demise of Minoan civilization. *Clim Past* 6, 525-530.
- Türkeş, M., 1996. Spatial and temporal analysis of annual rainfall variations in Turkey. *Int J Climatol* 16, 1057-1076.
- Türkeş, M., Erlat, E., 2003. Precipitation changes and variability in turkey linked to the North Atlantic oscillation during the period 1930-2000. *Int J Climatol* 23, 1771-1796.
- Türkeş, M., Erlat, E., 2009. Winter mean temperature variability in Turkey associated with the North Atlantic Oscillation. *Meteorol Atmos Phys* 105, 211-225.
- Vaganov, E.A., Hughes, M.K., Kirilyanov, A.V., Schweingruber, F.H., Silkin, P.P., 1999. Influence of snowfall and melt timing on tree growth in subarctic Eurasia. *Nature* 400, 149-151.
- Wanner, H., Beer, J., Butikofer, J., Crowley, T.J., Cubasch, U., Fluckiger, J., Goosse, H., Grosjean, M., Joos, F., Kaplan, J.O., Kuttel, M., Muller, S.A., Prentice, I.C., Solomina, O., Stocker, T.F., Tarasov, P., Wagner, M., Widmann, M., 2008. Mid- to Late Holocene climate change: an overview. *Quaternary Sci Rev* 27, 1791-1828.
- Weninger, B., Clare, L., Rohling, E.J., Bar-Yosef, O., Böhrer, U., Budja, M., Bundschuh, M., Feurdean, A., Gebel, H.G., Jöris, O., Linstadter, J., Mayewski, P., Mühlenbruch, T., Reingruber, A., Rollefson, G., Schyle, D., Thissen, L., Todorova, H., Zielhofer, C., 2009. The Impact of Rapid Climate Change on prehistoric societies during the Holocene in the Eastern Mediterranean. *Documenta Praehistorica* 36, 7-59.
- Ziv, B., Saaroni, H., Alpert, P., 2004. The factors governing the summer regime of the eastern Mediterranean. *Int J Climatol* 24, 1859-1871.







## CHAPTER 5

### RECORDS FROM OVACIK AND YENESU CAVES

#### 5.1 Abstract

In this chapter, preliminary results of currently inconclusive work on three Holocene stalagmite records from Ovacık and Yenesu caves in northern Turkey will be presented. These caves are close to Sofular (Chapter 2, this thesis) and Uzuntarla (Chapter 4, this thesis) caves respectively, and can in principle confirm the regional representativeness of Sofular and Uzuntarla records. However, their profiles possess dissimilarities from those of Sofular and Uzuntarla. Moreover, the two longer stable isotope profiles from Ovacık and Yenesu caves were determined not to be covering the most recent part of the Holocene, thus did not allow a comparison with meteorological records that could lead to more reliable interpretations. It is concluded that stalagmite stable isotope profiles may substantially differ from nearby stalagmite records due to local effects or other factors, which are hard to decipher with a lack of meteorological calibration.

#### 5.2 Introduction

Obtaining climate proxy records from stalagmites, as in the case of other natural archives, is a task that requires careful consideration of all factors that can lead to the observed proxy signals. Stalagmites even from the same cave can exhibit stable isotope profiles that differ from each other to a certain extent, for example owing to different hydrological routings (Fairchild et al., 2006). Differences between stalagmite records from two caves in the same climatic region can be larger due to complicating local factors. Therefore, stalagmite proxy records should be duplicated whenever possible, both using other stalagmites from the same cave, and with ones from nearby caves in the same climatic zone. Comparison of the most recent parts of stalagmite records with local meteorological records (calibration) proves very important in such cases, to find out the variables to which stalagmite proxies respond.

With an aim to support, and/or hopefully confirm the climatic signals inferred from Sofular and Uzuntarla caves (chapters 2 and 4), three stalagmite records from nearby Ovacık and Yenesu were analyzed.

#### 5.3 Ovacık and Yenesu Caves

Ovacık Cave (41°45'59" N, 32°28'28" E, entrance: 80 m asl) is similar to Sofular Cave (Chapter 2 in this thesis) in terms of its location with respect to the Black Sea (Fig. 5.1), with a somewhat lower altitude. A temperate, year-round wet climate dominates here, creating a dense vegetation. Yenesu Cave (41°36'51" N, 27°57'39" E, entrance: 160 m asl) is very close to Uzuntarla Cave (Fig. 5.1), where the semi-continental climate in inland northwestern Turkey gives way to the more humid Black Sea climate and forested terrain. The reader is referred to chapters 2 and 4 for full descriptions of the climatic characteristics of Ovacık and Yenesu cave sites, respectively.



**Fig. 5.1:** Locations of Ovacik and Yenesu Caves along with those of Sofular and Uzuntarla caves.

## 5.4 Material and Methods

Two stalagmites from Ovacik Cave (O-1, O-4; sampled in 2008) and one stalagmite from Yenesu Cave (Ye-4; sampled in 2005) were dated with  $^{230}\text{Th}$  methodology and analyzed for their stable isotopes ( $\delta^{13}\text{C}$  and  $\delta^{18}\text{O}$ ). For the stable isotope analysis, calcite samples were drilled continuously every 1 mm from O-1, a stalagmite over 1 m long. The first 36.5 mm of the much shorter O-4 was sampled at every 0.1 mm. 544 mm-long Ye-4 was drilled at every 0.5 mm. Larger quantity calcite samples were obtained from each stalagmite by a dental drill for  $^{230}\text{Th}$  dating. Further details on stable isotope analyses and  $^{230}\text{Th}$  dating method are given in Chapter 3 of this thesis, and were provided by Fleitmann et al. (2009) and Badertscher et al. (2011).

## 5.5 Results and Discussion

### 5.5.1 Chronology and Growth Rates

The age-depth plots of stalagmites O-1, O-4 and Ye-4 are given in Figs. 2, 3 and 4, respectively. Age models are based on linear interpolation through the stratigraphically ordered  $^{230}\text{Th}$  dates obtained for each stalagmite.

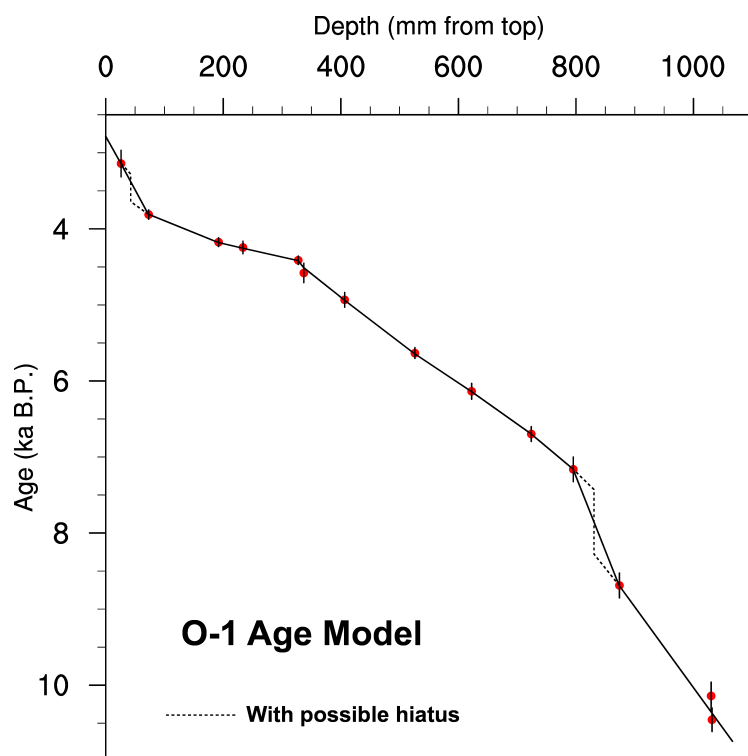


**Fig. 5.2:** Age model of stalagmite O-1.  $^{230}\text{Th}$  dates are marked with red dots, with their uncertainties attached. Dashed lines show the alternative age model with possible hiatus. B.P. Stands for 'before 1950'.

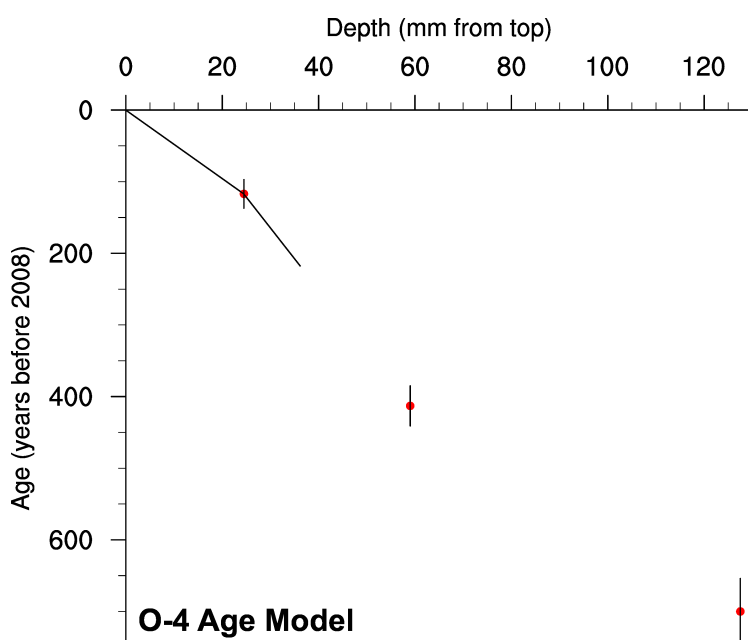


**Fig. 5.3:** Age model of stalagmite O-4.  $^{230}\text{Th}$  dates are marked with red dots, with their uncertainties attached.

### 5.5.1.1 O-1

The age model is based on 14  $^{230}\text{Th}$  dates, which are all in stratigraphic order except for the oldest two. This stalagmite grew from ~10.8 to 2.8 ka BP, with two possible hiatus between ~8.7 – 7.2 and ~3.8 – 3.1 ka BP (Fig. 5.2). Excluding those parts, the average growth rate is 0.24 mm per year, which is close to the typical values (~0.30 – 0.40 mm/yr) observed at moist Mediterranean sites (Fairchild et al., 2006).

### 5.5.1.2 O-4

The age model is based on 3  $^{230}\text{Th}$  dates, of which only one is within the range of stable isotope measurements (Fig. 5.3). This is a very recent stalagmite and was actively growing at the time of sampling, as also evident in the age model. Age errors are in the range of 6-16%, due to low  $^{230}\text{Th}/^{232}\text{Th}$  ratios (Appendix A), which is a known factor for large uncertainties (Richards and Dorale, 2003). The mean growth rate is 0.20 mm/yr.

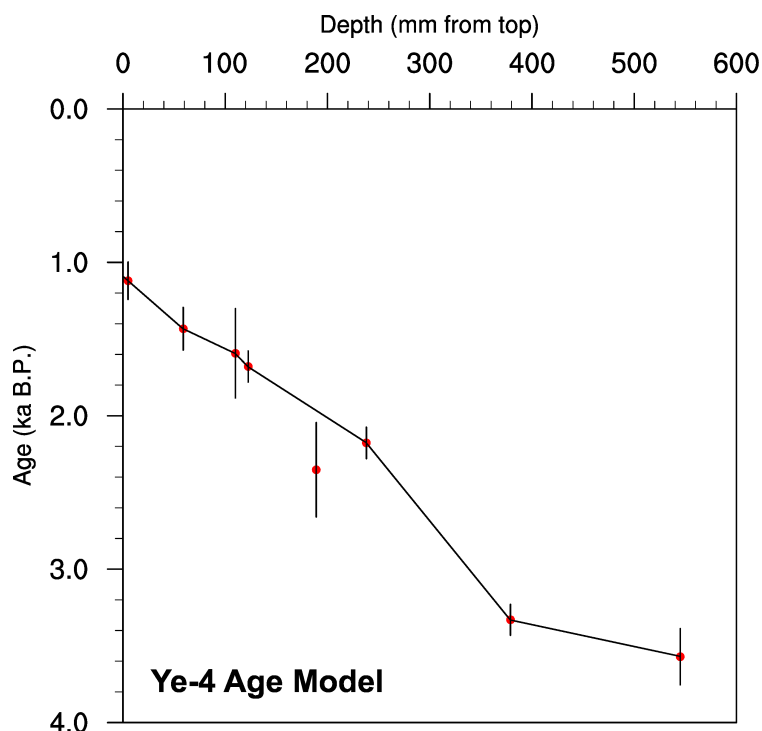


**Fig. 5.4:** Age model of stalagmite Ye-4.  $^{230}\text{Th}$  dates are marked with red dots, with their uncertainties attached. B.P. Stands for 'before 1950'.

### 5.5.1.3 Ye-4

7 out of 8 measured  $^{230}\text{Th}$  dates are in stratigraphic order in the age model of stalagmite Ye-4 (Fig. 5.4). Dates suffer from high uncertainties as a result of low  $^{230}\text{Th}/^{232}\text{Th}$  ratios (Appendix A). Growth was continuous between ~3.6 and 1.1 ka BP. The average growth rate is 0.34 mm/yr.

## 5.5.2 Stable isotope profiles and their comparison with those of Sofular and Uzuntarla caves

A total of 2519 stable isotope measurements were performed on these three stalagmites.

### 5.5.2.1 O-1

1076 stable isotope measurements on stalagmite O-1 resulted in a mean resolution of ~5.9 years.  $\delta^{18}\text{O}$  varies between -10.4 and -6.8‰ and follows a mild upward trend through the Holocene (Fig. 5.5a), reflecting the long term change in the isotopic composition of Black Sea waters as the Sofular record does. Shorter term variations in  $\delta^{18}\text{O}$  are controlled in this area by numerous climatic factors that can often operate in opposing ways (Chapter 2).  $\delta^{13}\text{C}$  ranges from -11.6 to -6.6‰, within the limits of typically observed values (-14 to -6‰) for temperate region stalagmites (McDermott, 2004). There are two prominent positive excursions of  $\delta^{13}\text{C}$  at ~4.5-4.0 ka BP (gray shade in Fig. 5.5b), implying a decrease in vegetation activity that could be attributed to aridity (e.g. Hellstrom et al., 1998). However, none of these match the timing of comparable more positive  $\delta^{13}\text{C}$  intervals in Sofular record (Fig. 5.5b). Moreover, growth rates (Fig. 5.5c) and initial  $^{234}\text{U}/^{238}\text{U}$  ratios (Fig. 5.5d) do not support the idea of arid conditions (see Chapter 2 for detailed explanation) during those positive  $\delta^{13}\text{C}$  excursions, especially at ~4.2 ka BP where the growth rates are the highest in the entire record (Fig. 5.5c) and the dating is robust (Fig. 5.5d). Moreover, stalagmite O-1 is old, thus does not allow a comparison of its stable isotope profile with recent meteorological data, which makes interpretations even harder. A positive

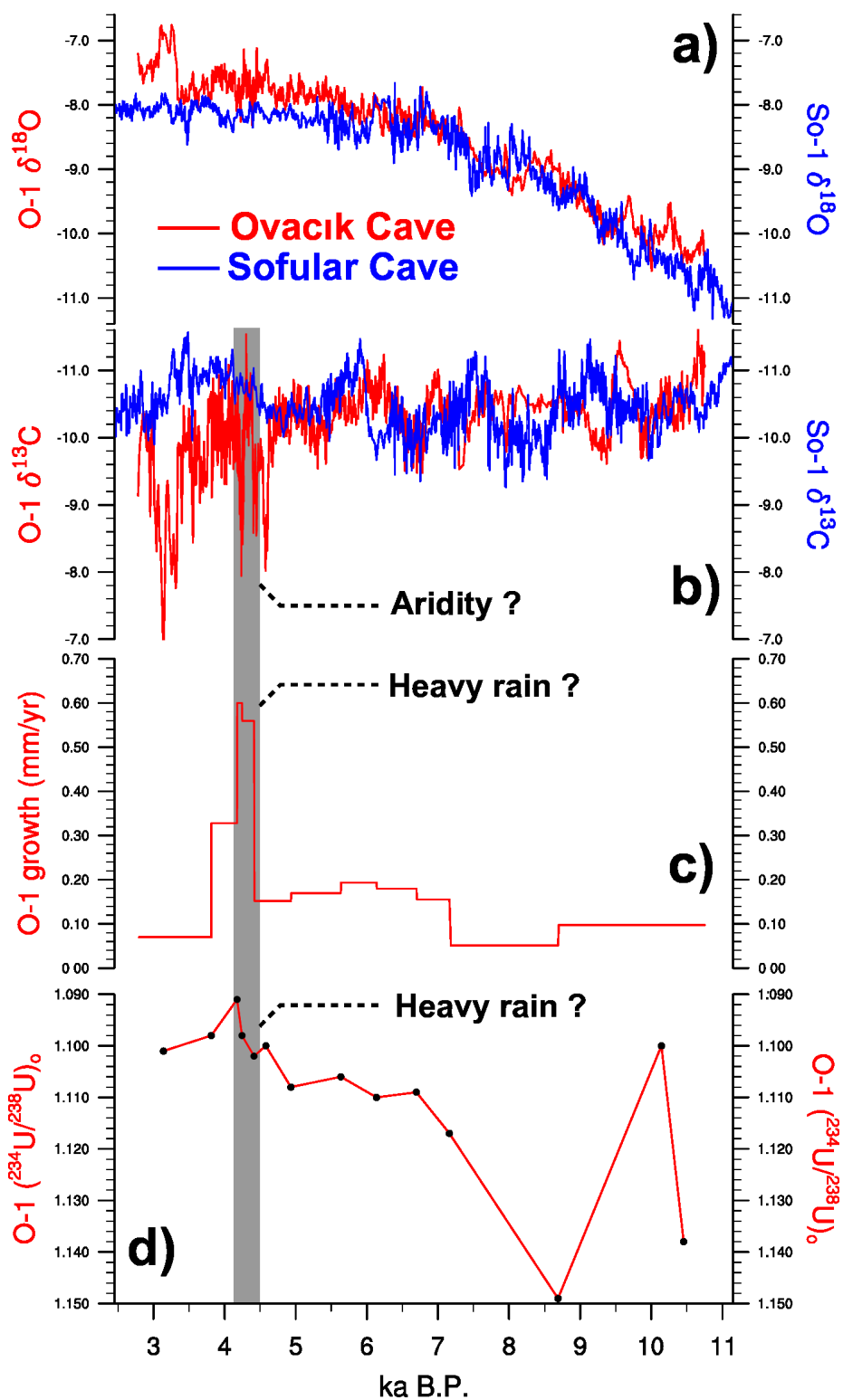


**Fig. 5.5:** Parameters of stalagmite O-1 (Ovacık Cave) along with stable isotope profile of stalagmite So-1 (Sofular Cave). B.P. Stands for 'before 1950'. **a)**  $\delta^{18}\text{O}$  (VPDB). **b)**  $\delta^{13}\text{C}$  (VPDB). **c)** Growth rate (mm/yr). **d)** Initial  $^{234}\text{U}/^{238}\text{U}$  ratio. Black dots on  $(^{234}\text{U}/^{238}\text{U})_0$  mark the  $^{230}\text{Th}$  dates.

correlation ( $r = 0.40$ ) between  $\delta^{18}\text{O}$  and  $\delta^{13}\text{C}$  time series of stalagmite O-1 implies the role of kinetic fractionation to a certain extent (Hendy, 1971).

To sum up, stalagmite O-1 does *currently* not provide sufficient data to allow reliable reconstructions of past climate variability on the Black Sea coast of Turkey. Its mismatch (especially of the  $\delta^{13}\text{C}$ ) with the more robust Sofular record reinforces this conclusion. The short-lived  $\delta^{13}\text{C}$  increase at  $\sim 4.2$  ka BP does probably have other causes than a widespread drought, which was hypothesized to have led to a societal collapse in northern Mesopotamia (Weiss et al., 1993). After all, considering the year-round wet character of the Black Sea climate that is unique within the greater Eastern Mediterranean region (see Chapter 2), it is not very plausible to argue for a severe and long lasting historical drought at Sofular and Ovacik cave sites.

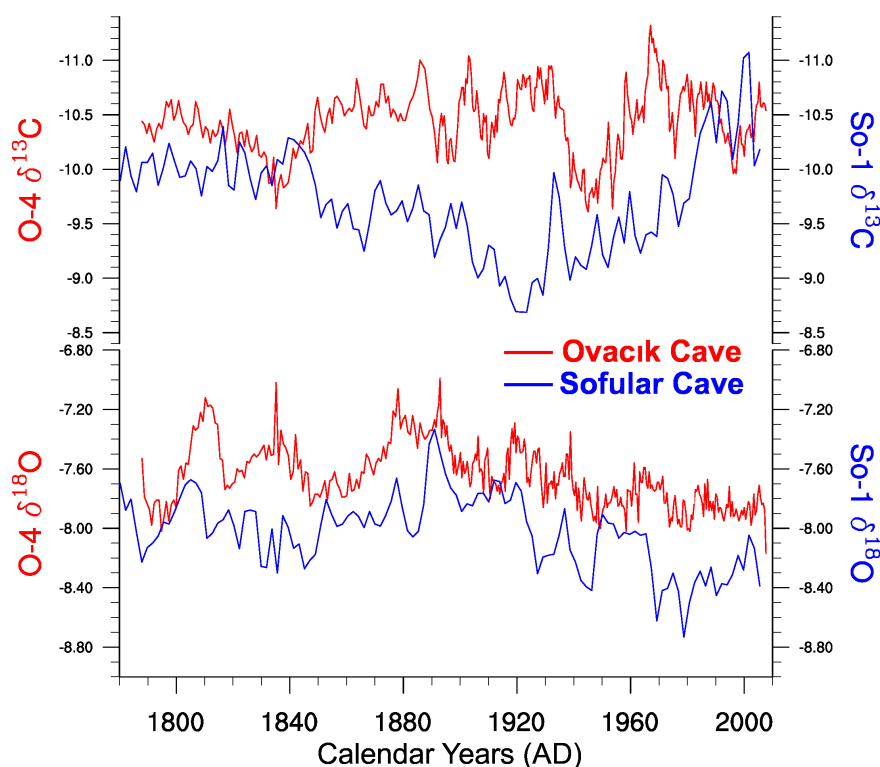


**Fig. 5.6:** Isotope profiles of stalagmite O-4 from the Ovacik Cave, compared with those of stalagmite So-1 from the Sofular Cave.

### 5.5.2.2 O-4

With 365 stable isotope measurements, stalagmite O-4 from the Ovacik Cave covers the period between 1787 and 2008 AD with sub-annual ( $\sim 0.6$  year) resolution. Comparison of its stable isotope profile with meteorological data did not yet reveal a convincing relationship, but the work is ongoing. A lack of correlation between  $\delta^{13}\text{C}$  and  $\delta^{18}\text{O}$  ( $r = -0.03$ ) implies that the two proxies are governed by different factors. In Fig. 5.6, O-4 record is presented in comparison with So-1 from the Sofular Cave.

### 5.5.2.3 Ye-4

1078 stable isotope measurements were done on the stalagmite Ye-4 from Yenesu Cave, resulting in a mean temporal resolution of  $\sim 2.3$  years over the period from  $\sim 3.6$  to 1.1 ka



BP. Correlation between  $\delta^{13}\text{C}$  and  $\delta^{18}\text{O}$  is quite high ( $r = 0.60$ ), implying that there was a common factor affecting the two parameters, one of them probably being kinetic fractionation (Hendy, 1971). The stable isotope profile of Ye-4 along with that of stalagmite U-1 from the Uzuntarla cave is given in Fig. 5.7. The similarity in the trends of  $\delta^{18}\text{O}$  profiles is obvious, whereas an eye catching common pattern in  $\delta^{13}\text{C}$  or in the shorter term variations in  $\delta^{18}\text{O}$  cannot be identified. Moreover, the range of variability in Ye-4's  $\delta^{18}\text{O}$  record is significantly narrower than that of U-1.

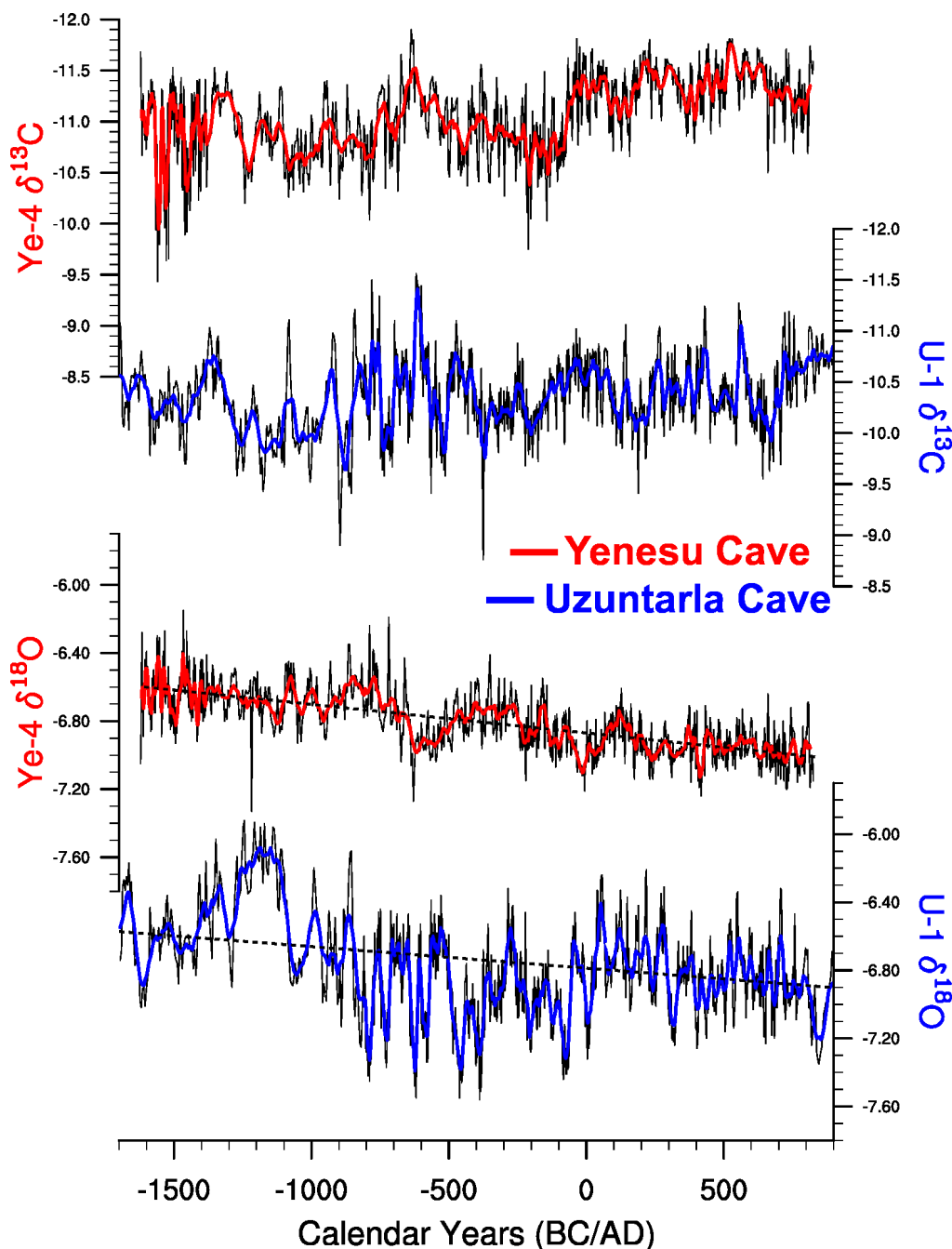


**Fig. 5.7:** Comparison of the stable isotope profiles of stalagmites Ye-4 (Yenesu Cave) and U-1 (Uzuntarla Cave). The upper and lower two panels are for  $\delta^{13}\text{C}$  and  $\delta^{18}\text{O}$ , respectively. The colored (red and blue) curves are the 10-point running averages, whereas the thin black curves show the raw data. Dashed black lines are the least squares linear trends of the  $\delta^{18}\text{O}$  profiles.

## 5.6 Conclusions

Three stalagmite records from Ovacık (O-1 and O-4) and Yenesu (Ye-4) caves were presented. It has been shown that their stable isotope profiles, especially  $\delta^{13}\text{C}$ , substantially differ from those of stalagmites from nearby Sofular and Uzuntarla caves. The two longer records (O-1 and Ye-4) do not cover the 20<sup>th</sup> century, thus they cannot be compared with meteorological records; which makes their interpretation harder.

## 5.7 References

- Badertscher, S., Fleitmann, D., Cheng, H., Edwards, R.L., Gokturk, O.M., Zumbuhl, A., Leuenberger, M., Tuysuz, O., 2011. Pleistocene water intrusions from the Mediterranean and Caspian seas into the Black Sea. *Nat Geosci* 4, 236-239.
- Fairchild, I.J., Smith, C.L., Baker, A., Fuller, L., Spötl, C., Matthey, D., McDermott, F., 2006. Modification and preservation of environmental signals in speleothems. *Earth-Sci Rev* 75, 105-153.
- Fleitmann, D., Cheng, H., Badertscher, S., Edwards, R.L., Mudelsee, M., Gökürk, O.M., Fankhauser, A., Pickering, R., Raible, C.C., Matter, A., Kramers, J., Tüysüz, O., 2009. Timing and climatic impact of Greenland interstadials recorded in stalagmites from northern Turkey. *Geophys Res Lett* 36, L19707.
- Hellstrom, J., McCulloch, M., Stone, J., 1998. A detailed 31,000-year record of climate and vegetation change, from the isotope geochemistry of two New Zealand speleothems. *Quaternary Res* 50, 167-178.
- Hendy, C.H., 1971. Isotopic geochemistry of speleothems: I. Calculation of effects of different modes of formation on isotopic composition of speleothems and their applicability as palaeoclimatic indicators. *Geochim Cosmochim Acta* 35, 801-824.
- Jex, C.N., Baker, A., Eden, J.M., Eastwood, W.J., Fairchild, I.J., Leng, M.J., Thomas, L., Sloane, H.J., 2011. A 500-yr speleothem-derived reconstruction of late autumn-winter precipitation, North East Turkey. *Quaternary Research*, In Press, doi:10.1016/j.yqres.2011.01.005.
- McDermott, F., 2004. Palaeo-climate reconstruction from stable isotope variations in speleothems: a review. *Quaternary Sci Rev* 23, 901-918.
- Richards, D.A., Dorale, J.A., 2003. Uranium-series chronology and environmental applications of speleothems. *Reviews in Mineralogy and Geochemistry* 52, 407-460.
- Weiss, H., Courty, M.A., Wetterstrom, W., Guichard, F., Senior, L., Meadow, R., Curnow, A., 1993. The genesis and collapse of 3rd millennium north Mesopotamian civilization. *Science* 261, 995-1004.





---

## CHAPTER 6

### SUMMARY AND FINAL CONCLUSIONS

#### 6.1 Summary

In this PhD thesis, 6 proxy records based on 8 stalagmites from caves in various regions of Turkey are presented; with an aim to better understand the climatic and environmental evolution of the Eastern Mediterranean region through the Holocene. To construct the records, a total of 9582 stable isotope ( $\delta^{13}\text{C}$  and  $\delta^{18}\text{O}$ ) measurements were performed and 128  $^{230}\text{Th}$  dates were obtained within the Holocene sections of the stalagmites. 3 of the 6 records provide conclusive results concerning some of the specific problems of the Holocene climate in this area. The summary of each chapter and their conclusions are given below.

In **Chapter 1**, the thesis was introduced by providing background information about the study area, material and methods used; along with the aim and outline of the thesis.

In **Chapter 2**, the Holocene profile of the Sofular Cave record from the southern coast of the Black Sea (northern Turkey) was presented. The robust age model for the stalagmite So-1 based on 41  $^{230}\text{Th}$  dates allows the construction of a record consisting of  $\delta^{18}\text{O}$ ,  $\delta^{13}\text{C}$ , growth rate and  $(^{234}\text{U}/^{238}\text{U})_0$  time series with a very high mean temporal resolution of 5.4 years for the stable isotope profile. The main conclusions of this chapter are as follows:

- $\delta^{13}\text{C}$ , growth rates and the  $(^{234}\text{U}/^{238}\text{U})_0$  time series proved to be more useful than  $\delta^{18}\text{O}$  in understanding the hydrological conditions over the southern Black Sea coast through the Holocene; as the direct effect of climatic changes on the  $\delta^{18}\text{O}$  is masked by changes in the  $\delta^{18}\text{O}$  of Black Sea surface water. High growth rates and low  $(^{234}\text{U}/^{238}\text{U})_0$  between 9.6 and 5.4 ka BP, which coincide with the early- to mid-Holocene wet period and sapropel deposition in the Eastern Mediterranean, show that the southern Black Sea region experienced times of enhanced and more intense precipitation in concert with regional trends. However, the  $\delta^{13}\text{C}$  record does not indicate an increase in effective moisture level, probably due to water-excess related non-equilibration of seepage waters with soil  $\text{CO}_2$ , or, less likely, to a rainfall deficit in the vegetation growing season.

- Of the previously suggested climatic mechanisms for the early- to mid-Holocene wet period, there is evidence in Sofular record supporting two of the scenarios, albeit without a firm conclusion: a) The enhanced fall / winter precipitation mechanism with increased summer aridity, due to elevated summertime sea surface temperatures (Tzedakis, 2007). b) A regional summer monsoon mechanism involving the Black Sea and the Mediterranean, previously proposed by Arz et al. (2003) for the northern Red Sea involving only the Mediterranean. There are disagreements among the Eastern Mediterranean records concerning the timing of the wet period, complicating the issue even further. More high-quality paleoclimate records are needed in order to eliminate one of the scenarios, as well as to explain the timing discrepancies.

- The influence of Rapid Climate Change events (RCCs, Mayewski et al., 2004) on the southern Black Sea coast is unclear; probably due to the local effects of the Black Sea (e.g.

sea effect precipitation) and the North Anatolian mountain range. Nevertheless, the long-term anomaly centered at 8.2 ka (Rohling and Palike, 2005) is present in Sofular Cave record as a decrease in rainfall.

In **Chapter 3**, a new high resolution proxy record for winter temperatures in southern Turkey was presented. Covering the last ~5700 years, this record is based on the  $\delta^{13}\text{C}$  profile of a stalagmite from the Kocain Cave near Antalya. During the time of meteorological observations,  $\delta^{13}\text{C}$  values in this stalagmite match the variations in the amount of decadal snowfall, which closely follows decadal winter temperatures. It is shown, for the first time, that stalagmite  $\delta^{13}\text{C}$  can have more negative values as a response to increased snowfall, rather than to increased rainfall above the cave; this is most probably due to preferential infiltration and higher soil wetting ability of snowmelt. The main conclusions concerning the climate of the last 5700 years and its relationship with cultural changes are as follows.

- There is a good agreement between periods of major cold in the Kocain Cave record and widespread glacier advances; which independently confirms our interpretation of stalagmite  $\delta^{13}\text{C}$  as a snowfall and winter temperature proxy.

- Winter warmth in southern Turkey during the 20<sup>th</sup> century AD is matched and exceeded several times in the last ~5700 years, especially during the time of the Minoan civilization in Crete between ~2400 and 1100 BC.

- While a persistent positive North Atlantic Oscillation during the Medieval Warm Period is only partially supported by the Kocain record, our results contradict the idea of generally negative NAO during the Little Ice Age.

- Both cold and warm extremes can lead to societal crisis or collapse, as implied by the Kocain Cave record. This record provides strong evidence for the previously hypothesized influence of extreme cold and drought on the uprisings in the 16<sup>th</sup> century AD Ottoman empire. The 4.2 ka BP event in northern Mesopotamia may primarily be a cold event, rather than widespread aridification. Large-scale extremes not encountered in the instrumental era may have led to climatic patterns and regional responses that are unknown today, especially in the case of Bronze Age collapse in the Eastern Mediterranean. The time around the Bronze Age collapse is the warmest in the entire Kocain record.

- Our hypotheses, specifically the one linking  $\delta^{13}\text{C}$  to snowfall will be further tested in the future through analysis of new stalagmites from Kocain Cave, as well as monitoring studies in the cave and its environment.

In **Chapter 4**, a new, highly resolved (2.6 years on average) paleoclimate proxy record covering the last ~4.1 ka was presented. The record is based on the stable isotopes ( $\delta^{18}\text{O}$  and  $\delta^{13}\text{C}$ ) of a stalagmite from the Uzuntarla Cave located in southeastern Balkan region (northwestern Turkey). Both proxies were shown to respond to more than one climatic variable, which makes their paleoclimatic interpretation difficult. Yet, reasonable conclusions can be inferred by taking other records and also regional climate

characteristics into account.

-  $\delta^{18}\text{O}$  in the Uzuntarla record displays a clear 'temperature effect', responding both to temperature variations and the seasonality of precipitation.

-  $\delta^{13}\text{C}$  is, to some extent, a proxy for water excess, but is also influenced by summer heat. Using the Kocain Cave record (Chapter 3 in this thesis),  $\delta^{18}\text{O}$  and  $\delta^{13}\text{C}$  can be interpreted more clearly during the last 4.1 ka.

- The decline in the Uzuntarla  $\delta^{18}\text{O}$  as a response to cooler periods is often compensated by a shift in the seasonality of precipitation, blurring both signals. Yet, this is in good agreement with the regional climate characteristics.

- In the Eastern Mediterranean, the warm period coinciding with the Minoan civilization in Crete, seems to be warmer than any time within the last 4.1 ka, including the 20<sup>th</sup> century.

- If influenced by any climatic factor, the Bronze Age collapse must have been triggered by a widespread drought, and not by a cooling event.

In **Chapter 5**, three stalagmite records from Ovacık (O-1 and O-4) and Yenesu (Ye-4) caves, which are very close to Sofular (Chapter 2) and Uzuntarla (Chapter 4) caves respectively, were presented; with an aim of confirming the regional representativeness of Sofular and Uzuntarla records. However, it has been shown that the stable isotope profiles of stalagmites from Ovacık and Yenesu caves, especially  $\delta^{13}\text{C}$ , substantially differ from those of stalagmites from Sofular and Uzuntarla caves. The two longer records (O-1 and Ye-4) do not cover the 20<sup>th</sup> century, thus they cannot be compared with meteorological records; which makes their interpretation harder.

## 6.2 Final Conclusions and Outlook

It has been shown that stalagmites, with their potential ability to record various climatic and environmental parameters, are valuable natural archives to study the Holocene climate. However, they have also their own shortcomings. First of all, the signature of the more subtle Holocene climatic variations (compared to glacial-interglacial shifts) can be overridden by factors that are not related to climate. This is probably what was observed in the diverging stable isotope profiles of stalagmites from nearby caves in Turkey. At this point, monitoring in caves and choosing actively growing samples (both of which are not always possible) prove essential to find out the factors influencing stalagmite proxies. Moreover, in the absence of annual layering and fast growth, dating uncertainties of the 'contaminated' samples (i.e. samples with high  $^{232}\text{Th}$  content due to detrital material) become a problem on short time scales within the Holocene; by, for example, not allowing a robust determination of climatically extreme years. Determining those would also lead to a better interpretation of the proxies.

Nevertheless, stalagmites should continue to serve as natural archives for the Holocene, as caves are widely distributed in the climatically diverse Eastern Mediterranean region. Only a well distributed network of paleoclimate proxy records can lead to a better and non-

simplistic understanding of the Holocene climate in this area, as well as its responses to hemispheric and global forcing mechanisms.

### **6.3 References**

- Arz, H.W., Lamy, F., Patzold, J., Muller, P.J., Prins, M., 2003. Mediterranean moisture source for an early-Holocene humid period in the northern Red Sea. *Science* 300, 118-121.
- Mayewski, P.A., Rohling, E.J., Stager, J.C., Karlen, W., Maasch, K.A., Meeker, L.D., Meyerson, E.A., Gasse, F., van Kreveld, S., Holmgren, K., Lee-Thorp, J., Rosqvist, G., Rack, F., Staubwasser, M., Schneider, R.R., Steig, E.J., 2004. Holocene climate variability. *Quaternary Res* 62, 243-255.
- Rohling, E.J., Palike, H., 2005. Centennial-scale climate cooling with a sudden cold event around 8,200 years ago. *Nature* 434, 975-979.
- Tzedakis, P.C., 2007. Seven ambiguities in the Mediterranean palaeoenvironmental narrative. *Quaternary Sci. Rev.* 26, 2042-2066.







## APPENDIX A

### DATA

The data sets presented in this work can be found on the CD enclosed, which includes the following folders:

1. Stable isotope ( $\delta^{13}\text{C}$  and  $\delta^{18}\text{O}$ ) measurements.
2. All  $^{230}\text{Th}$  dates measured at the Department of Geology and Geophysics, University of Minnesota (USA).
3. All  $^{230}\text{Th}$  dates measured at the Institute of Geological Sciences, University of Bern (Switzerland).

## APPENDIX B

### PUBLICATIONS

During his PhD study, Ozan Mert Göktürk contributed to and became a co-author on two research articles, which can be found in the following pages.



## Timing and climatic impact of Greenland interstadials recorded in stalagmites from northern Turkey

D. Fleitmann,<sup>1,2</sup> H. Cheng,<sup>3</sup> S. Badertscher,<sup>1,2</sup> R. L. Edwards,<sup>3</sup> M. Mudelsee,<sup>4</sup> O. M. Göktürk,<sup>1,2</sup> A. Fankhauser,<sup>1</sup> R. Pickering,<sup>1</sup> C. C. Raible,<sup>2,5</sup> A. Matter,<sup>1</sup> J. Kramers,<sup>1</sup> and O. Tüysüz<sup>6</sup>

Received 14 July 2009; revised 17 August 2009; accepted 19 August 2009; published 6 October 2009.

[1] A 50 kyr-long exceptionally well-dated and highly resolved stalagmite oxygen ( $\delta^{18}\text{O}$ ) and carbon ( $\delta^{13}\text{C}$ ) isotope record from Sofular Cave in northwestern Turkey helps to further improve the dating of Greenland Interstadials (GI) 1, and 3–12. Timing of most GI in the Sofular record is consistent within  $\pm 10$  to 300 years with the “iconic” Hulu Cave record. Larger divergences ( $>500$  years) between Sofular and Hulu are only observed for GI 4 and 7. The Sofular record differs from the most recent NGRIP chronology by up to several centuries, whereas age offsets do not increase systematically with depth. The Sofular record also reveals a rapid and sensitive climate and ecosystem response in the eastern Mediterranean to GI, whereas a phase lag of  $\sim 100$  years between climate and full ecosystem response is evident. Finally, results of spectral analyses of the Sofular isotope records do not support a 1,470-year pacing of GI. **Citation:** Fleitmann, D., et al. (2009), Timing and climatic impact of Greenland interstadials recorded in stalagmites from northern Turkey, *Geophys. Res. Lett.*, 36, L19707, doi:10.1029/2009GL040050.

### 1. Introduction

[2] The last glacial period is marked by rapid variations in climate termed Greenland interstadials (GI; also known as Dansgaard-Oeschger events). While the spatial extent and climatic impact of GI is well documented [Voelker, 2002], uncertainties with respect to their absolute timing exist. Uranium-series dated ( $^{230}\text{Th}$ ) stalagmites [Wang et al., 2001; Genty et al., 2003; Burns et al., 2003; Wang et al., 2006; Spötl et al., 2006] have been used to develop a more coherent and absolute chronology of GI. To date, the Hulu Cave stalagmite oxygen isotope record captures GI 1–21 in detail, though its resolution is rather coarse (50–200 years) and spacing of  $^{230}\text{Th}$  dates averages 1,600 years [Wang et al., 2001]. Other stalagmite records covering this period are discontinuous or do not show well-expressed GI in their isotopic profiles [e.g., Genty et al., 2003] (Figure 1). Additional

$^{230}\text{Th}$ -dated stalagmites are thus required for further validation and, if necessary, refinement of the Hulu record. This is of paramount importance as the Hulu time series is being used as a ‘reference record’ for other paleoclimate records [e.g., Svensson et al., 2008; Skinner, 2008], and even to constrain radiocarbon calibration [Weninger and Joris, 2008; Hughen et al., 2006]. Here we present a 50 kyr-long stalagmite oxygen ( $\delta^{18}\text{O}$ ) and carbon ( $\delta^{13}\text{C}$ ) isotope record from Sofular Cave located at the Black Sea in northwestern Turkey (Figure 1 and auxiliary material Text S1).<sup>7</sup> A set of 98  $^{230}\text{Th}$  dates with very small errors of  $\sim 0.25$ –2.5% and highly resolved ( $\sim 20$  year resolution)  $\delta^{18}\text{O}$  and  $\delta^{13}\text{C}$  profiles allow us to assign precise ages to GI 1 (Bølling-Allerød (BA)), and 3–13.

[3] Furthermore, the Sofular time series fills a large spatial gap of precisely-dated, highly-resolved and long terrestrial paleoclimate records in the northeastern Mediterranean, and provides unambiguous evidence for the climatic and environmental impact of GI in this area, where current key-paleoclimate time series, such as the Lago Grande di Monticchio, and Soreq Cave records from Southern Italy and Israel respectively [Allen et al., 1999; Bar-Matthews et al., 2003], do not show a well developed GI (Figure 1).

### 2. Cave Location and Modern Climatology

[4] Sofular (41°25′N, 31°56′E; So-1 and So-2) and Ovacik caves (41°46′N, 32°02′E; O-1) are located in northwestern Turkey. Precipitation in this region averages  $\sim 1,200$  mm  $\text{yr}^{-1}$ , with  $\sim 75\%$  occurring between September and April (Figures S1 and S2). Moisture originates mainly from the Black Sea and, to lesser extent, from the Mediterranean and Marmara Sea. Climate in northwestern Turkey is strongly tied to the North Atlantic realm and representative for the northeastern part of the Mediterranean (Text S1 and Figure S3). Vegetation above both caves is marginally affected by human activity and consists of trees, shrubs and, to a lesser extent, grass (Figure S4).

### 3. Methods and Sample Description

[5] Three large active stalagmites, ranging between 1–1.75 m in height, were collected from Sofular Cave (stalagmites So-1 and So-2) and Ovacik Cave (stalagmite O-1) A total of 121  $^{230}\text{Th}$  dates and 5,485 stable isotope measurements were performed, although the main focus was on stalagmite So-1.

<sup>1</sup>Institute of Geological Sciences, University of Bern, Bern, Switzerland.

<sup>2</sup>Oeschger Centre for Climate Change Research, University of Bern, Bern, Switzerland.

<sup>3</sup>Department of Geology and Geophysics, University of Minnesota-Twin Cities, Minneapolis, Minnesota, USA.

<sup>4</sup>Climate Risk Analysis, Hannover, Germany.

<sup>5</sup>Climate and Environmental Physics, Physics Institute, University of Bern, Bern, Switzerland.

<sup>6</sup>Eurasia Institute of Earth Sciences, Istanbul Technical University, Istanbul, Turkey.

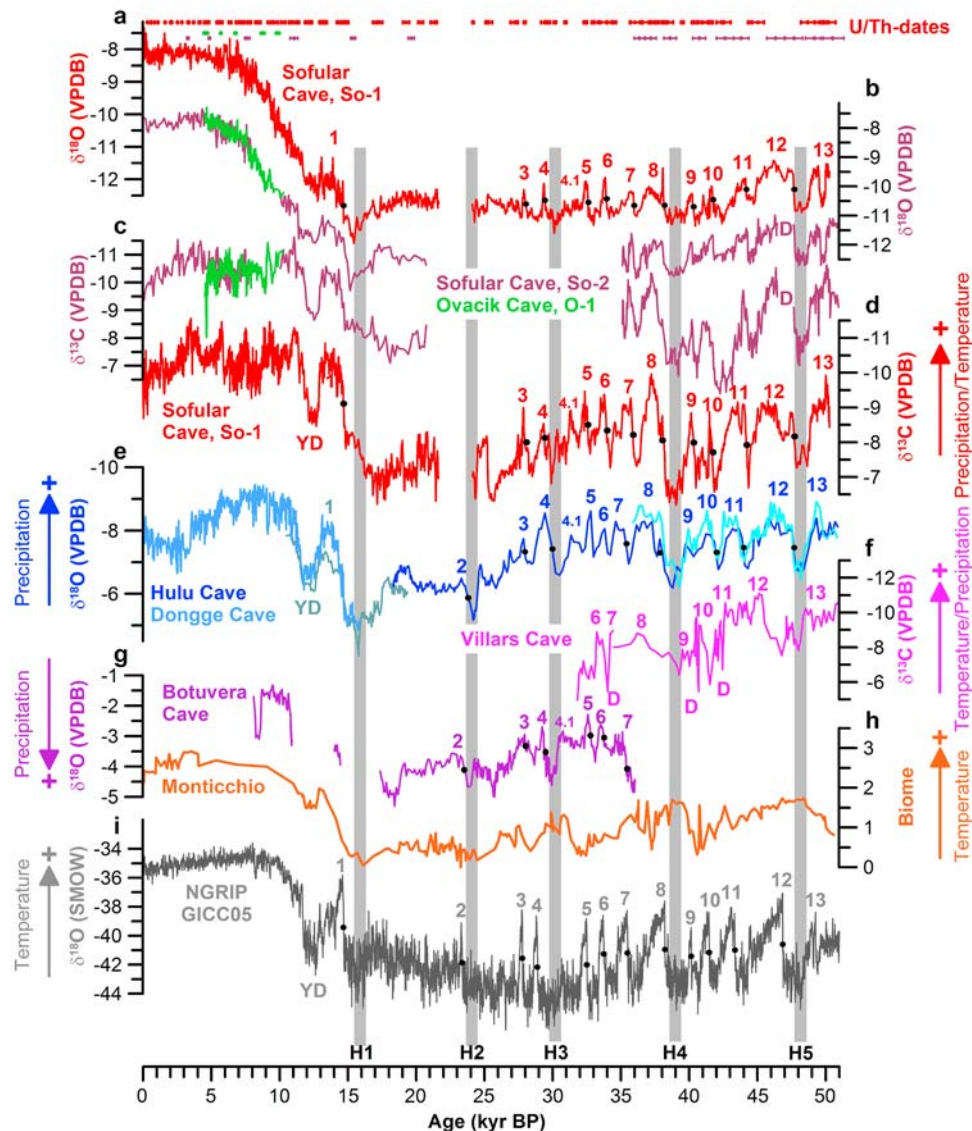


**Figure 1.** (a–d) The  $\delta^{18}\text{O}$  and  $\delta^{13}\text{C}$  time series of stalagmites So-1 and So-2 from Sofular Cave and O-1 from Ovatick Cave. Color-coded points with error bars denote  $^{230}\text{Th}$  dates. (e) Hulu and Dongge caves records from China [Wang *et al.*, 2001; Dykoski *et al.*, 2005]. (f) Villars Cave  $\delta^{13}\text{C}$  record, southwestern France [Genty *et al.*, 2003]. (g) Botuvera Cave  $\delta^{18}\text{O}$  record, Brazil [Wang *et al.*, 2006]. (h) Pollen record from Lago Grande di Monticchio from southern Italy [Allen *et al.*, 1999]. (i) NGRIP  $\delta^{18}\text{O}$ -profile from Greenland [Svensson *et al.*, 2008]. Numbers denote GI. Grey shaded bars denote Heinrich (H) events 1–5 [Bond *et al.*, 1993]. Letter D in the Sofular (So-2) and Villars Cave isotope profiles denote discontinuities.

[6]  $^{230}\text{Th}$  dating of stalagmite So-1 was made on a multi-collector inductively coupled plasma mass spectrometer (MC-ICP-MS, Thermo-Finnigan-Neptune) at the Minnesota Isotope Laboratory, University of Minnesota (Table S1). Further  $^{230}\text{Th}$  dating on all stalagmites was done on a Nu Instruments<sup>®</sup> MC-ICP-MS at the Geological Institute, University of Bern (Table S2). Detailed information on analytical procedures is provided in Texts S2 and S3 accompanying this article.

[7] Stable isotope analyses were performed on a Finnigan Delta V Advantage mass spectrometer equipped with an automated carbonate preparation system (Gas Bench-II) at the Institute of Geological Sciences, University of Bern. Precision of  $\delta^{13}\text{C}$  and  $\delta^{18}\text{O}$  measurements is 0.06‰ and 0.07‰ ( $1\sigma$ -error) respectively.

[8] Uranium concentrations of  $\sim 0.5$  ppm and low common thorium ( $^{232}\text{Th}$ ) result in especially precise  $^{230}\text{Th}$  ages for So-1; almost all of them are in stratigraphic order (Figure S5). Age models of stalagmites So-1 and O-1 are based on linear interpolation between  $^{230}\text{Th}$  dates. Chronology of So-2 was adjusted within age uncertainties to the more precisely dated stalagmite So-1, which grew nearly continuously over the last 50.3 kyr before present (BP, “present” is defined as 1950 AD), except of a hiatus between 21.2 and 24.8 kyr BP.

#### 4. Interpretation of Stable Isotope Profiles

[9] Isotope profiles of all stalagmites are very similar, indicating that So-1  $\delta^{18}\text{O}$  and  $\delta^{13}\text{C}$  values are not biased by

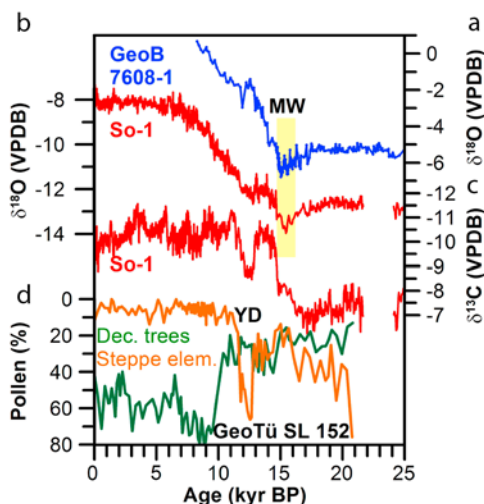


**Figure 2.** Comparison between Sofular Cave isotope profiles and marine sediment records from the Black and Aegean Seas. (a and b) The comparison between  $\delta^{18}\text{O}$  records from the western Black Sea (GeoB 7608-1) [Bahr *et al.*, 2008] and from Sofular Cave (So-1). Yellow bar marks the interval enhanced input of isotopically depleted melt water (MW). (c and d) The comparison between the So-1  $\delta^{13}\text{C}$  time series with a pollen record from the Aegean Sea (green line = deciduous trees and orange line = steppe pollen assemblages) [Kotthoff *et al.*, 2008].

site-, cave- or sample-specific effects (e.g., kinetic fractionation effects), and furthermore that the So-1 record can be used with confidence for environmental and climatic reconstructions. Interpretation of the So-1  $\delta^{18}\text{O}$  record is not simple as  $\delta^{18}\text{O}$  can be influenced by various climate variables, such as variations in surface and cave air temperatures, seasonality of precipitation, storm tracks and ice volume [McDermott, 2004]. To what extent these climate-related factors influence  $\delta^{18}\text{O}$  values in our stalagmites is not fully clear. However, well expressed GI in the So-1 and So-2  $\delta^{18}\text{O}$  records suggest that decadal- to centennial-scale variations of 0.5–1.5‰ in  $\delta^{18}\text{O}$  relate to climate; most likely to changes in temperature and seasonality of precipitation. On longer time-scales, So-1  $\delta^{18}\text{O}$  values are primarily influenced by changes in  $\delta^{18}\text{O}$  of Black Sea surface water, as revealed by the close match between So-1 and core GeoB 7608-1 from the western Black Sea [Bahr *et al.*, 2008] (Figure 2). The drop in  $\delta^{18}\text{O}$  between ~16.5 and 14.8 kyr BP due to enhanced inflow of isotopically depleted melt water [Bahr *et al.*, 2008], the subdued nature of GI 1 (BA) and the continuous increase in  $\delta^{18}\text{O}$  between ~15 and 7 kyr BP are features of both records. Thus, the Black Sea was the dominant source of moisture even during the late Pleistocene.

[10] Factors governing So-1  $\delta^{13}\text{C}$  values in stalagmites are the type and density of vegetation, and soil microbial activity [Baker *et al.*, 1997; Genty *et al.*, 2003]; all of these factors are primarily dependent on effective moisture and temperature. Stalagmite  $\delta^{13}\text{C}$  values of  $-12\text{‰}$  are characteristic for  $\text{C}_3$  (trees and shrubs) and values of  $-6\text{‰}$  for  $\text{C}_4$  (grasses) plants above the cave [Baker *et al.*, 1997]. Generally, a warmer and wetter climate in northwestern Turkey would promote a higher proportion of  $\text{C}_3$  plants (trees and shrubs), denser vegetation and enhanced soil productivity, leading to more

negative  $\delta^{13}\text{C}$  calcite values. Thus, stalagmite  $\delta^{13}\text{C}$  values are sensitive proxies for climate-driven changes of the local ecosystem. Modern stalagmite  $\delta^{13}\text{C}$  values of  $-10\text{‰}$  are in good agreement with the  $\text{C}_3$  dominated vegetation above Sofular and Ovacik caves.

## 5. Ecosystem Response to GI

[11] Between 50.3 and 14.6 kyr BP So-1  $\delta^{13}\text{C}$  values of around  $-8\text{‰}$  are indicative of more  $\text{C}_4$  plants, lower plant density and soil microbial activity due to colder and drier climatic conditions. This observation agrees with pollen evidence for enhanced steppe ( $\text{C}_4$  plants; Figure 2) and reduced arboreal vegetation in the central and eastern Mediterranean [Bottema, 1995; Allen *et al.*, 1999; Kotthoff *et al.*, 2008]. In the Sofular time series GI 1 and 3–13 are characterized by negative shifts of 1–3‰ in  $\delta^{13}\text{C}$  within a few decades to centuries (transition times were calculated by ramp regressions) (Figure S6 and Table S3), and reveal a greater proportion of  $\text{C}_3$  plants and higher soil productivity due to increasing temperatures and effective moisture. Such rapid changes in vegetation have been also observed in pollen assemblages from southern Italy (Figure 1h) and Greece, although identification of GI is difficult in both records [Allen *et al.*, 1999; Tzedakis *et al.*, 2002]. Combined  $\delta^{18}\text{O}$  and  $\delta^{13}\text{C}$  measurements hold further information on climate and ecosystem coupling at the transition into a GI. In the So-1  $\delta^{13}\text{C}$  time series, the full transition into GI takes place within  $252 \pm 87$  years (GI 8 not included), slower compared to  $121 \pm 99$  years in the So-1  $\delta^{18}\text{O}$  record, and  $62 \pm 14$  years in NGRIP (values derive from the mean and standard deviation of all transitions in So-1 and NGRIP; Figure 3a and Table S3). While the onset of GI is almost simultaneous in the So-1  $\delta^{18}\text{O}$  and  $\delta^{13}\text{C}$  time series, the slightly slower transition into GI in the So-1  $\delta^{13}\text{C}$  record suggests that the ecosystem reached a kind of equilibrium with climate within ~250 years, if the equilibrium was reached at all during shorter GI.

[12] Another interesting feature of So-1 is the nature of Termination I. In contrast to pollen records from the eastern Mediterranean [Bottema, 1995; Kotthoff *et al.*, 2008], the So-1  $\delta^{13}\text{C}$  record does not exhibit a time lag of several hundreds to thousands of years between climate and vegetation at the onset of the BA and early Holocene (Figure 2). Rather, the rapid decrease of So-1  $\delta^{13}\text{C}$  values at the onset of the BA (~14.6 kyr B.P.) and the Holocene (~10.5 kyr B.P.) suggest a fast re-vegetation with trees and shrubs ( $\text{C}_3$  plants). This observation supports the presumption that parts of the Black Sea Mountains were glacial refugia for temperate trees [Leroy and Arpe, 2007], which facilitated their rapid re-advance at the onset of the BA and Holocene. Overall, the So-1  $\delta^{13}\text{C}$  time series complements and extends pollen records from the eastern Mediterranean much further back in time, and provides, due to its precise chronology and high resolution, clear evidence for a rapid ecosystem response to GI.

## 6. Timing of GI

[13] GI and the Younger Dryas (YD) are clearly discernable in both So-1 isotope profiles and more explicit than in the Hulu and Villars caves records (Figure 1). This is important, as the more closely Sofular resembles NGRIP [Svensson *et al.*, 2008] and GISP2 [Meese *et al.*, 1997], the

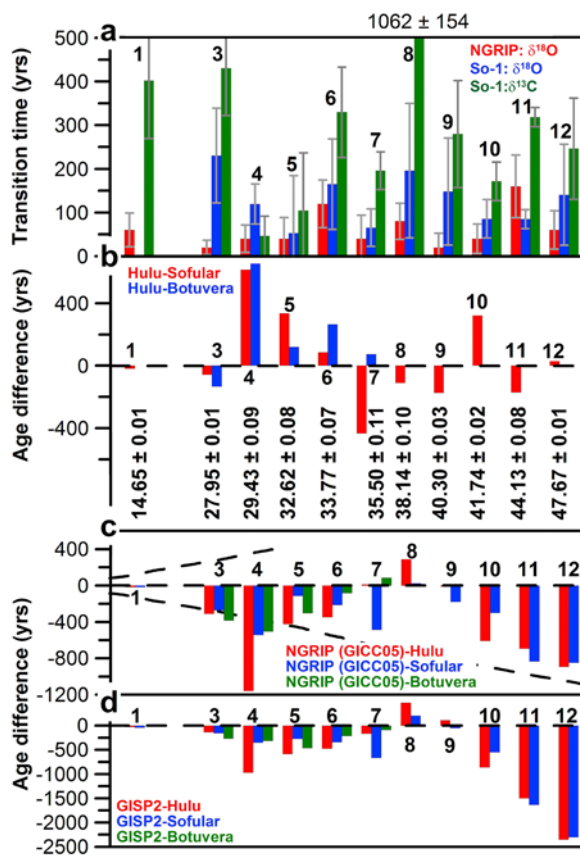


**Figure 3.** Transition time into GI in Sofular and NGRIP and comparison of stalagmite and ice core chronologies. Numbers denote GI. (a) Transition time into GI for NGRIP [Svensson *et al.*, 2008] and Sofular. Error bars denote ramp function uncertainties derived from bootstrap simulations (Text S4 and Table S3) [Mudelsee, 2000]. (b) Age offsets of midpoints of transitions into GI 1–13 between stalagmite chronologies from Hulu [Wang *et al.*, 2001], Sofular and Botuvera [Wang *et al.*, 2006] caves (Table S4). Numbers denote age estimates for GI based on the best fit between at least two stalagmite records. (c) Age offsets for midpoints of transitions into GI between NGRIP and Sofular and Hulu. Dashed lines denote  $1\sigma$  error of the NGRIP chronology. (d) Age offsets for midpoints of transitions into GI between GISP2 [Meese *et al.*, 1997] and Sofular and Hulu.

better GI can be dated and synchronized. Midpoints of isotopic transitions into GI 1–12 (referred as midpoints hereinafter) were determined by statistical ramp function regression for the Hulu and Sofular  $\delta^{18}\text{O}$  records; provided that the transition was defined by sufficiently many data points [Mudelsee, 2000] (Figures 1 and S6 and Table S4). The Villars record was not used because of its weakly expressed GI (Figure 1f). The comparison between Hulu-Sofular (Hu-So)  $\delta^{18}\text{O}$  records reveals small age offsets for GI 1 ( $\Delta t_{\text{Hu-So}} = -13$  yrs), 3 ( $\Delta t_{\text{Hu-So}} = -75$  yrs), 5 ( $\Delta t_{\text{Hu-So}} = 112$  yrs), 6 ( $\Delta t_{\text{Hu-So}} = 134$  yrs), 8 ( $\Delta t_{\text{Hu-So}} = -321$  yrs), 9 ( $\Delta t_{\text{Hu-So}} = -166$  yrs), 10 ( $\Delta t_{\text{Hu-So}} = 252$  yrs), 11 ( $\Delta t_{\text{Hu-So}} = -195$  yrs) and 12 ( $\Delta t_{\text{Hu-So}} = -9$  yrs), all of them are within dating uncertainties (Figure 3b and Table S5). Higher divergences are only observed for GI 4 ( $\Delta t_{\text{Hu-So}} = 524$  yrs) and 7 ( $\Delta t_{\text{Hu-So}} = -554$  yrs), and likely a combination of (1)  $^{230}\text{Th}$

dating uncertainties, (2) lower temporal resolution of Hulu, and (3) errors introduced by age model construction. In Hulu GI 4 is characterized by a broad peak in  $\delta^{18}\text{O}$ , which is in contrast to the relatively narrow nature of this event in Sofular, NGRIP and GISP2. Age estimate for the midpoint of GI 4 in the Botuvera (Bo) Cave record from Brazil [Wang *et al.*, 2006] (Figure 1g), differs also from Hulu ( $\Delta t_{\text{Hu-Bo}} = 613$  yrs), but is in good agreement with Sofular ( $\Delta t_{\text{So-Bo}} = 89$  yrs) (Figure 3b). However, the So-1 chronology seems to have an anomalous GI 7 timing, which is older as compared to Hulu and Botuvera (Figure 3b). Overall, the timing of most GI is broadly consistent between the Sofular, Hulu, and Botuvera caves records.

[14] Another important aspect of this study is the evaluation of the most recent NGRIP (GICC05) chronology [Svensson *et al.*, 2008]. The NGRIP-Sofular comparison shows non-systematic age offsets (Figure 3c). While age estimates for the midpoints of GI, are synchronous within stated  $1\sigma$ -age uncertainties of the NGRIP GICC05 chronology, larger age differences are observed for GI 4 ( $\Delta t_{\text{NGRIP-So}} = -586$  yrs), 7 ( $\Delta t_{\text{NGRIP-So}} = -493$  yrs), 11 ( $\Delta t_{\text{NGRIP-So}} = -839$  yrs), and 12 ( $\Delta t_{\text{NGRIP-So}} = -855$  yrs) (Figure 3c). NGRIP-Hulu age offsets are similar, GI 11 ( $\Delta t_{\text{NGRIP-Hu}} = -644$  yrs) and 12 ( $\Delta t_{\text{NGRIP-Hu}} = -846$  yrs) seem to be too young in NGRIP (Figure 3c). Even larger discrepancies are observed between GISP2-Sofular and GISP2-Hulu (Figure 3d), particularly for GI 10 ( $\Delta t_{\text{GISP2-So}} = -553$  yrs;  $\Delta t_{\text{GISP2-Hu}} = -806$  yrs), 11 ( $\Delta t_{\text{GISP2-So}} = 1636$  yrs;  $\Delta t_{\text{GISP2-Hu}} = -1441$  yrs), and 12 ( $\Delta t_{\text{GISP2-So}} = -2303$  yrs;  $\Delta t_{\text{GISP2-Hu}} = -2294$  yrs). Overall, ice core chronologies seem to be consistently too young, whereas age offsets of GI between the Greenland ice cores and Hulu and Sofular do not increase systematically with depth. GI 7–9 seem to deviate from the general trend of generally younger ages in NGRIP and GISP2 relative to the cave records, though the reason for this deviation is yet unknown.

## 7. Conclusions

[15] Based on the best fit between absolutely dated stalagmites from Sofular, Hulu and Botuvera, a more robust chronological framework for GI 1, 3–12 can now be provided. This is one prerequisite for an improved radiocarbon age scale beyond  $\sim 24$  kyr BP [Hughen *et al.*, 2006; Weninger and Joris, 2008], improvement of chronologies of ice core and sediment records, and determination of the pacing of GI. Whether GI follow an underlying cycle of  $\sim 1,500$  years is controversially discussed [You *et al.*, 1997; Rahmstorf, 2003]. Spectral analysis of the So-1  $\delta^{18}\text{O}$  and  $\delta^{13}\text{C}$  time series do not show a significant peak around 1,500 years (Figure S7) and, thus, point to a rather stochastic forcing of GI [Ditlevsen *et al.*, 2005]. Finally, the Sofular Cave record shows, for the first time, unequivocal evidence for a rapid and sensitive climate and ecosystem response in the eastern Mediterranean to GI, and thus bears important climatic information for the Black Sea area which has been a stronghold for Neanderthal populations during the late Pleistocene [Finlayson, 2008].

[16] **Acknowledgments.** This work was supported by the Swiss National Science Foundation (grant PP002-110554/1 to D. F.), the U.S. National Science Foundation (ESH 0502535 to R. L. E. and H. C.), the

Gary Comer Science and Education Foundation (CP41 to R. L. E.), the NCCR Climate (to C. C. R.), and Istanbul Technical University (grant ITU-BAP-32491 to O. T.).

## References

- Allen, J. R. M., et al. (1999), Rapid environmental changes in southern Europe during the last glacial period, *Nature*, *400*, 740–743, doi:10.1038/23432.
- Bahr, A., F. Lamy, H. W. Arz, C. Major, O. Kwiecien, and G. Wefer (2008), Abrupt changes of temperature and water chemistry in the late Pleistocene and early Holocene Black Sea, *Geochem. Geophys. Geosyst.*, *9*, Q01004, doi:10.1029/2007GC001683.
- Baker, A., E. Ito, P. L. Smart, and R. F. McEwan (1997), Elevated and variable values of  $^{13}\text{C}$  in speleothems in a British cave system, *Chem. Geol.*, *136*, 263–270, doi:10.1016/S0009-2541(96)00129-5.
- Bar-Matthews, M., A. Ayalon, M. Gilmour, A. Matthews, and C. J. Hawkesworth (2003), Sea-land oxygen isotopic relationships from planktonic foraminifera and speleothems in the eastern Mediterranean region and their implication for paleorainfall during interglacial intervals, *Geochim. Cosmochim. Acta*, *67*, 3181–3199, doi:10.1016/S0016-7037(02)01031-1.
- Bond, G., W. Broecker, S. Johnsen, J. McManus, L. Labeyrie, J. Jouzel, and G. Bonani (1993), Correlations between climate records from the Atlantic sediments and Greenland ice, *Nature*, *365*, 143–147, doi:10.1038/365143a0.
- Bottema, S. (1995), The Younger Dryas in the eastern Mediterranean, *Quat. Sci. Rev.*, *14*, 883–891, doi:10.1016/0277-3791(95)00069-0.
- Burns, S. J., D. Fleitmann, A. Matter, J. Kramers, and A. A. Al-Subbary (2003), Indian Ocean climate and an absolute chronology over Dansgaard/Oeschger events 9 to 13, *Science*, *301*, 1365–1367, doi:10.1126/science.1086227.
- Ditlevsen, P. D., M. S. Kristensen, and K. K. Andersen (2005), The recurrence time of Dansgaard-Oeschger events and limits on the possible periodic component, *J. Clim.*, *18*, 2594–2603, doi:10.1175/JCLI3437.1.
- Dykoski, C. A., et al. (2005), A high-resolution, absolute-dated Holocene and deglacial Asian monsoon record from Dongge Cave, China, *Earth Planet. Sci. Lett.*, *233*, 71–86, doi:10.1016/j.epsl.2005.01.036.
- Finlayson, C. (2008), On the importance of coastal areas in the survival of Neanderthal populations during the late Pleistocene, *Quat. Sci. Rev.*, *27*, 2246–2252, doi:10.1016/j.quascirev.2008.08.033.
- Genty, D., D. Blamart, R. Ouahdi, M. Gilmour, A. Baker, J. Jouzel, and S. Van-Exter (2003), Precise dating of Dansgaard-Oeschger climate oscillations in western Europe from stalagmite data, *Nature*, *421*, 833–837, doi:10.1038/nature01391.
- Hughen, K., J. Southon, S. Lehman, C. Bertrand, and J. Turnbull (2006), Marine-derived  $^{14}\text{C}$  calibration and activity record for the past 50000 years updated from the Cariaco Basin, *Quat. Sci. Rev.*, *25*, 3216–3227, doi:10.1016/j.quascirev.2006.03.014.
- Kotthoff, U., U. C. Muller, J. Pross, G. Schmiedl, I. T. Lawson, and H. Schulz (2008), Lateglacial and Holocene vegetation dynamics in the Aegean region: An integrated view based on pollen data from marine and terrestrial archives, *Holocene*, *18*, 1019–1032, doi:10.1177/0959683608095573.
- Leroy, S. A. G., and K. Arpe (2007), Glacial refugia for summer-green trees in Europe and south-west Asia as proposed by ECHAM3 time-slice atmospheric model simulations, *J. Biogeogr.*, *34*, 2115–2128, doi:10.1111/j.1365-2699.2007.01754.x.
- McDermott, F. (2004), Palaeo-climate reconstruction from stable isotope variations in speleothems: A review, *Quat. Sci. Rev.*, *23*, 901–918, doi:10.1016/j.quascirev.2003.06.021.
- Meese, D. A., A. J. Gow, R. B. Alley, G. A. Zielinski, P. M. Grootes, M. Ram, K. C. Taylor, P. A. Mayewski, and J. F. Bolzan (1997), The Greenland Ice Sheet Project 2 depth-age scale: Methods and results, *J. Geophys. Res.*, *102*, 26,411–26,423, doi:10.1029/97JC00269.
- Mudelsee, M. (2000), Ramp function regression: A tool for quantifying climate transitions, *Comput. Geosci.*, *26*, 293–307, doi:10.1016/S0098-3004(99)00141-7.
- Rahmstorf, S. (2003), Timing of abrupt climate change: A precise clock, *Geophys. Res. Lett.*, *30*(10), 1510, doi:10.1029/2003GL017115.
- Skinner, L. C. (2008), Revisiting the absolute calibration of the Greenland ice-core age-scales, *Clim. Past Discuss.*, *4*, 295–302.
- Spötl, C., A. Mangini, and D. A. Richards (2006), Chronology and paleo-environment of Marine Isotope Stage 3 from two high-elevation speleothems, Austrian Alps, *Quat. Sci. Rev.*, *25*, 1127–1136, doi:10.1016/j.quascirev.2005.10.006.
- Svensson, A., et al. (2008), A 60 000 year Greenland stratigraphic ice core chronology, *Clim. Past Discuss.*, *4*, 47–57.
- Tzedakis, P. C., I. T. Lawson, M. R. Frogley, G. M. Hewitt, and R. C. Preece (2002), Buffered tree population changes in a Quaternary refugium: Evolutionary implications, *Science*, *297*, 2044–2047, doi:10.1126/science.1073083.
- Voelker, A. H. L. (2002), Global distribution of centennial-scale records for Marine Isotope Stage (MIS) 3: A database, *Quat. Sci. Rev.*, *21*, 1185–1212, doi:10.1016/S0277-3791(01)00139-1.
- Wang, Y. J., H. Cheng, R. L. Edwards, Z. S. An, J. Y. Wu, C. C. Shen, and J. A. Dorale (2001), A high-resolution absolute-dated late Pleistocene monsoon record from Hulu Cave, China, *Science*, *294*, 2345–2348, doi:10.1126/science.1064618.
- Wang, X. F., A. S. Auler, R. L. Edwards, H. Cheng, E. Ito, and M. Solheid (2006), Interhemispheric anti-phasing of rainfall during the last glacial period, *Quat. Sci. Rev.*, *25*, 3391–3403, doi:10.1016/j.quascirev.2006.02.009.
- Weninger, B., and O. A. Joris (2008), A  $^{14}\text{C}$  age calibration curve for the last 60 ka: The Greenland-Hulu U/Th timescale and its impact on understanding the middle to upper Paleolithic transition in western Eurasia, *J. Hum. Evol.*, *55*, 772–781, doi:10.1016/j.jhevol.2008.08.017.
- Yiou, P., K. Fuhrer, L. D. Meeke, J. Jouzel, S. Johnsen, and P. A. Mayewski (1997), Paleoclimatic variability inferred from the spectral analysis of Greenland and Antarctic ice-core data, *J. Geophys. Res.*, *102*, 26,441–26,454, doi:10.1029/97JC00158.

S. Badertscher, A. Fankhauser, D. Fleitmann, O. M. Göktürk, J. Kramers, A. Matter, and R. Pickering, Institute of Geological Sciences, University of Bern, CH-3012 Bern, Switzerland. (fleitm@geo.unibe.ch)

H. Cheng and R. L. Edwards, Department of Geology and Geophysics, University of Minnesota-Twin Cities, Minneapolis, MN 55455, USA.

M. Mudelsee, Climate Risk Analysis, D-30167 Hannover, Germany.

C. C. Raible, Oeschger Centre for Climate Change Research, University of Bern, CE-3012 Bern, Switzerland.

O. Tüysüz, Eurasia Institute of Earth Sciences, Istanbul Technical University, 80626 Istanbul, Turkey.



# Pleistocene water intrusions from the Mediterranean and Caspian seas into the Black Sea

S. Badertscher<sup>1,2\*</sup>, D. Fleitmann<sup>1,2\*</sup>, H. Cheng<sup>3,4</sup>, R. L. Edwards<sup>4</sup>, O. M. Göktürk<sup>1,2</sup>, A. Zumbühl<sup>2</sup>, M. Leuenberger<sup>2,5</sup> and O. Tüysüz<sup>6</sup>

**The hydrological balance of the Black Sea is governed by riverine input and by the exchange with the Mediterranean Sea through the shallow Bosphorus Strait. These sources have distinctly different oxygen isotope ( $\delta^{18}\text{O}$ ) signatures. Therefore, the  $\delta^{18}\text{O}$  of Black Sea water directly reflects the presence or absence of a connection with the Mediterranean Sea, as well as hydrological changes in the vast watersheds of the Black and Caspian seas<sup>1–3</sup>. However, the timing of late to middle Pleistocene water intrusions to the Black Sea is poorly constrained in sedimentary sequences<sup>4,5</sup>. Here we present a stacked speleothem  $\delta^{18}\text{O}$  record from Sofular Cave in northern Turkey that tracks the isotopic signature of Black Sea surface water, and thus allows a reconstruction of the precise timing of hydrological shifts of the Black Sea. Our record, which extends discontinuously over the last 670,000 years, suggests that the connection between the Black Sea and Mediterranean Sea has been open for a significant period at least twelve times since 670,000 yr ago, more often than previously suggested<sup>4,5</sup>. Distinct minima in the Sofular  $\delta^{18}\text{O}$  record indicate at least seven intervals when isotopically depleted freshwater from the Caspian Sea entered the Black Sea. Our data provide precisely dated evidence for a highly dynamic hydrological history of the Black Sea.**

The modern hydrology of the Black Sea (BS) is strongly governed by the discharge of major Eurasian rivers (for example, the Danube, Dniester and Dnieper) and water exchange with the Mediterranean Sea (MS) through the shallow Bosphorus Strait (~35 mbsl) (Supplementary Fig. S1). The connection with the MS has been interrupted repeatedly over the last ~3 Myr, causing the BS to oscillate between lacustrine and marine conditions<sup>1</sup>. However, only the last incursion, at ~9.4 kyr BP, has been studied in detail<sup>2,3,6</sup>. The precise timing and nature of earlier shifts between a fresh to brackish BS are not known because BS sediment sequences older than 50 kyr cannot be dated accurately<sup>1,4,5</sup>. Thus, it remains elusive whether earlier intrusions of MS water resulted from global sea level oscillations or changes in the Bosphorus sill depth due to erosion, sedimentation or local tectonics<sup>7</sup>. Furthermore, there have been episodic intrusions of water from the Caspian Sea (CS) through the Manych–Kerch spillway into the BS, the last one occurring between ~16.5 and ~14.5 kyr BP (refs 2–4,8). However, the precise timing

and nature of earlier intrusions is, like their Mediterranean counterparts, unknown.

To provide more precise dates for major hydrological shifts of the BS, we present an absolutely dated speleothem  $\delta^{18}\text{O}$  record, extending back to 670 kyr BP, from six stalagmites (So-1, 2, 4, 6, 14B, 17A) collected from Sofular Cave. The cave is located 10 km from the southern BS coast in Turkey (Fig. 1; Supplementary Fig. S1), and the  $\delta^{18}\text{O}$  of its speleothems is an excellent recorder of fluctuations in the  $\delta^{18}\text{O}$  of BS surface water due to transitions between lacustrine and marine phases, and to intrusions of CS water<sup>9</sup>. The cave's climate is characterized by high relative humidity (>90%) and constant temperatures ( $11.8 \pm 0.2$  °C). Local precipitation averages  $1,200 \text{ mm yr}^{-1}$ . The prevalence of northerly and north-westerly winds throughout the year<sup>9</sup> (Supplementary Figs S2–S4) results in the BS being an important source of moisture (see Supplementary Information). A total of 224 <sup>230</sup>Th-ages reveal that the stalagmites are up to ~670 kyr old. However, the stacked Sofular record is not continuous, with gaps that span the intervals ~21.6–24.1, 81.8–86.3, 122.9–127.7, 133.2–159.6, 235.8–284.9, 307.0–476.0 and 516.0–563.0 kyr BP (Supplementary Fig. S5, Tables S1 and S2). The Sofular  $\delta^{18}\text{O}$  record consists of 9,300 stable isotope measurements, with values ranging between  $-7.5$  and  $-17.5$ ‰ (VPDB; Figs 2, 3; Supplementary Table S3).

Given the excellent reproducibility of the Sofular  $\delta^{18}\text{O}$  profiles (Fig. 2c), we conclude that calcite  $\delta^{18}\text{O}$  values are not compromised by kinetic effects, and thus constitute a reliable proxy for the  $\delta^{18}\text{O}$  of meteoric precipitation. Today, the  $\delta^{18}\text{O}$  of precipitation in Turkey is influenced by air temperature ('temperature effect'; ref. 10). At our cave site this effect is in the order of  $+0.26$ ‰ °C<sup>-1</sup> (Supplementary Fig. S6). When this temperature effect is added to the temperature effect associated with calcite precipitation from water ( $-0.24$ ‰ °C<sup>-1</sup>; ref. 11), the net effect between air temperature and stalagmite  $\delta^{18}\text{O}$  is almost zero, indicating that the 10‰ range in  $\delta^{18}\text{O}$  is not directly related to temperature (Fig. 3). Furthermore, the long-term trend in the Sofular  $\delta^{18}\text{O}$  profile is markedly different from that seen in the Lake Ammersee record<sup>12</sup> (located in the drainage basin of the BS), which reflects temperature-driven changes in the  $\delta^{18}\text{O}$  of precipitation in central Europe (Fig. 2a). In contrast to Ammersee, the Sofular  $\delta^{18}\text{O}$  profile (Fig. 2c) shows no clear Bølling–Allerød (BA) and Younger Dryas (YD), and a smooth linear increase into the Holocene. Between

<sup>1</sup>Institute of Geological Sciences, University of Bern, Baltzerstr. 1 + 3, 3012 Bern, Switzerland, <sup>2</sup>Oeschger Centre for Climate Change Research, University of Bern, Zähringerstr. 25, 3012 Bern, Switzerland, <sup>3</sup>Institute of Global Environmental Change, Xi'an Jiaotong University, 710049 Xi'an, Shaanxi, China,

<sup>4</sup>Department of Geology and Geophysics, University of Minnesota, 310 Pillsbury Drive SE, Minneapolis, Minnesota 55455-0231, USA, <sup>5</sup>Climate and Environmental Physics, University of Bern, Siedlerstr. 5, 3012 Bern, Switzerland, <sup>6</sup>Eurasia Institute of Earth Sciences, Istanbul Technical University, Maslak 34469, Istanbul, Turkey. \*e-mail: badertscher@geo.unibe.ch; fleitmann@geo.unibe.ch.

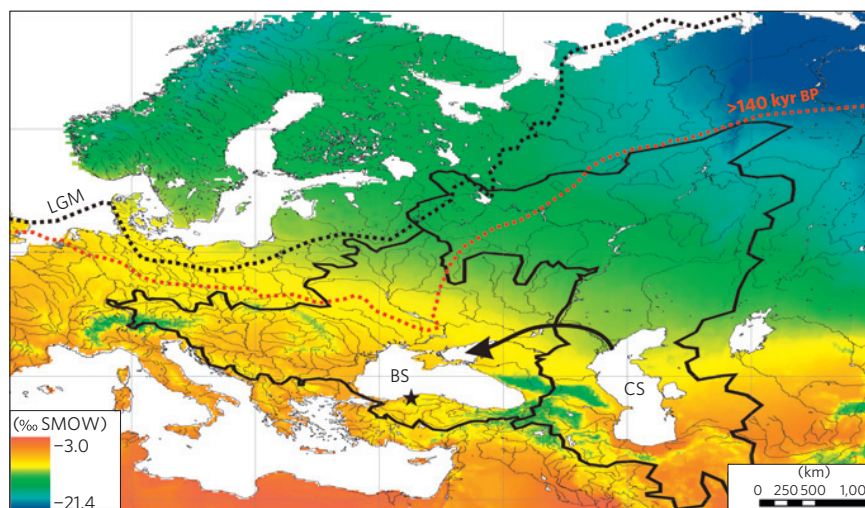


**Figure 1 | Map of Black Sea (BS) and Caspian Sea (CS) drainage basins (black lines).** Colours denote the interpolated mean annual oxygen isotope composition of precipitation (after [www.waterisotopes.org](http://www.waterisotopes.org)). The black star marks Sofular Cave. The arrow denotes the Manych-Kerch spillway, which connects the CS with the BS. The maximum ice sheet extent during the last glacial maximum (LGM) and the Saalian (140–180 kyr BP) (redrawn after ref. 25) are also shown.

10.5 and 7 kyr BP, the Sofular  $\delta^{18}\text{O}$  values increase by  $\sim 2.5\text{‰}$  whereas Ammersee increases by only  $\sim 0.4\text{‰}$ . These disparities reveal that long-term changes in the Sofular  $\delta^{18}\text{O}$  record are strongly influenced by other factors.

A major change in the source of moisture, for example from a BS to a MS water vapour source, is also unlikely. The deglacial trend in the Sofular  $\delta^{18}\text{O}$  record is opposite to that in the Soreq Cave (Fig. 2b) and Mediterranean lake records, which are closely related to the  $\delta^{18}\text{O}$  of MS surface water<sup>13,14</sup>. Rather, we suggest that the mean  $\delta^{18}\text{O}$  of precipitation reaching Sofular exhibits a greater dependence on the  $\delta^{18}\text{O}$  of the BS surface water ('water vapour source effect'; ref. 11). This sea-land oxygen isotopic coupling is substantiated by the close correspondence between the Sofular and the BS ostracod  $\delta^{18}\text{O}$  records (Fig. 2d). The decrease in  $\delta^{18}\text{O}$  between  $\sim 16.5$  and 14.8 kyr BP (related to the inflow of isotopically depleted water from the CS; refs 2–5), the subdued nature of the BA and YD, and the near-monotonic increase of  $\sim 6\text{‰}$  in  $\delta^{18}\text{O}$  between  $\sim 15$  and 9 kyr BP are visible in both the terrestrial and the marine isotopic records (Fig. 2c,d). This long-term increase in  $\delta^{18}\text{O}$  across the last deglaciation reflects the slow adjustment of the large water body of the BS ( $517,000 \text{ km}^3$ ) to the relatively small volume of riverine input (presently at  $\sim 350 \text{ km}^3 \text{ yr}^{-1}$ ;  $-6$  to  $-10\text{‰}$  VSMOW), and precipitation (presently at  $\sim 230 \text{ km}^3 \text{ yr}^{-1}$ ;  $\sim -10\text{‰}$  VSMOW; refs 15–17). In addition, the inflow of isotopically enriched Mediterranean water (presently at  $\sim 300 \text{ km}^3 \text{ yr}^{-1}$ ;  $1.8\text{‰}$  VSMOW, ref. 15) since  $9.4 \pm 0.5$  kyr BP has further increased the  $\delta^{18}\text{O}$  of BS deep water (presently at  $-1.7\text{‰}$  VSMOW), resulting in a slow equilibration (within  $\sim 1,000$ – $2,000$  yr) of the BS surface water (presently at  $\sim -2.4\text{‰}$  VSMOW) with deep water<sup>2,3,15–17</sup>. The inflow of more enriched MS water has been estimated to account for a change of  $\sim 2\text{‰}$  of BS water<sup>3,15</sup>, which is in good agreement with the observed slow increase of  $1.7\text{‰}$  in the Sofular  $\delta^{18}\text{O}$  record since  $\sim 9.5$  kyr BP. Overall, there is strong evidence for a close coupling between changes in the  $\delta^{18}\text{O}$  of BS water and stalagmite calcite. This sea-land relationship allows us to use our precisely dated stalagmites to reconstruct hydrological oscillations of the BS in detail.

On the basis of the clear visual correlation between the documented isotopic evolution during the last deglaciation and early Holocene (Fig. 2), we suggest that stalagmite  $\delta^{18}\text{O}$  values of around  $-8.5 \pm 1\text{‰}$  (error accounts for possible second order effects of evaporation, temperature and isotopic composition of precipitation) are characteristic of time intervals when a connection

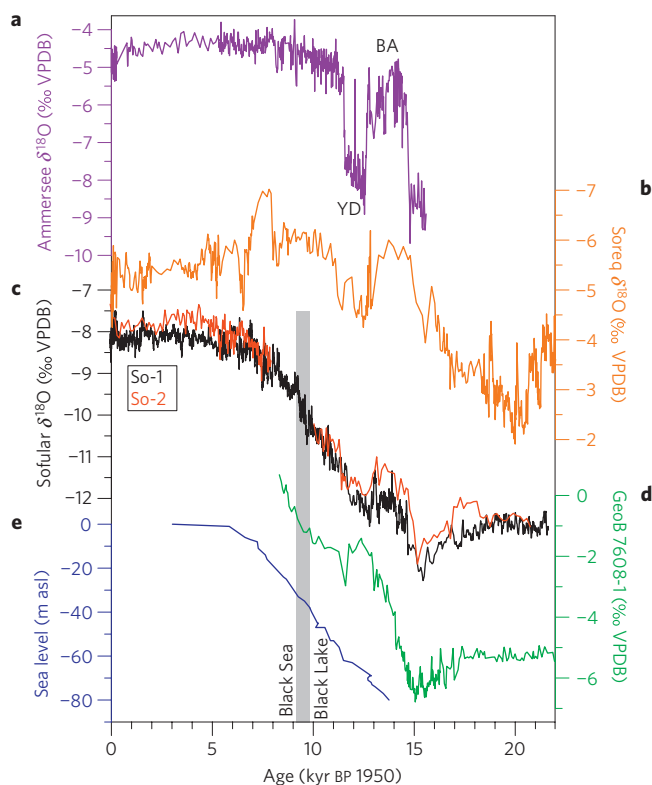


**Figure 2 | Last deglacial and Holocene  $\delta^{18}\text{O}$  variations and global sea level.** Grey vertical bar indicates the timing of the connection between the Black Sea and Mediterranean Sea. **a**, Ammersee  $\delta^{18}\text{O}$  record<sup>12</sup>. **b**, Soreq Cave  $\delta^{18}\text{O}$  record<sup>13</sup>. **c**,  $\delta^{18}\text{O}$  profiles of stalagmites So-1 and So-2 from Sofular Cave. **d**,  $\delta^{18}\text{O}$  record of Black Sea core GeoB 7608-1 (ref. 2). **e**, Sea-level record from Tahitian corals<sup>29</sup>.

between the BS and MS was established. Thus, the Sofular  $\delta^{18}\text{O}$  profile provides evidence for at least twelve time intervals (Fig. 3; Supplementary Table S4) within the last 670 kyr when water exchange between the BS and MS was established. These intervals coincide (within age uncertainties) with sea levels<sup>18,19</sup> higher than the current Bosphorus sill depth of  $\sim 35$  mbsl for at least the period spanning currently available sea-level reconstructions (that is, the

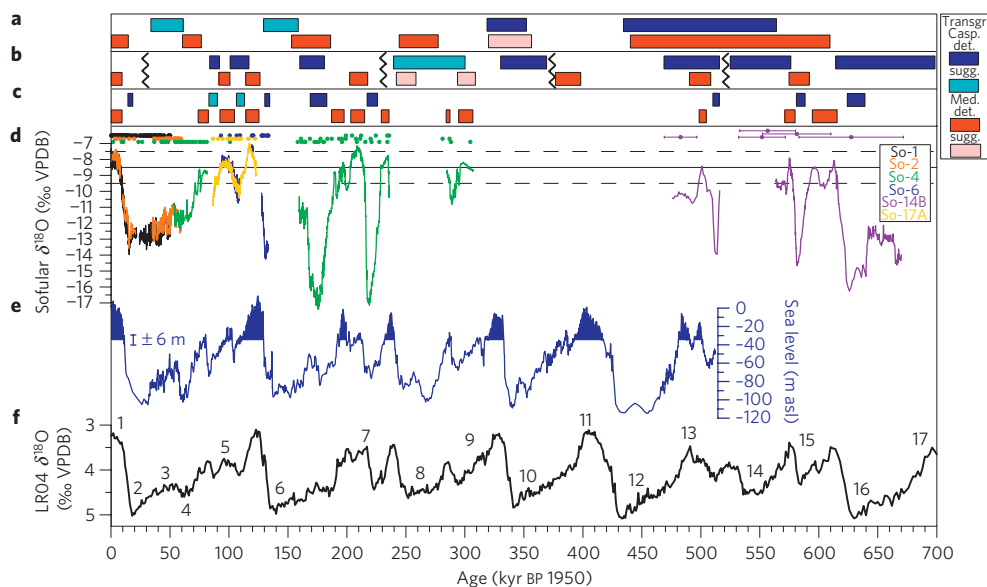


**Figure 3 | Stacked Sofular  $\delta^{18}\text{O}$  record in comparison with sedimentary records from the Black Sea and global sea level. a**, Faunal evidence for water intrusions from the MS (red) and CS (blue) into the BS (ref. 5). **b**, Faunal evidence for water intrusions from the MS (red) and CS (blue) into the BS (ref. 4). Black lines denote discontinuities in the sedimentary sequence. **c**, Sofular stalagmite evidence for water intrusions from the MS (red) and CS (blue) into the BS. **d**, Sofular  $\delta^{18}\text{O}$  record, with the colours and colour-coded dots with error bars denoting different stalagmites and  $^{230}\text{Th}$ -ages respectively. Solid horizontal line (black) indicates the threshold value of  $-8.5 \pm 1\%$  VPDB. **e**, Global sea-level curve<sup>18,19</sup> (the error is  $\pm 6$  m). Blue shaded area marks periods when global sea level was above the Bosphorus sill depth of  $\sim -35$  mbsl. **f**, LR04 stacked isotope record<sup>30</sup>. Numbers denote marine isotope stages (MIS).

last 520 kyr BP; refs 18,19). For the last 240 kyr BP, the number of intrusions of Mediterranean water in the Sofular record is broadly consistent with those identified in poorly dated sediment sequences from the BS (refs 4,5). The close association between sea level and intrusion of MS water suggests that the Bosphorus sill depth only fluctuated slightly around its present depth of  $\sim 35$  mbsl from at least marine isotope stage (MIS) 15 ( $\sim 520$  kyr BP; Fig. 3). Although this is surprising, considering local tectonic uplift (North Anatolian fault) and isostatic response<sup>20</sup>, it is plausible that these processes, combined with sedimentation and stream downcutting, have resulted in the sill depth remaining fairly constant. As intrusions of Mediterranean water were apparently intimately linked to global sea level, there were most likely more intrusions during MIS 9, 11 and 13, when sea levels were also above  $\sim 35$  mbsl. Unfortunately, MIS 9, 11 and 13 have yet to be recovered from Sofular Cave speleothems.

The Sofular time series shows distinct negative isotope excursions with  $\delta^{18}\text{O}$  values as low as  $-17.5\%$  at around 175, 220, 515, 580 and 630 kyr BP, and before Terminations I and II (Fig. 3; Supplementary Fig. S7). Such negative Sofular  $\delta^{18}\text{O}$  values have been interpreted as reflecting the inflow of isotopically depleted water from the CS via the shallow Manych–Kerch (currently at 26 masl) spillway into the BS (refs 2,3,8). Although the modern  $\delta^{18}\text{O}$  of CS water ( $-2.7$  to  $-1.7\%$  VSMOW) is almost identical to that of BS water ( $-2.4$  to  $-1.7\%$  VSMOW) (ref. 21), the  $\delta^{18}\text{O}$  of CS water was significantly lower at times of increased freshwater discharge because of the inflow of melt water from the Eurasian ice sheets, diversion of rivers, and higher runoff coefficients and reduced evaporation under colder climatic conditions<sup>22–25</sup>. This is also because of the generally more negative  $\delta^{18}\text{O}$  values of precipitation in the drainage area of the CS compared with the BS (Fig. 1), as is evident, for instance, from the difference of  $\sim 3\%$  in  $\delta^{18}\text{O}$  between runoff from the Volga ( $\sim -12.5\%$  VSMOW;  $\sim 80\%$  of total water inflow into the CS) and Danube Rivers ( $\sim -10\%$  VSMOW;  $\sim 60\%$  of total water inflow into the BS; ref. 26). Estimates for maximum total annual runoff of CS water into the BS during Termination I range from 1,000 to 1,500  $\text{km}^3 \text{yr}^{-1}$ , which is up to five times higher than current total river discharge into the BS (ref. 8). Clearly, such a high

discharge of isotopically depleted water would lead to more negative  $\delta^{18}\text{O}$  values of BS water, and, thus, of precipitation at Sofular (Fig. 3). Furthermore, the marked negative shifts in the Sofular  $\delta^{18}\text{O}$  profile are broadly consistent with faunal evidence for intrusions of CS water identified in sediment sequences from the BS (Fig. 3). In addition to CS water, a larger volume of isotopically depleted riverine water (melt water) could also have been delivered from the northern BS drainage area (for example, via the Dniestr and Dniepr) where the  $\delta^{18}\text{O}$  of precipitation is more depleted (Fig. 1).

It is striking that the negative excursions in the Sofular  $\delta^{18}\text{O}$  profile are  $\sim 3\%$  lower before  $\sim 160$  kyr BP than during the well-documented enhanced input of CS water between 16.5 and 14.5 kyr BP (Fig. 2; ref. 2). This suggests that the discharge of isotopically depleted water into the BS was considerably higher before  $\sim 160$  kyr BP owing to a greater extent of ice sheets in the northern drainage basin of the BS and CS during the middle Pleistocene<sup>24,25,27</sup> (Fig. 1). Our hypothesis is supported by the reconstruction of ice-sheet extent in Eurasia for different glacial periods. Compared with the last glacial maximum, the Late Saalian (180–140 kyr BP) ice sheet was  $\sim 56\%$  larger and extended further east and southeast over Eurasia<sup>28</sup>. Furthermore, there is clear evidence that ice sheets in Eurasia were much larger during the middle than during the late Pleistocene<sup>27</sup>. This implies that runoff of isotopically depleted water into the BS and CS was considerably higher than during the late Pleistocene, as indicated by very low Sofular  $\delta^{18}\text{O}$  values at around 175, 220, 515, 580 and 630 kyr BP.

Overall, the Sofular record shows strong evidence for a highly dynamic hydrological history of the BS, with more inundations of water from the Mediterranean and Caspian seas than previously thought. Precisely dated records such as ours are crucial for providing more accurate chronologies for ice sheet dynamics in Eurasia and for long sediment sequences from the BS, which in turn can be used to reconstruct the paleoclimate in this poorly explored region<sup>9</sup>.

## Methods

Stable isotope measurements were performed on a Finnigan Delta V Advantage mass spectrometer equipped with an automated carbonate preparation system

(Gas-Bench-II) at the Institute of Geological Sciences, University of Bern. The precision of the  $\delta^{13}\text{C}$  and  $\delta^{18}\text{O}$  measurements is 0.06‰ and 0.07‰ ( $1\sigma$ -error), respectively.

$^{230}\text{Th}$  dating was conducted using a multicollector inductively coupled mass spectrometer (MC-ICP-MS, Nu Instruments) at the Institute of Geological Sciences, University of Bern (Supplementary Table S1) and a MC-ICP-MS (Thermo-Finnigan Neptune) at the Department of Geology and Geophysics, University of Minnesota (Supplementary Table S2). Detailed information on analytical procedures is provided in the Supplementary Information accompanying this article.

Received 22 December 2010; accepted 10 February 2011;  
published online 13 March 2011

## References

- Deuser, W. G. Late-Pleistocene and Holocene history of Black Sea as indicated by stable-isotope studies. *J. Geophys. Res.* **77**, 1071–1077 (1972).
- Bahr, A. *et al.* Abrupt changes of temperature and water chemistry in the late Pleistocene and early Holocene Black Sea. *Geochem. Geophys. Geosyst.* **9**, Q01004 (2008).
- Major, C. O. *et al.* The co-evolution of Black Sea level and composition through the last deglaciation and its paleoclimatic significance. *Quat. Sci. Rev.* **25**, 2031–2047 (2006).
- Zubakov, V. A. Climatostratigraphic scheme of the Black Sea Pleistocene and its correlation with the oxygen isotope scale and glacial events. *Quat. Res.* **29**, 1–24 (1988).
- Svitoch, A. A., Selivanov, A. O. & Yanina, T. A. Paleohydrology of the Black Sea Pleistocene basin. *Wat. Resour.* **27**, 655–664 (2000).
- Ryan, W. B. F. *et al.* An abrupt drowning of the Black Sea shelf. *Mar. Geol.* **138**, 119–126 (1997).
- Gökasan, E. *et al.* On the origin of the Bosphorus. *Mar. Geol.* **140**, 183–199 (1997).
- Chepalyga, A. L. *The Black Sea Flood Question: Changes in Coastline, Climate and Human Settlement* Ch. 6 (Springer, 2007).
- Fleitmann, D. *et al.* Timing and climatic impact of Greenland interstadials recorded in stalagmites from northern Turkey. *Geophys. Res. Lett.* **36**, L19707 (2009).
- Bowen, G. J. & Revenaugh, J. Interpolating the isotopic composition of modern meteoric precipitation. *Wat. Resour. Res.* **39**, 1299–1311 (2003).
- Lachniet, M. S. Climatic and environmental controls on speleothem oxygen-isotope values. *Quat. Sci. Rev.* **28**, 412–432 (2009).
- von Grafenstein, U., Erlenkeuser, H., Brauer, A., Jouzel, J. & Johnsen, S. J. A mid-European decadal isotope-climate record from 15,500 to 5,000 years BP. *Science* **284**, 1654–1657 (1999).
- Bar-Matthews, M., Ayalon, A., Gilmour, M., Matthews, A. & Hawkesworth, C. J. Sea-land oxygen isotopic relationships from planktonic foraminifera and speleothems in the Eastern Mediterranean region and their implication for paleorainfall during interglacial intervals. *Geochim. Cosmochim. Acta* **67**, 3181–3199 (2003).
- Roberts, N. *et al.* Stable isotope records of Late Quaternary climate and hydrology from Mediterranean lakes: The ISOMED synthesis. *Quat. Sci. Rev.* **27**, 2426–2441 (2008).
- Swart, P. K. The oxygen and hydrogen isotopic composition of the Black-Sea. *Deep-Sea Res. A* **38**, S761–S772 (1991).
- Özsoy, E., Rank, D. & Salihoglu, I. Pycnocline and deep mixing in the Black Sea: Stable isotope and transient tracer measurements. *Estuar. Coast. Shelf Sci.* **54**, 621–629 (2002).
- Soulet, G. *et al.* Glacial hydrologic conditions in the Black Sea reconstructed using geochemical pore water profiles. *Earth Planet. Sci. Lett.* **296**, 57–66 (2010).
- Siddall, M. *et al.* Sea-level fluctuations during the last glacial cycle. *Nature* **423**, 853–858 (2003).
- Rohling, E. J. *et al.* Comparison between Holocene and Marine Isotope Stage-11 sea-level histories. *Earth Planet. Sci. Lett.* **291**, 97–105 (2010).
- Oktyay, F. Y. *et al.* The effects of the North Anatolian Fault zone on the latest connection between Black Sea and Sea of Marmara. *Mar. Geol.* **190**, 367–382 (2002).
- Ferronsky, V. I. *et al.* Investigation of water-exchange processes in the Caspian Sea on the basis of isotopic and oceanographic data. *Wat. Resour.* **30**, 15–28 (2003).
- Yanko-Hombach, V., Gilbert, A. S. & Dolukhanov, P. Controversy over the great flood hypotheses in the Black Sea in light of geological, paleontological, and archaeological evidence. *Quat. Int.* **167**, 91–113 (2007).
- Sidorchuk, A. Y., Panin, A. V. & Borisova, O. K. Morphology of river channels and surface runoff in the Volga River basin (East European Plain) during the Late Glacial period. *Geomorphology* **113**, 137–157 (2009).
- Mangerud, J. *et al.* Ice-dammed lakes and rerouting of the drainage of northern Eurasia during the last Glaciation. *Quat. Sci. Rev.* **23**, 1313–1332 (2004).
- Svensden, J. I. *et al.* Late quaternary ice sheet history of northern Eurasia. *Quat. Sci. Rev.* **23**, 1229–1271 (2004).
- Froehlich, K. Evaluating the water balance of inland seas using isotopic tracers: The Caspian Sea experience. *Hydrol. Process.* **14**, 1371–1383 (2000).
- Astakhov, V. Middle Pleistocene glaciations of the Russian north. *Quat. Sci. Rev.* **23**, 1285–1311 (2004).
- Colleoni, F., Krinner, G., Jakobsson, M., Peyaud, V. & Ritz, C. Influence of regional parameters on the surface mass balance of the Eurasian ice sheet during the peak Saalian (140 kya). *Global Planet. Change* **68**, 132–148 (2009).
- Bard, E. *et al.* Deglacial sea-level record from Tahiti corals and the timing of global meltwater discharge. *Nature* **382**, 241–244 (1996).
- Lisiecki, L. E. & Raymo, M. E. A Pliocene–Pleistocene stack of 57 globally distributed benthic  $\delta^{18}\text{O}$  records. *Paleoceanography* **20**, PA1003 (2005).

## Acknowledgements

Support of the Swiss National Science Foundation (grant PP002-110554/1 to D.F.), the US National Science Foundation (ESH 0502535 to R.L.E. and H.C.), the Gary Comer Science and Education Foundation (CP41 to R.L.E.) and Istanbul Technical University (grant ITU-BAP-332491 to O.T.) facilitated this work. We would like to thank P. C. Tzedakis and M. Siddall for providing their data and for helpful discussions.

## Author contributions

D.F. and O.T. initiated the project. S.B., A.Z., O.M.G. and D.F. performed the stable isotope analysis. H.C., S.B. and R.L.E. conducted the uranium-series analysis. S.B. and D.F. wrote the paper.

## Additional information

The authors declare no competing financial interests. Supplementary information accompanies this paper on [www.nature.com/naturegeoscience](http://www.nature.com/naturegeoscience). Reprints and permissions information is available online at <http://npg.nature.com/reprintsandpermissions>. Correspondence and requests for materials should be addressed to S.B. or D.F.

---

## APPENDIX C

### CONFERENCE CONTRIBUTIONS (only the first-name contributions included)

1. Göktürk, O.M., Badertscher, S., Pickering, R., Fankhauser, A., Kramers, J., Tüysüz, O., Matter, A., Fleitmann, D., 2008. Stalagmites from Northern Turkey: Potential Climate Proxies for the Last Three Millennia. Poster presented in the meeting *9<sup>th</sup> Swiss Global Change Day, Bern, Switzerland, April 1, 2008*.
2. Göktürk, O.M., Fleitmann, D., Badertscher, S., Pickering, R., Fankhauser, A., Tüysüz, O., Matter, A., Kramers, J., 2008. Stalagmites from Turkey: Potential Climate Proxies for the Holocene. Extended abstract submitted to and poster presented in the symposium *Climate Extremes During Recent Millennia and their Impact on Mediterranean Societies, Athens, Greece, September 14-16, 2008*.
3. Göktürk, O.M., Fleitmann, D., Badertscher, S., Cheng, H., Pickering, R., Fankhauser, A., Tüysüz, O., Matter, A., Kramers, J., 2009. A High Resolution Late Glacial and Holocene Stalagmite Stable Isotope Record From The Southern Black Sea Coast. Abstract submitted to and oral presentation given in the *64<sup>th</sup> Geological Congress of Turkey, Ankara, Turkey, April 13-17, 2009*.
4. Göktürk, O.M. and Akçar, N., 2009. The Role of Air-Sea Interaction in the Precipitation Variability of the Southern Black Sea Coast. Abstract submitted to and oral presentation given in the conference *Geology of the Black Sea Region, Ankara, Turkey, October 5-8, 2009*.
5. Göktürk, O.M., Fleitmann, D., Badertscher, S., Cheng, H., Edwards, L., Laudanski, P., Tüysüz, O., Kramers, J., 2010. Late Holocene Stalagmites from Turkey: What Do They Actually Record? Poster presented in the meeting *11<sup>th</sup> Swiss Global Change Day, Bern, Switzerland, April 20, 2008*.
6. Göktürk, O.M., Fleitmann, D., Badertscher, S., Cheng, H., Edwards, L., Laudanski, P., Fankhauser, A., Tüysüz, O., Kramers, J., 2010. Stalagmite Records From Turkey Exhibit Varied Isotopic Responses and Reveal Regional Complexity of Late Holocene Climate in the Eastern Mediterranean. Abstract submitted to and oral presentation given in the *3<sup>rd</sup> workshop of the 'Dated Speleothems – Archives of the Paleoenvironment' (DAPHNE), Innsbruck, Austria, June 30 - July 2, 2010*.
7. Göktürk, O.M., Fleitmann, D., Badertscher, S., Cheng, H., Edwards, L., Fankhauser, A., Tüysüz, O., Kramers, J., 2010. *Climate on the southern Black Sea coast during the Holocene: Implications from the Sofular Cave record*. Abstract submitted to and oral presentation given in the *8<sup>th</sup> Swiss Geoscience Meeting: Extremes in Space and Time, Fribourg, Switzerland, November 19-20, 2010*.



---

**APPENDIX D****DECLARATION****Erklärung**

gemäss Art. 28 Abs. 2 RSL 05

Name/Vorname: *Göktürk Ozan Mert*  
Matrikelnummer: *07-126-063*  
Studiengang: *Doktorat Phil-nat. (Climate Sciences)*

Bachelor       Master       Dissertation

Titel der Arbeit: *Climate in the Eastern Mediterranean through the Holocene  
inferred from Turkish stalagmites*

Leiter der Arbeit: *SNF-Prof. Dr. Dominik Fleitmann*

Ich erkläre hiermit, dass ich diese Arbeit selbstständig verfasst und keine anderen als die angegebenen Quellen benutzt habe. Alle Stellen, die wörtlich oder sinngemäss aus Quellen entnommen wurden, habe ich als solche gekennzeichnet. Mir ist bekannt, dass andernfalls der Senat gemäss Artikel 36 Absatz 1 Buchstabe o des Gesetzes vom 5. September 1996 über die Universität zum Entzug des auf Grund dieser Arbeit verliehenen Titels berechtigt ist.

Bern, 10. Mai 2011





## APPENDIX E

### CURRICULUM VITAE

#### **Ozan Mert Göktürk**

Date of birth: 23. January 1979

Nationality: Turkish

#### **University education**

2007 – 2011    Dissertation at the Institute of Geological Sciences,  
University of Bern, Switzerland

PhD thesis:        *Climate in the Eastern Mediterranean through the  
Holocene inferred from Turkish stalagmites*

Supervisor:        SNF-Prof. Dr. Dominik Fleitmann

2003 – 2005    Master study in Climate and Marine Sciences at the  
Eurasia Institute of Earth Sciences, Istanbul Technical University, Turkey

Degree:            Master of Science in Climate and Marine Sciences

Master Thesis:    *North Sea – Caspian pattern its influence on the  
hydrological parameters over Turkey*

Supervisor:        Prof. Dr. Mehmet Karaca

1997 – 2003    Bachelor study in the Mechanical Engineering Department of the  
Faculty of Engineering, Middle East Technical University, Ankara, Turkey

Degree:            Bachelor of Science in Mechanical Engineering

#### **Primary and Secondary Education**

1990 – 1997    Kocaeli Anatolian High School, Middle and High Sections, Izmit, Turkey

1986 – 1990    Orta Anadolu Primary School, Kırıkkale, Turkey